THE PROCEEDINGS OF THE PHYSICAL SOCIETY

Section A

VOL. 64, PART 12 — 1 December 1951 — No. 384 A

CONTENTS

	PAGE
Professor S. CHAPMAN (President 1949–1950)	*Frontispiece*
Dr. A. L. HODSON. The Temperature Effect of Extensive Air Showers	1061
Mr. A. C. CLARK and Miss S. N. RUDDLESDEN. The Disintegration of Light Nuclei by Meson Capture	1064
Dr. F. A. EL-BEDEWI. Range–Energy Relation for Protons in Ilford C2 Dry Emulsion	1079
Dr. H. S. GREEN and Dr. H. MESSEL. The Differential Cross Section for High Energy Nucleon–Nucleon Collisions and the Mean Square Angle of Scatter	1083
Dr. H. KUHN and Dr. G. K. WOODGATE. Nuclear Spin and Magnetic Moment of Rhodium $^{103}_{45}$Rh	1090
Dr. R. G. MOORHOUSE. Slow Neutron Scattering by Ferromagnetic Crystals	1097
Mr. J. M. ZIMAN. Antiferromagnetism by the Bethe Method	1108
Dr. D. W. PASHLEY. Asymmetrical Electron Diffraction Effects from Single Crystals of Silver	1113
Dr. J. J. O'DWYER. Field Dependence of the Dielectric Constant	1125
Letters to the Editor :	
Mr. J. H. BLACKWELL and Dr. A. D. MISENER. Approximate Solution of a Transient Heat Flow Problem	1132
Dr. E. P. GEORGE and Dr. P. T. TRENT. Observations on the Interactions of μ-Mesons Underground	1134
Dr. B. BLEANEY and Mr. K. D. BOWERS. Nuclear Spin of $^{53}_{24}$Chromium	1135
Dr. J. W. GARDNER. Interference in the Directional Correlation of Conversion Electrons	1136
Mr. D. L. PURSEY. Theoretical Discussion of the Beta Decay of ^{32}P	1138
Mr. D. J. LITTLER, Mr. E. E. LOCKETT and Mr. B. T. PRICE. The G.L.E.E.P. as an Absolute Standard of Thermal Neutron Density	1139
Obituary Notices :	
LESLIE JOHN COMRIE	1141
LEONARD GEORGE GRIMMETT	1143
JOHN R. LOOFBOUROW	1144
EDWARD MALLETT	1145
HANTARO NAGAOKA	1146
FRANK BENNETT YOUNG	1147
ARNOLD SOMMERFELD	1148
STUART ARTHUR FRANK WHITE	1149
Miss JESSIE S. CHREE	1150
ALLAN FERGUSON (brief note: Obituary Notice next year)	1150
Contents for Section B	1150
Abstracts for Section B	1151
Subject Index, Section A, Vol. 64	1153
Index of Authors (with Titles), Section A, Vol. 64	1161
Index to Reviews of Books, Section A, Vol. 64	1169

Price to non-members 10*s.* net, by post 6*d.* extra. Annual subscription: £5 5*s.*

Composite subscription for both Sections A and B: £9 9*s.*

Published by

THE PHYSICAL SOCIETY

1 Lowther Gardens, Prince Consort Road, London S.W.7

The Hall-mark of a WRP Precision Built Microscope

PRIOR MICROSCOPES

are still made by expert craftsmen to those exacting standards of optical and mechanical precision which have made them so universally acceptable amongst discerning users.

W. R. PRIOR & CO. LTD.

28A DEVONSHIRE STREET, LONDON, W.1.

WELbeck 4695

PROCEEDINGS OF THE PHYSICAL SOCIETY

ADVERTISEMENT RATES

The *Proceedings* are divided into two parts, A and B. The charge for insertion is £18 for a full page in either Section A or Section B, £30 for a full page for insertion of the same advertisement in both Sections. The corresponding charges for part pages are:

½ page	£9 5 0	£15 10 0
¼ page	£4 15 0	£8 0 0
⅛ page	£2 10 0	£4 5 0

Discount is 20% for a series of six similar insertions and 10% for a series of three.

The printed area of the page is $8\frac{1}{2}'' \times 5\frac{1}{2}''$, and the screen number is 100.

Copy should be received at the Offices of the Physical Society six weeks before the date of publication of the *Proceedings*.

THE PHYSICAL SOCIETY

VOLUME XIV of the REPORTS ON PROGRESS IN PHYSICS

A comprehensive annual review by specialist authors. The contents are as follows:

W. C. PRICE. Recent Advances in Ultra-Violet Absorption Spectroscopy.

W. E. LAMB, Jr. Anomalous Fine Structure of Hydrogen and Singly Ionized Helium.

H. KUHN. New Techniques in Optical Interferometry.

E. WOLF. Diffraction Theory of Aberrations.

A. B. MEINEL. The Spectrum of the Airglow and the Aurora.

B. J. MASON and F. H. LUDLAM. The Microphysics of Clouds.

M. DEUTSCH. Angular Correlations in Nuclear Reactions.

G. D. ROCHESTER and W. V. G. ROSSER. Nuclear Interactions of Cosmic Rays.

E. W. FOSTER. Nuclear Effects in Atomic Spectra.

N. C. GERSON. A Critical Survey of Ionospheric Temperatures.

W. V. MAYNEORD. Some Applications of Nuclear Physics in Medicine.

The price is **50***s*. 0*d*. Members: One copy at **27***s*. **6***d*.
Postage and packing 1*s*.

Further information can be obtained from

THE PHYSICAL SOCIETY

1 Lowther Gardens, Prince Consort Road, London S.W.7

HANDBOOK
OF THE
PHYSICAL SOCIETY'S
35th EXHIBITION
OF
SCIENTIFIC INSTRUMENTS
AND APPARATUS
1951

lxxii + 244 pp.; 121 illustrations
5*s.* ; *by post* 6*s.*

Orders, with remittances, to
THE PHYSICAL SOCIETY
1 Lowther Gardens, Prince Consort Road,
London S.W.7

611

DESIGN ENGINEERS!
Seamless one-piece
METAL BELLOWS

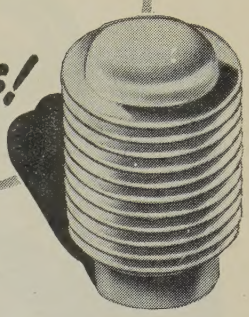

Combining the properties of :
1. A compression spring capable of repeated flexing.
2. A container which can be hermetically sealed.
3. A packless gland.

HYDRAULICALLY FORMED BY A PROCESS UNIQUE IN THIS COUNTRY

FOR Automatic coolant regulation. Movement for pressure change. Packless gland to seal spindle in high vacua. Reservoir to accept liquid expansion. Dashpot or delay device. Barometric measurement or control. Pressurised couplings where vibration or movement is present. Dust seal to prevent ingress of dirt. Pressure reducing valves. Hydraulic transmission. Distance thermostatic control. Low torque flexible coupling. Pressure sealed rocking movement. Pressurised rotating shaft seals. Aircraft pressurised cabin control. Refrigeration expansion valves. Thermostatic Steam Traps. Pressure amplifiers. Differential pressure measurements. Thermostatic operation of louvre or damper. *Write for List No.* V. 500-1.

Drayton METAL BELLOWS
Drayton Regulator and Instrument Co. Ltd., West Drayton, Middlesex

PHYSICAL SOCIETY SPECIALIST GROUPS

OPTICAL GROUP

The Physical Society Optical Group exists to foster interest in and development of all branches of optical science. To this end, among other activities, it holds meetings about five times a year to discuss subjects covering all aspects of the theory and practice of optics, according to the papers offered.

COLOUR GROUP

The Physical Society Colour Group exists to provide an opportunity for the very varied types of workers engaged on colour problems to meet and to discuss the scientific and technical aspects of their work. Five or six meetings for lectures and discussions are normally held each year, and reprints of papers are circulated to members when available. A certain amount of committee work is undertaken, and reports on Defective Colour Vision (1946) and on Colour Terminology (1948) have already been published.

LOW TEMPERATURE GROUP

The Low Temperature Group was formed to provide an opportunity for the various groups of people concerned with low temperatures—physicists, chemists, engineers, etc.—to meet and become familiar with one another's problems. The group seeks to encourage investigations in the low temperature field and to assist in the correlation and publication of data.

ACOUSTICS GROUP

The Acoustics Group was formed to meet the long-felt need for a focus of acoustical studies in Great Britain. The scope includes the physiological, architectural, psychological and musical aspects of acoustics as well as the fundamental physical studies on intensity transmission and absorption of sound. The Group achieves its object by holding discussion meetings, by the circulation of reprints and by arranging symposia on selected acoustical topics.

Further information may be obtained from the Offices of the Society :
1 Lowther Gardens, Prince Consort Road, London S.W.7.

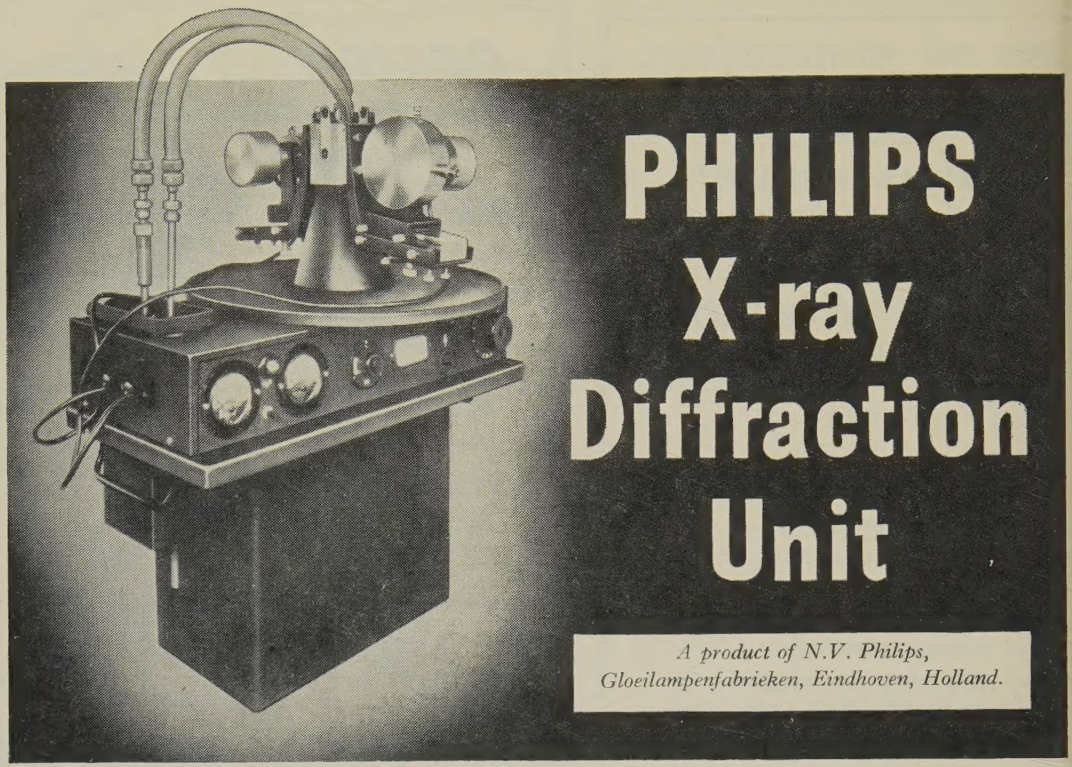

This apparatus constitutes the ideal flexible diffraction machine. With a power unit rated at 60 kvp. 20 ma. any of the modern techniques can be readily employed. Among the many applications for this machine are:—

CHEMICAL IDENTIFICATION · PHASE ANALYSIS · SOLID SOLUBILITY STUDY · SINGLE CRYSTAL STUDIES · PARTICLE SIZE MEASUREMENTS · METALLOGRAPHIC STUDIES · MOLECULAR WEIGHT DETERMINATION · STRUCTURE IDENTIFICATION · STRESS ANALYSIS · FIBRE STUDIES · PROCESS CONTROL · ORIENTATION STUDIES

PRECISION MADE · GENEROUSLY RATED · ALWAYS READY FOR USE

Fully descriptive catalogue on request

PHILIPS ELECTRICAL
LIMITED

Manufacturers of:
X-RAY EQUIPMENT FOR ALL PURPOSES · ELECTRO-MEDICAL APPARATUS · LAMPS AND LIGHTING EQUIPMENT · SOUND AMPLIFYING EQUIPMENT · MAGNETIC FILTERS · BATTERY CHARGERS AND RECTIFIERS

PHILIPS ELECTRICAL LIMITED, X-RAY DEPARTMENT, CENTURY HOUSE, SHAFTESBURY AVENUE, LONDON, W.C.2.

(XB 731B)

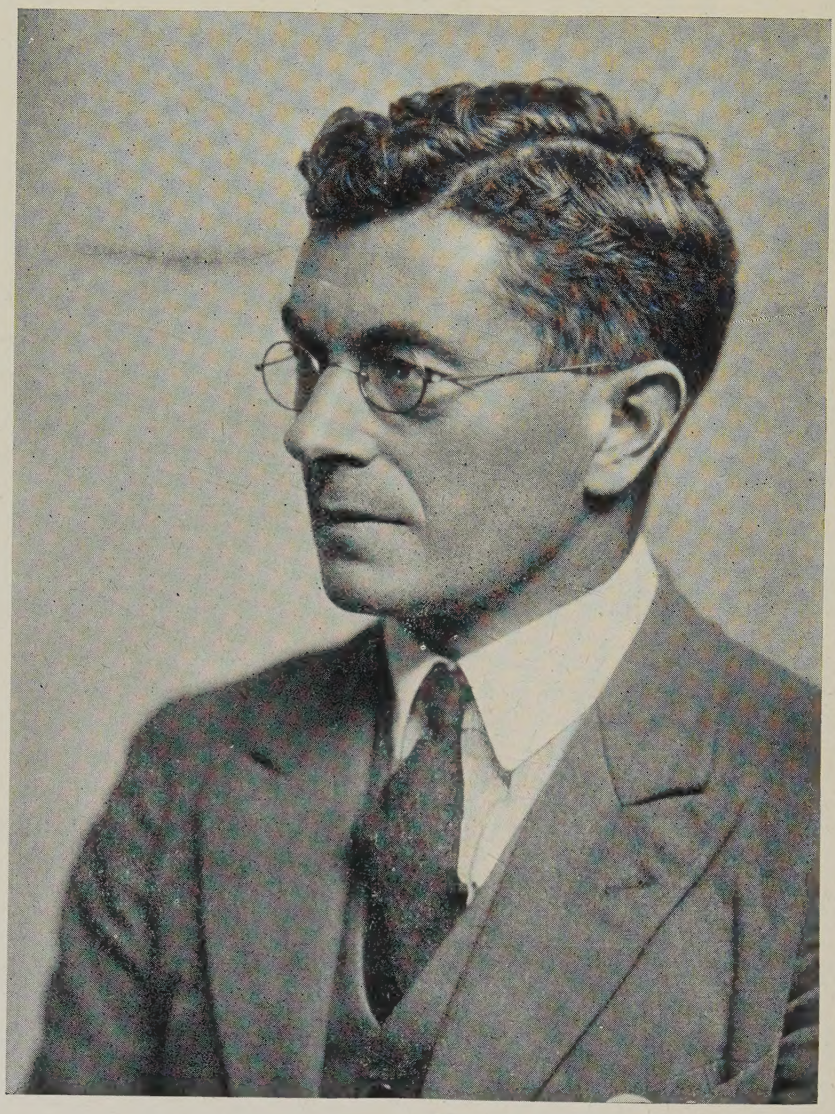

PROFESSOR S. CHAPMAN, M.A., D.Sc., F.R.S.,
President of the Physical Society 1949–1950.

(*Note*—Prof. Chapman's Presidential Address is published in the October 1951 *Proceedings*, Section B, page 833.)

THE PROCEEDINGS OF
THE PHYSICAL SOCIETY

Section A

VOL. 64, PART 12 1 December 1951 No. 384 A

The Temperature Effect of Extensive Air Showers

BY A. L. HODSON
The Physical Laboratories, The University, Manchester

Communicated by P. M. S. Blackett; *MS. received 3rd July* 1951

ABSTRACT. Extensive air showers have been recorded at sea level over a period of nine months. The data show a fairly good correlation between the shower rate and the air temperature at about one cascade unit above the apparatus, e.g. at the 950 mb. level. A temperature coefficient of $-(0{\cdot}38\pm0{\cdot}11)\%$ per °C. at this level is indicated. This may be explained by the dependence of the lateral spread of an extensive shower on the air density.

§1. INTRODUCTION

In a homogeneous atmosphere the root mean square lateral spread of a cascade shower is proportional to the length of the cascade unit (Blatt 1949) which in turn is inversely proportional to the air density ρ. The dependence of the lateral spread on ρ, and thus on the air temperature, leads us to expect a seasonal variation of the rate of extensive showers at sea level.

The shower rate observed with a fixed arrangement of counter trays depends on ρ in three different ways:

(*a*) The effective area of the counter trays is proportional to ρ^2. Since varying the areas of the counter trays by a factor f produces a change of f^γ in the shower rate (where γ is the exponent of the integral density spectrum of extensive showers), a dependence of the order of $\rho^{2\gamma}$ is thus introduced into the shower rate.

(*b*) The effective separation of the counter trays is proportional to ρ. Now the shower rate recorded by counter trays a distance r apart varies approximately as $r^{-\alpha}$ where α lies between 0·1 and 0·5, depending on the experimental arrangement and on the altitude (Auger *et al.* 1939, Daudin and Daudin 1949, Kraybill 1949). The shower rate is therefore modified by a further factor $\rho^{-\alpha}$.

(*c*) A counter tray is liable to be discharged by showers whose cores fall within a distance proportional to the root mean square lateral spread, i.e. within an area proportional to ρ^{-2}.

The variation of the lateral spread with air density is therefore expected to produce a total dependence of the shower rate on air density of the form $\rho^{2\gamma-2-\alpha}$.

Now Jánossy (1948, p. 323) has shown that most of the lateral spread of a shower observed at a given atmospheric depth is due to scattering in the previous

one or two cascade units. The lateral spread at a given depth in the earth's atmosphere is therefore more correctly given by taking ρ equal to the density at one cascade unit above the apparatus.

At constant pressure, the shower rate is thus expected to depend on the absolute temperature T at one cascade unit above the apparatus roughly as $T^{-(2\gamma-2-\alpha)}$, i.e. to have a temperature coefficient of the order of

$$\frac{1}{N}\left(\frac{dN}{dT}\right) = -(2\gamma-2-\alpha)\frac{100}{T}\,\%\text{ per °C.}$$

$$= -\frac{(2\gamma-2-\alpha)}{2{\cdot}8}\,\%\text{ per °C.} \qquad \ldots\ldots(1)$$

The existence of a temperature effect in extensive air showers was suggested by Euler (1940) and by Daudin and Daudin (1949), but no observational evidence has previously been reported.

§ 2. EXPERIMENTAL RESULTS

Threefold coincidences were recorded between counter trays A, B, C (Figure 1) during the period April 1950–January 1951, the apparatus being situated in a heated laboratory under a light roof. The average hourly shower rate (corrected to 76 cm. Hg) for each monthly period is given in the Table and plotted in Figure 2. Also shown in Figure 2 is the average air temperature at the 950 mb. level measured at Liverpool during the same period. (We are indebted to the Air Ministry for the temperature data.)

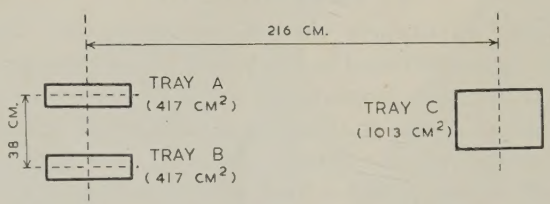

Figure 1.

Period 1950	Recording time (hours)	No. of showers	Average rate per hour in period.	Average air temperature at 950 mb. (°F.)
April–May	688	8038	$11{\cdot}68 \pm 0{\cdot}13$	43·8
May–June	727	8196	$11{\cdot}27 \pm 0{\cdot}12$	52·6
June–July	688	7714	$11{\cdot}21 \pm 0{\cdot}13$	54·1
July–Aug.	556	6241	$11{\cdot}22 \pm 0{\cdot}14$	53·7
Aug.–Sept.	530	6449	$11{\cdot}12 \pm 0{\cdot}14$	51·9
Sept.–Oct.	606	6735	$11{\cdot}11 \pm 0{\cdot}14$	47·9
Oct.–Nov.	538	6265	$11{\cdot}64 \pm 0{\cdot}15$	40·3
Nov.–Dec.	300	3448	$11{\cdot}49 \pm 0{\cdot}20$	37·5
Dec.–Jan. '51.	352	4073	$11{\cdot}57 \pm 0{\cdot}18$	31·9

The results indicate a fairly definite correlation of the shower rate with air temperature. An analysis of the data gives the temperature coefficient of extensive showers at sea level as $-(0{\cdot}21 \pm 0{\cdot}06)\%$ per °F. or $-(0{\cdot}38 \pm 0{\cdot}11)\%$ per °C. (The errors quoted here and elsewhere are standard deviations.)

The choice of pressure level for the correlation is based on the theoretical considerations above. If these are correct the shower data should give the highest correlation for a pressure level of about 950 mb. Unfortunately, the

temperature variation shows little change over a wide range of pressure levels, and because of the limited statistical accuracy of the shower data it is not possible to distinguish between various levels. For example, the seasonal variation of the air temperature at the 500 mb. level differed from that at the 950 mb. level by less than 10%. The correlation and regression coefficients for these two levels are thus not significantly different.

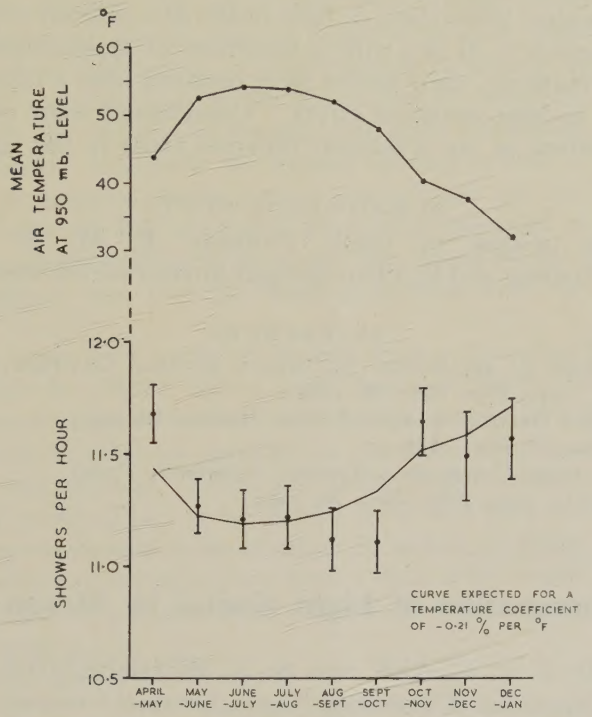

Figure 2. The seasonal variation of extensive air showers.

From experiments to be published shortly, the value of γ for the showers recorded by the arrangement of Figure 1 was found to be $\gamma = 1{\cdot}445 \pm 0{\cdot}014$. The value of α applicable to the present apparatus is probably of the same order as the value found by Kraybill (1949) at 720 m. with a threefold arrangement of counters ($\alpha \sim 0{\cdot}1$). From expression (1) we thus expect a temperature coefficient of the order of $-0{\cdot}3\%$ per °c. This is quite consistent with the observed value.

§ 3. OTHER VARIATIONS

Since data were available for the number of showers recorded during each hourly period, a search was also made for a possible solar daily variation and for a sidereal variation.

No significant solar daily variation was found, a Fourier analysis of the data giving the amplitude of the first harmonic as $(0{\cdot}30 \pm 0{\cdot}61)\%$. The amplitude of the average daily variation of air temperature during the period of the experiment was 1·2°F. (Compare this with the amplitude of the seasonal temperature variation, Figure 2 (of the order of 11°F.).) Assuming the temperature coefficient found above a solar diurnal variation of amplitude $0{\cdot}25\%$ is expected.

The analysis of the sidereal data gave the amplitude of the first harmonic of the sidereal variation as $(1{\cdot}15 \pm 0{\cdot}61)\%$ with the 'maximum' at 2330 hours sidereal time. The average primary energy of the showers recorded was probably of the order of 5×10^{14} ev. It is clear that even for primary cosmic rays of this energy no large sidereal variation exists. Since the average energy of the showers recorded by an arrangement of counters increases with the total counter spread a much larger effect might be observed with counter trays, say, 50 m. apart. Daudin and Daudin (1949) claim to have observed a sidereal variation of 1–5% (for counter spreads 5–70 m.) with a maximum at approximately 1800 hours sidereal time. However, their results were obtained over a rather short period and are subject to large statistical errors. Considerably more data are needed to establish whether or not a sidereal variation exists in the very high energy primaries.

ACKNOWLEDGMENTS

The author wishes to thank Professor P. M. S. Blackett and Drs. D. W. N. Dolbear and H. Elliot for their interest in this work.

REFERENCES

Auger, P., Maze, R., and Robley, R., 1939, *C. R. Acad. Sci., Paris*, **208**, 1641.
Blatt, J. M., 1949, *Phys. Rev.*, **75**, 1584.
Daudin, J., and Daudin, A., 1949, *J. Phys. Radium*, **10**, 394.
Euler, H., 1940, *Z. Phys.*, **116**, 73.
Jánossy, L., 1948, *Cosmic Rays* (Oxford : University Press).
Kraybill, H. L., 1949, *Phys. Rev.*, **76**, 1092.

The Disintegration of Light Nuclei by Meson Capture

By A. C. Clark and S. N. Ruddlesden
Department of Theoretical Physics, Liverpool University

Communicated by H. Fröhlich; *MS. received* 19*th June* 1951

ABSTRACT. The disintegration by π^--meson capture of the elements helium and carbon is discussed. Two types of meson theory, scalar and pseudo-scalar, are considered. The relative probabilities of the various modes of disintegration of helium are calculated and the energy spectra of the most likely one, viz. proton emission, are shown. The disintegration of carbon into two α-particles and one singly charged particle is considered, using a simple α-particle model. The energy spectra and angular correlations of the α-particles obtained by a direct transition and by a transition via an excited state of ^{8}Be are compared.

§1. INTRODUCTION

The production of 'stars' by the capture of negative π-mesons in nuclei is a well-known phenomenon which it is hoped may provide some information about the form of the interaction between mesons and nucleons. The stars formed by the disintegration of heavy nuclei do not provide such information since these have been explained satisfactorily by Le Couteur (1950) using the evaporation theory of Bohr and Kalckar (1937), which is based on rather general considerations and is independent of the meson–nucleon interaction. The criteria for the applicability of evaporation theory, that

(*a*) the excitation energy given to the nucleus must be much less than its binding energy, and (*b*) the number of particles in the nucleus must be great enough for approximate thermodynamic equilibrium to be attained between emission of particles, are not obeyed when a light nucleus captures a meson. In this case the concept of a compound nucleus has only a limited meaning and the disintegration must be considered as a direct process, as indeed must the emission of one high-energy particle from a heavy nucleus (Tamor 1950). This direct transition requires the use of first order perturbation theory and the results of applying this theory may be expected to show some dependence on the meson–nucleon interaction. Considerations favouring the study of very light nuclei are the reduction in the effects due to statistical factors and the simplification in the analysis of experiments upon decreasing the number of particles concerned. Helium is the lightest element to emit a charged particle on capturing a negative meson, so it was chosen as the subject of our investigations; also the ^{4}He nucleus (α-particle) is regarded as a constituent of heavier nuclei, which enables us to apply our results to the disintegration of carbon (or oxygen) into two (or three) α-particles and one singly charged particle.

The direct capture by nuclei of mesons from a beam has been studied by Massey and Corben (1939), Sakata and Tanikawa (1939) and Bruno (1948), who found capture times of order 10^{-6} second for mesons of a few volts energy; their results may be taken as applying to π-mesons since a strong interaction with nucleons was assumed. Fermi and Teller (1947) estimated the time taken by a meson of energy 2 kev. to be slowed down and captured into the lowest Bohr orbit about a nucleus to be about 10^{-13} second, in solids. Thus one can assume that meson capture takes place from a Bohr orbit, usually the lowest one; this is in agreement with experiments, which show that a meson usually comes to rest before creating a star.

Possible basic capture processes are

$$\mathrm{P}+\pi^-\rightarrow\mathrm{N}, \qquad \ldots\ldots(1)$$

$$\mathrm{P}+\pi^-\rightarrow\mathrm{N}+\pi^0, \qquad \ldots\ldots(2)$$

$$\mathrm{P}+\pi^-\rightarrow\mathrm{N}+\gamma, \qquad \ldots\ldots(3)$$

where P, N, π^-, π^0 and γ represent a proton, neutron, negative π-meson, neutral π-meson and γ-ray respectively. Recent experiments at Berkeley (Aamodt *et al.* 1950) on the capture of π-mesons in hydrogen have shown that in ^{1}H, where process (1) is forbidden by conservation of momentum, both (2) and (3) occur, while in ^{2}H (2) is not observed and (1) and (3) occur with about equal probabilities. In heavier nuclei, where the binding energy is too great to permit (2), (3) is expected to be rare and process (1) is here assumed. The validity of this assumption can be checked experimentally by considering conservation of energy and momentum for a disintegration in which only one neutron is emitted: in particular, for the disintegration $^4\mathrm{He}+\pi^-\rightarrow{}^3\mathrm{H}+\mathrm{n}$ the triton has a fixed energy, of about 30 Mev., if no secondary particle (or quantum) is emitted. Recent work by Menon, Muirhead and Rochat (1950, referred to as M.M.R.) offers some, though inconclusive, evidence on this point from stars which are identified as $^{12}\mathrm{C}+\pi^-\rightarrow 2\,{}^4\mathrm{He}+{}^3\mathrm{H}+\mathrm{n}$.

The discovery by Bjorkland *et al.* (1950) of a neutral π-meson which decays into two γ-rays and the work of Yang (1950 a) showing that such a meson must

have spin 0 lead one to expect that the spin of the charged π-meson is also zero, as does much other indirect evidence. Mesons of spin 0 occur in both the scalar and pseudoscalar theories: the interactions used in this paper, between which it is hoped that experiments might differentiate, are the non-relativistic approximations to those given by these two theories, viz. $\psi(\mathbf{r})$ and $\boldsymbol{\sigma}.\nabla\psi(\mathbf{r})$, where $\psi(\mathbf{r})$ is the meson wave function at the position of the nucleon and $\boldsymbol{\sigma}$ is the nucleon spin operator. If instead of estimating actual cross sections one estimates the relative probabilities of one nucleus splitting in various ways after capturing a meson and the energy spectra of the emitted particles, many uncertainties due to our lack of detailed knowledge of the way in which the meson approaches the nucleus, the strength of the interaction and the form of the nuclear wave functions are eliminated. For each disintegration we refer to a 'standard' energy spectrum (defined in §2) which is independent of the meson interaction. This spectrum is effectively that due to a constant interaction, but neglects the antisymmetry of the wave functions; it is convenient both as a rough approximation and for comparing the effects of different interactions.

Another way of differentiating between the two theories, proposed by Yang (1950 b), depends on measurements of the relative polarization of the γ-rays produced when the neutral π-meson disintegrates.

§2. GENERAL METHOD

In this section the method of calculation is described in general terms which are later applied to specific problems; where necessary ^{3}He is used as a simple but typical example. Since it is the relative probabilities of the different modes of disintegration of one nucleus which are to be calculated, certain constant factors, common to all such modes, are omitted. First order perturbation theory gives the transition probability for a particular mode of disintegration as

$$\int \Sigma |H|^2 \, d\rho_E = \int W \, d\rho_E \quad \text{writing} \quad W = \Sigma |H|^2, \qquad \ldots\ldots(4)$$

where H is the matrix element for transition to one of the possible final states, $d\rho_E$ is the number of momentum states per unit energy of the final system, the summation is over all spin states and the integration is over all momentum states. The energy spectrum $P(\epsilon_1)$ of one of the emitted particles is given by

$$P(\epsilon_1)\, d\epsilon_1 \propto {\epsilon_1}^{1/2}\, d\epsilon_1 \int W \, d\rho_E', \qquad \ldots\ldots(5)$$

where ${\epsilon_1}^{1/2}\, d\epsilon_1\, d\rho_E' = d\rho_E$. The total kinetic energy E available in the final state is given by $E =$ meson mass $-$ difference of binding energies in initial and final states; the value of the meson mass is taken as 290 electron masses.

The matrix element for a disintegration is

$$H = \int \Psi_F^* G \Psi_I, \qquad \ldots\ldots(6)$$

where Ψ_I and Ψ_F are the wave functions describing the initial and final states of the nucleons and G is the meson interaction operator, which may be written as

$$G = \sum_{\text{nucleons}} G_i \Gamma_i, \qquad \ldots\ldots(7)$$

where Γ is the operator which converts a proton into a neutron, and is zero when applied to a neutron, and for a scalar meson

$$G_{1i} = \psi(\mathbf{r}_i), \qquad \ldots\ldots(8)$$

while for a pseudo-scalar meson $G_{2i} = \boldsymbol{\sigma}_i.\nabla_i\psi(\mathbf{r}_i)$, $\qquad \ldots\ldots(9)$

where $\psi(\mathbf{r}_i)$ is the meson wave function at the position of the ith nucleon and $\boldsymbol{\sigma}$ is the nucleon spin operator. Since the 'correct' forms of Ψ_I and Ψ_F are not known it is convenient to represent all nuclei by gaussian wave functions and all emitted particles by plane waves. All the wave functions are antisymmetrized with the help of the quantity $\epsilon_{ij\ldots s}$, where

$$\epsilon_{ij\ldots s}=\begin{cases}+1 \text{ if } ij\ldots s \text{ is an even permutation of } 1, 2\ldots n\\ -1 \text{ if } ij\ldots s \text{ is an odd permutation of } 1, 2\ldots n\\ 0 \text{ otherwise.}\end{cases}$$

For example, in the complete disintegration of ^{3}He the initial wave function is

$$\Psi_I=(3!)^{-1/2}\exp\left\{-a\sum_1^3 r_{ij}^2\right\}\sum_{ijk}\alpha_i\alpha_j\beta_k\eta_i\xi_j\eta_k\epsilon_{ijk} \qquad \ldots\ldots(10)$$

and a typical final wave function is

$$\Psi_F=(3!)^{-1/2}\sum_{ijk}\psi_{ijk}\alpha_i\alpha_j\beta_k\eta_i\xi_j\xi_k\epsilon_{ijk}, \qquad \ldots\ldots(11)$$

where† $$\psi_{ijk}=V^{-1}\exp\{i(\mathbf{k}_1.\mathbf{r}_i+\mathbf{k}_2.\mathbf{r}_j+\mathbf{k}_3.\mathbf{r}_k)\},$$

α, β and ξ, η are the spin and isotopic spin functions, r_{ij} is the distance between the ith and jth nucleons, V is the (large) volume in which the events take place, and $\hbar\mathbf{k}_1$, $\hbar\mathbf{k}_2$ and $\hbar\mathbf{k}_3$ are the momenta of the emitted particles. Following Bruno (1948) the value of the constant a used throughout is given by $a^{-1/2}=4{\cdot}0\times10^{-13}$ cm.

The question of the orthogonality of the wave functions Ψ_I and Ψ_F will now be discussed briefly. It will be noted that in the above example Ψ_I and Ψ_F are orthogonal by virtue of the change in isotopic spin but, in the approximation of charge-independent forces, one might expect their spatial parts, $\psi_I=\exp\{-a\Sigma_1^3 r_{ij}^2\}$ and $\psi_F=\psi_{123}$, to be orthogonal; these may be made so, artificially, by introducing $\psi_F'=(1-d\exp\{-g\Sigma_1^3 r_{ij}^2\})\psi_F$, with suitable values of d and g. This factor will reduce, in the region of small r_{ij}, the contribution to any matrix element between ψ_I and ψ_F, as would an increase in $\mathbf{k}_i$ in this region due to the action of nuclear forces. If the spatial parts of the initial and final wave functions are orthogonal any constant term in the meson interaction G will give no contribution to the matrix element. Using the scalar meson interaction G_1 it has been found that the matrix element $\int\Psi_F^*G_1\Psi_I$ after omitting the contribution due to the constant term in G_1 can be identified with the matrix element $\int\Psi_F'^*G_1\Psi_I$ in the limiting case $g\gg a$. For $d=0{\cdot}5$ we find $a/g\simeq0{\cdot}07$ and a calculation has shown that the proton energy spectra from these two matrix elements differ, at any point of non-vanishing probability, by less than about 2% and that the difference between the total probabilities of proton emission is also about 2%. This provides some justification for the use of non-orthogonal wave functions with omission of the constant term. In the case of ^{4}He such a constant term is automatically eliminated by the antisymmetry properties of the wave functions.

To obtain $W=\Sigma|H|^2$ where $H=\int\Psi_F^*G\Psi_I$ one may first integrate over the spin and isotopic spin variables and sum over all final states; this gives W in

† The nuclear wave functions ψ_{ijk}, ... ψ_I and ψ_F should not be confused with $\psi(\mathbf{r})$, the meson wave function.

terms of integrals I_i involving only the spatial wave functions ψ_I and ψ_F and that part O_i of the interaction operator G_i which is independent of spin. The nature of the wave functions is such that each integral I_i can be expressed in the form

$$I_i = \int \psi_F^* O_i \psi_I = \int \psi_F^* \psi_I \frac{\int O_i \exp(-\rho_i r_i^2 - i\boldsymbol{\lambda}_i . \mathbf{r}_i)\, d\mathbf{r}_i}{\int \exp(-\rho_i r_i^2 - i\boldsymbol{\lambda}_i . \mathbf{r}_i)\, d\mathbf{r}_i}, \quad \ldots\ldots(12)$$

where ρ_i and $\boldsymbol{\lambda}_i$ are independent of the operator O and depend on a and $\mathbf{k}_i$ respectively. In this integral, I, the coordinates $\mathbf{r}$ are referred to the centre of mass of the system and integration over the centre-of-mass coordinate is omitted since this gives only a constant factor, after ensuring conservation of momentum. Thus

$$W = |\int \psi_F^* \psi_I|^2 \times \text{an expression which depends on the interaction } G. \quad \ldots\ldots(13)$$

This separation makes it possible to compare the energy spectra obtained from different interactions not only with each other but with a standard spectrum given by

$$W_0 = |\int \psi_F^* \psi_I|^2. \quad \ldots\ldots(14)$$

To obtain these expressions W one must first determine the meson wave function $\psi(\mathbf{r})$ which occurs in G. The meson is considered to be in the lowest Bohr orbit about the nucleus before capture; the wave function for this orbit, $\exp(-\gamma r)$, which was used in our earlier calculations (Ruddlesden and Clark 1949) should be modified to take into account the spread of charge over the nucleus. The wave function now used behaves like $\exp(-\gamma r)$ at large $\mathbf{r}$ but inside the nucleus it may be written as

$$\psi(\mathbf{r}) = A - r^2 + \text{higher terms}; \quad \ldots\ldots(15)$$

the higher terms make little contribution to the result and are neglected.

§ 3. DISINTEGRATION OF ^{3}He AND ^{4}He

The individual cases will now be dealt with in more detail, starting with ^{3}He which can disintegrate in only two ways, viz.

$$^3\text{He} + \pi^- \rightarrow {}^1\text{H} + 2\text{n} \quad \text{and} \quad {}^3\text{He} + \pi^- \rightarrow {}^2\text{H} + \text{n}.$$

Applying the method and wave functions of the previous section to the first of these gives, for final states in which the proton has momentum $\hbar\mathbf{k}_1$ and the neutrons have momenta $\hbar\mathbf{k}_2$ and $\hbar\mathbf{k}_3$, for interaction G_1: $W_1 = I_2^2 + I_3^2 + (I_2 - I_3)^2$ where I_i is defined as

$$I_i = \int \psi_F^* O_{1i} \psi_I, \text{ where } O_{1i} = \psi(\mathbf{r}_i) \quad \ldots\ldots(16)$$

and, for interaction G_2: $W_2 = \mathbf{J}_2^2 + \mathbf{J}_3^2 + (\mathbf{J}_2 - \mathbf{J}_3)^2$, where

$$\mathbf{J}_i = \int \psi_F^* \mathbf{O}_{2i} \psi_I, \text{ with } \mathbf{O}_{2i} = \nabla_i \psi(\mathbf{r}_i). \quad \ldots\ldots(17)$$

On integration the standard expression W_0 becomes

$$W_0 = \left| \int \psi_F^* \psi_I \right|^2 = \frac{(2\pi)^6}{V^2 3^3 \beta^6} \exp\left(-\frac{1}{\beta} \sum_1^3 k_i^2 \right), \text{ writing } \beta = 6a,$$

$$= \frac{(2\pi)^6}{V^2 3^3 \beta^6} \exp\left(-\frac{2ME}{\hbar^2 \beta} \right) \quad \text{since } \sum_1^3 \frac{\hbar^2 k_i^2}{2M} = E,$$

where M is the mass of a nucleon.

To obtain the proton energy spectra these expressions for W must be integrated over the density of states $d\rho_E$ which, since conservation of momentum allows the elimination of one variable ($\mathbf{k}_3$), is given by

$$d\rho_E\, dE = \left(\frac{V}{8\pi^3}\right)^2 d\mathbf{k}_1\, d\mathbf{k}_2. \qquad \ldots\ldots(18)$$

We may now write $$\int W\, d\rho_E = \frac{V^2}{(2\pi)^6} \int d\mathbf{k}_1 \frac{d}{dE} \int W\, d\mathbf{k}_2,$$

the region of integration being $k_1^2 + k_2^2 + \mathbf{k}_1.\mathbf{k}_2 \leqslant ME/\hbar^2$. Thus the spectrum of the proton energy $\epsilon_1 = \hbar^2 k_1^2/2M$ is given by

$$P(\epsilon_1)\, d\epsilon_1 \propto \epsilon_1^{1/2}\, d\epsilon_1 \frac{d}{dE} \int W\, d\mathbf{k}_2.$$

The proton spectra obtained from the above expressions W_0, W_1 and W_2 and normalized to the same value are shown in Figure 1.

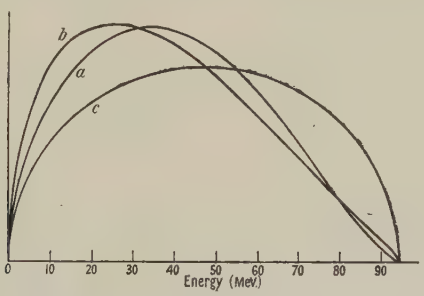

Figure 1. Energy spectrum of protons from $^3\mathrm{He} + \pi^- \rightarrow {}^1\mathrm{H} + 2\mathrm{n}$: *a*, scalar meson; *b*, pseudo-scalar meson ; *c*, ' standard '.

A typical wave function to describe the alternative process of deuteron emission is

$$\Psi_F = (3!)^{-1/2} \sum_{ijk} \psi_{ijk} \alpha_i \alpha_j \beta_k \eta_i \xi_j \xi_k \epsilon_{ijk},$$

where $$\psi_{ijk} = V^{-1/2} \left(\frac{2a}{\pi}\right)^{3/4} \exp\{-ar_{ij}^2 + \tfrac{1}{2}i\mathbf{k}.(\mathbf{r}_i + \mathbf{r}_j) - i\mathbf{k}.\mathbf{r}_k\},$$

with spatial part $\psi_F = \psi_{123}$. Integrating the matrix elements for this process over the spin variables and summing over all final states with deuteron momentum $\hbar\mathbf{k}$ gives $W_1 = 3I_1^2/2$ and $W_2 = \frac{1}{2}\mathbf{J}_1^2 + \mathbf{J}_2^2 + (\mathbf{J}_1 - \mathbf{J}_2)^2$, where I_i and $\mathbf{J}_i$ are again defined by equations (16) and (17). On integration, the standard expression W_0 for deuteron emission becomes

$$W_0 = \frac{2^6\pi^6}{V5^3\beta^6} \left(\frac{\beta}{3\pi}\right)^{3/2} \exp(-2ME/\hbar^2\beta), \text{ again writing } \beta = 6a.$$

For two-particle emission $d\rho_E\, dE = \{V/(2\pi)^3\}\, d\mathbf{k}$; only one deuteron energy is permitted and its probability, $\int W\, d\rho_E$, is compared with the probability of proton emission. The expressions W_1, W_2 and W_0 above give the relative probability of proton to deuteron emission as 23 : 1 (scalar interaction), 125 : 1 (pseudo-scalar interaction), and 60 : 1 (by integrating W_0 over the density of states) respectively.

^{4}He can disintegrate in three ways, viz.

$$^4\mathrm{He} + \pi^- \rightarrow {}^1\mathrm{H} + 3\mathrm{n}, \quad {}^4\mathrm{He} + \pi^- \rightarrow {}^2\mathrm{H} + 2\mathrm{n}, \quad {}^4\mathrm{He} + \pi^- \rightarrow {}^3\mathrm{H} + \mathrm{n}.$$

The ^{4}He wave function is

$$\Psi_{\alpha \mathrm{I}} = (4!)^{-1/2} \exp\left(-a\sum_1^4 r_{ij}^2\right) \sum_{ijkl} \alpha_i\alpha_j\beta_k\beta_l\eta_i\xi_j\eta_k\xi_l\epsilon_{ijkl}, \quad \ldots\ldots(19)$$

with spatial part

$$\psi_{\alpha \mathrm{I}} = \exp\left(-a\sum_1^4 r_{ij}^2\right). \quad \ldots\ldots(20)$$

A typical final wave function is

$$\Psi_{\alpha \mathrm{F}} = (4!)^{-1/2} \sum_{ijkl} \psi_{ijkl}\alpha_i\alpha_j\beta_k\beta_l\eta_i\xi_j\xi_k\xi_l\epsilon_{ijkl}, \quad \ldots\ldots(21)$$

with spatial part

$$_\alpha\psi_{\mathrm{F}} = \psi_{1234}, \quad \ldots\ldots(22)$$

where for example

$\psi_{ijkl} = V^{-3/2} \exp\{i(\mathbf{k}_1.\mathbf{r}_i + \mathbf{k}_2.\mathbf{r}_j + \mathbf{k}_3.\mathbf{r}_k + \mathbf{k}_4.r_l)\}$ for proton emission,

$\psi_{ijkl} = V^{-1}\left(\frac{2a}{\pi}\right)^{3/4} \exp\{-ar_{ij}^2 + \frac{1}{2}i\mathbf{k}_1.(\mathbf{r}_i + \mathbf{r}_j) + i(\mathbf{k}_2.\mathbf{r}_k + \mathbf{k}_3.\mathbf{r}_l)\}$ for deuteron emission,

$\psi_{ijkl} = V^{1/2}\left(\frac{2a\sqrt{3}}{\pi}\right)^{3/2} \exp\{-a(r_{ij}^2 + r_{jk}^2 + r_{ki}^2) + \frac{1}{3}i\mathbf{k}_1.(\mathbf{r}_i + \mathbf{r}_j + \mathbf{r}_k) + i\mathbf{k}_2.\mathbf{r}_l\}$ for triton emission.

For each mode of disintegration the expressions W_1, W_2 and W_0 corresponding to final states in which the charged particle has momentum $\hbar\mathbf{k}_1$ are evaluated, giving for proton emission

$$W_1 = 2\{(I_2 - I_3)^2 + (I_3 - I_4)^2 + (I_2 - I_4)^2\}, \quad \ldots\ldots(23)$$

$$W_2 = 2\{(\mathbf{J}_2 - \mathbf{J}_3)^2 + (\mathbf{J}_3 - \mathbf{J}_4)^2 + (\mathbf{J}_2 - \mathbf{J}_4)^2\}, \quad \ldots\ldots(24)$$

$$W_0 = \left|\int \psi_{\alpha \mathrm{F}}^* \psi_{\alpha \mathrm{I}}\right|^2 = \frac{8\pi^9}{V^3\alpha^9} \exp\left(-\frac{2ME}{\hbar^2\alpha}\right), \quad \ldots\ldots(25)$$

writing $\alpha = 8a$ and

$$E = \text{kinetic energy available in final state} = \sum_1^4 \frac{\hbar^2 k_i^2}{2M},$$

where, as before,

$$I_i = \int \psi_{\alpha \mathrm{F}}^* O_{1i} \psi_{\alpha \mathrm{I}} \text{ with } O_{1i} = \psi(\mathbf{r}_i) \text{ and } \mathbf{J}_i = \int \psi_{\alpha \mathrm{F}}^* \mathbf{O}_{2i} \psi_{\alpha \mathrm{I}} \text{ with } \mathbf{O}_{2i} = \nabla_i \psi(\mathbf{r}_i);$$

for deuteron emission

$$W_1 = 3(I_3 - I_4)^2, \quad \ldots\ldots(26)$$

$$W_2 = (2\mathbf{J}_1 + \mathbf{J}_3 + \mathbf{J}_4)^2 + 2(\mathbf{J}_3 - \mathbf{J}_4)^2, \quad \ldots\ldots(27)$$

$$W_0 = V^{-2}\left(\frac{2}{3}\right)^3 \left(\frac{\pi}{\alpha}\right)^{15/2} \exp\left(-\frac{2ME}{\hbar^2\alpha}\right); \quad \ldots\ldots(28)$$

for triton emission

$$W_1 = 2(I_1 - I_4)^2, \quad \ldots\ldots(29)$$

$$W_2 = 2(\mathbf{J}_1 - \mathbf{J}_4)^2, \quad \ldots\ldots(30)$$

$$W_0 = V^{-1}(12)^{3/2}\left(\frac{2\pi}{7\alpha}\right)^6 \exp\left(-\frac{2ME}{\hbar^2\alpha}\right). \quad \ldots\ldots(31)$$

From these expressions the relative probabilities of proton, deuteron or triton emission are found to be

140 : 15 : 1 for scalar interaction G_1,
450 : 20 : 1 for pseudo-scalar interaction G_2,
320 : 30 : 1 by integrating W_0 over the density of states. $\quad \ldots\ldots(31\,a)$

It appears that the probability of triton emission is very small and that proton emission will predominate. If the deuteron radius is increased by replacing, in its wave function, a by a' ($<a$) the only result is an alteration in the probability of deuteron emission, from ^{4}He, by a factor $(a'/a)^{3/2}(2/3+a'/3a)^{-3}$—putting $a'=\frac{1}{2}a$ reduces this probability by about 40%. The proton energy spectrum $P(\epsilon_1)\propto\epsilon_1^{1/2}\int W\,d\mathbf{k}_2\,d\mathbf{k}_3$ for each expression W_0, W_1 and W_2 is shown in Figure 2. The corresponding neutron spectra are shown in Figure 3; these show a stronger dependence on the meson interaction but the neutron spectrum would presumably be more difficult to determine experimentally than would the proton spectrum.

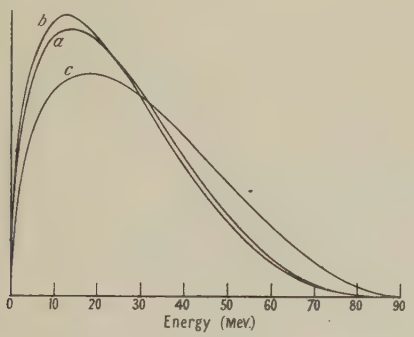

Figure 2. Energy spectrum of protons from $^4\mathrm{He}+\pi^-\rightarrow{}^1\mathrm{H}+3\mathrm{n}$:

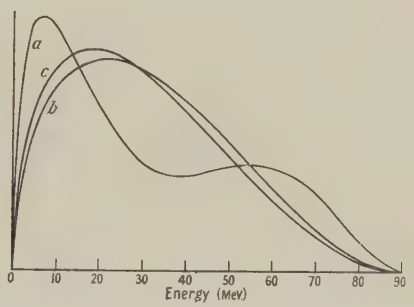

Figure 3. Energy spectrum of neutrons from $^4\mathrm{He}+\pi^-\rightarrow{}^1\mathrm{H}+3\mathrm{n}$:

a, scalar meson ; *b*, pseudo-scalar meson ; *c*, 'standard'.

§ 4. DISINTEGRATION OF ^{12}C AND ^{16}O

The calculations are now extended to cover the disintegration of carbon (or oxygen) into two (or three) α-particles and one singly charged particle by ascribing an α-particle structure to these nuclei. As the use of totally antisymmetric wave functions for these nuclei would involve too much labour, in this treatment the interchange of nucleons between α-particles is neglected; this is equivalent to assuming that the time required for the disintegration to take place is short compared with the lifetime of an α-particle in the nucleus. The wave function used to describe such a carbon nucleus is

$$\Psi_{\mathrm{CI}}=\Psi_\alpha^{\,1}\Psi_\alpha^{\,2}\Psi_\alpha^{\,3}\exp\left(-b\sum_1^3 R_{ij}^{\,2}\right), \qquad \ldots\ldots(32)$$

where R_{ij} is the distance between the centres of the ith and jth α-particles, b is a constant and $\Psi_\alpha^{\,i}$ is the ^{4}He wave function of the last section (equation (19)). The final wave function to describe the disintegration into two α-particles and a singly charged particle is

$$\Psi_{\mathrm{CF}}=\Psi_\alpha^{\,1}\Psi_\alpha^{\,2}\Psi_{\alpha\mathrm{F}}^{\,3}\exp\{i(\boldsymbol{\chi}_1\cdot\mathbf{R}_1+\boldsymbol{\chi}_2\cdot\mathbf{R}_2)\}, \qquad \ldots\ldots(33)$$

where $\hbar\boldsymbol{\chi}_1$ and $\hbar\boldsymbol{\chi}_2$ are the momenta of the α-particles and $\Psi_{\alpha\mathrm{F}}$ is given by equation (21). In this case $\Sigma_1^3\mathbf{r}_i=4\mathbf{R}_3$ and $\Sigma_1^3\mathbf{k}_i=\boldsymbol{\chi}_3$; conservation of momentum gives $\Sigma_1^3\boldsymbol{\chi}_i=0$ and reference to the centre of mass gives $\Sigma_1^3\mathbf{R}_i=0$. Corresponding wave functions and relations hold for nuclei containing more than three α-particles. The interactions G_1 and G_2 are just as before and each matrix element

$$H=\int\Psi_{\mathrm{CF}}^{*}G\Psi_{\mathrm{CI}}=V^{-1}\int\exp\{-i(\boldsymbol{\chi}_1\cdot\mathbf{R}_1+\boldsymbol{\chi}_2\cdot\mathbf{R}_2)\}\Psi_{\alpha\mathrm{F}}^{*}G\Psi_{\alpha\mathrm{I}}\exp\left\{-b\sum_1^3 R_{ij}^{\,2}\right\},$$

omitting the α-particle normalization factors. Similarly, for the disintegration of a nucleus composed of n α-particles into $n-1$ free α-particles and a singly charged particle,

$$H = V^{-(n-1)/2} \int \exp\left(-i \sum_1^{n-1} \boldsymbol{\chi}_i \cdot \mathbf{R} - b \sum_1^{n} R_{ij}^2\right) \Psi_{\alpha F}^* G \Psi_{\alpha I}. \quad \ldots\ldots(34)$$

This differs from the matrix element for the corresponding helium disintegration only in the space functions; thus integration over the spin variables and summation over the final states gives the same expressions for W_1 and W_2 as previously (equations (23), (24); (26), (27); (29), (30)) where I_i and $\mathbf{J}_i$ are now expressed in terms of the wave functions

$$\psi_I = \exp\left(-b \sum_1^{n} R_{ij}^2\right) \psi_{\alpha I} \quad \text{and} \quad \psi_F = V^{-(n-1)/2} \exp\left(i \sum_1^{n-1} \boldsymbol{\chi}_i \cdot \mathbf{R}_i\right) \psi_{\alpha F}.$$

Evaluation of $W_0 = |\int \psi_F^* \psi_I|^2$ for the three modes of disintegration considered gives

$$W_0 = V^{-(n+2)} \alpha^{-3} Q \text{ for proton emission,} \quad \ldots\ldots(35)$$

$$W_0 = V^{-(n+1)} \{3\sqrt{(\alpha\pi)}\}^{-3} Q \text{ for deuteron emission,} \quad \ldots\ldots(36)$$

$$W_0 = V^{-n} (7^2\pi/4\sqrt{3})^{-3} Q \text{ for triton emission,} \quad \ldots\ldots(37)$$

where

$$\left.\begin{aligned} Q &= \left[\frac{4c\pi^{n+2}}{n\alpha(2c\alpha)^n}\right]^3 \exp\left(-\frac{2ME}{\hbar^2\alpha} - \gamma x\right), \\ \alpha &= 8a, \quad 0 \leqslant \frac{\hbar^2}{8ME} \sum_1^n \chi_i^2 = x \leqslant 1, \quad c = \frac{nb}{2\alpha}, \end{aligned}\right\} \quad \ldots\ldots(38)$$

and

$$\gamma = \frac{1-c}{c} \frac{2ME}{\hbar^2\alpha}. \quad \ldots\ldots(39)$$

This important factor W_0 is no longer constant as in the helium case but depends on the way the meson rest energy is shared between the kinetic energy of the centre of mass of all the α-particles and the kinetic energy relative to its centre of mass of the split α-particle. The extent of this dependence is governed by the parameter γ which is a function of the constant c occurring in the initial wave function. $0<c<1$: the lower limit corresponds to a set of free α-particles; at the upper limit the spatial part of the wave function degenerates into $\exp[-(a/n)\Sigma_1^{4n} r_{ij}^2]$ which cannot be antisymmetrized since all $4n$ nucleons are then equivalent. The wave function is not a sufficiently good approximation to allow the value of c to be determined from the nuclear radius. It is easily shown that the standard energy spectrum (i.e. the spectrum obtained from W_0) of an α-particle emitted in one of the above disintegrations is given by

$$P(\epsilon)\, d\epsilon \propto e^{-\gamma t}(1-t)^m t^{1/2}\, dt \int_0^{\gamma(1-t)} e^{-u} \left(1 - \frac{u}{\gamma(1-t)}\right)^m u^{3n/2-4}\, du, \quad \ldots\ldots(40)$$

where $0 \leqslant t = n\epsilon/(n-1)E \leqslant 1$, ϵ is the energy of the α-particle, n is the number of α-particles in the initial nucleus and $m = 7/2$, 2 or $1/2$ according as a proton, deuteron or triton is emitted. The value of E, and hence of γ, varies slightly with the particular disintegration considered: in the case of proton emission from carbon $c = 1/2$ gives $\gamma \simeq 12$. The α-spectrum for this disintegration is shown in Figure 4 for various values of γ. For $\gamma = 12$ the α-spectra of W_1 and W_2 have also been calculated and are found to be indistinguishable from one another numerically: these and the corresponding standard spectrum are shown in Figure 5, together with a comparison spectrum of $W =$ constant. Using the same

value of γ ($=12$) for carbon, oxygen and neon the standard α-spectra of the disintegration of these elements with proton emission are, numerically, almost identical. The carbon and oxygen α-spectra for $c=1/2$ are found to be in fair agreement with the experimental results of M.M.R. The relative probabilities

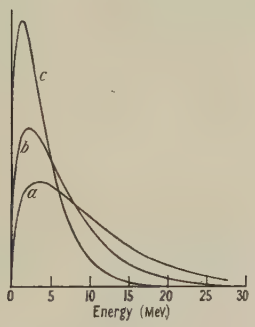

Figure 4. 'Standard' energy spectrum of α-particles from $^{12}C+\pi^- \rightarrow 2^4He+^1H+3n$: *a*, $\gamma=6$; *b*, $\gamma=12$; *c*, $\gamma=24$.

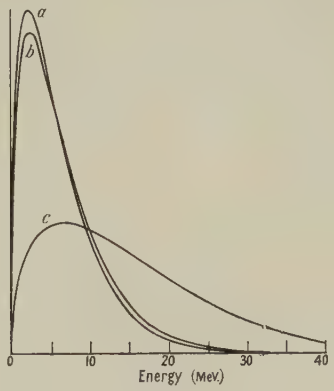

Figure 5. Energy spectrum of α-particles from $^{12}C+\pi^- \rightarrow 2^4He+^1H+3n$ with $\gamma=12$: *a*, scalar and pseudo-scalar mesons; *b*, 'standard'; *c*, statistical factor.

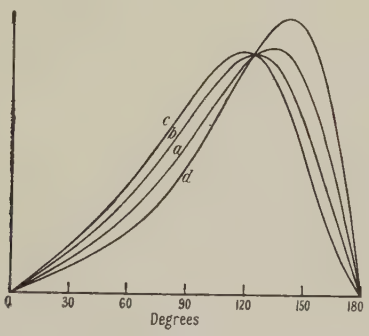

Figure 6. Angular correlation of α-particles from $^{12}C+\pi^- \rightarrow 2\,^4He+^1H+3n$: *a*, *b*, *c*, scalar meson with $\gamma \simeq 0$, 12, ∞ respectively; *d*, pseudo-scalar meson and 'standard' (all γ).

of proton, deuteron or triton emission given by W_0 for $\gamma_{\text{proton}}=12$ are: carbon 118:16:1, oxygen 67:13:1. The dependence of these ratios on the value of γ and on the type of interaction considered is shown in the Table, which gives the probability of proton emission relative to that of triton emission from carbon (in processes in which two α-particles are also emitted).

γ	(0)	6	12	24	(∞)
scalar	(54)	78	102	153	(187)
pseudo-scalar	(50)	102	174	238	(343)
'standard'	(17)	68	118	169	(205)

When more than one charged particle is emitted in a disintegration the angle between two such particles can be measured and the distribution of this angle may be found. In the disintegration

$$^{12}C+\pi^- \rightarrow 2\,^4He+^1H+3n \qquad \ldots\ldots(41)$$

the angular correlation of the two α-particles is given by

$$N(\theta)\,d\theta = d\theta \int W\,d\rho_E'', \qquad \ldots\ldots(42)$$

where $d\rho_E'' \, d\theta = d\rho_E$ and θ is the angle between the two α-particles. W_0 and W_2 are independent of the distribution of kinetic energy amongst the three α-particles and this leads to angular distributions identical with that for a constant matrix element. W_1 depends on the kinetic energy of the centre of mass of the split α-particle and yields an angular distribution somewhat different from the standard case and depending, slightly, on c. Figure 6 shows the variation of $N_1(\theta)$ with c and the standard $N_0(\theta)$ for this disintegration. Preliminary experimental results, communicated by Rochat (private communication), are as follows:

Angle θ (deg.)	0–30	30–60	60–90	90–120	120–150	150–180
No. of events $N(\theta)$	5	12	7	6	11	1

§ 5. INDIRECT DISINTEGRATION OF ^{12}C

The scheme (41) is not the only one which can describe the disintegration of ^{12}C on a simple α-particle model; an intermediate state may be involved, represented by

$$\left.\begin{aligned} {}^{12}\mathrm{C} + \pi^- &\rightarrow {}^{8}\mathrm{Be}^* + {}^{1}\mathrm{H} + 3\mathrm{n}, \\ {}^{8}\mathrm{Be}^* &\rightarrow 2\ {}^{4}\mathrm{He}. \end{aligned}\right\} \qquad \ldots\ldots(43)$$

An analogous scheme has been suggested by Telegdi and Zünti (1950) to explain the experiments on the photo-disintegration of ^{12}C into three α-particles. They obtained agreement with the measured α-particle energy spectrum by assuming that the only state of ^{8}Be involved was the excited state at 3 MeV. With the same assumption it is possible to calculate the energy spectrum and angular correlation of the α-particles produced by process (43). The results of the previous section show that it is possible to neglect the meson interaction and also the spins of the nucleons when calculating the α-spectrum for process (41). This should also be true when an intermediate state is involved.

Taking the wave function of the intermediate state to be

$$\phi_{\mathrm{F}} = V^{-2} \exp\left(i \sum_1^4 \mathbf{k}_j \,.\, \mathbf{r}_j + i\mathbf{k} \,.\, \mathbf{R}\right) \phi(\boldsymbol{\rho}) \psi_\alpha{}^1 \psi_\alpha{}^2, \qquad \ldots\ldots(44)$$

where $\hbar\mathbf{k}$ is the momentum of $^{8}Be^*$, $\mathbf{R}$ its centre of gravity and $\phi(\boldsymbol{\rho})$ its internal wave function ($\boldsymbol{\rho}$ is the distance between the α-particles composing $^{8}Be^*$), leads to

$$W_0 = \pi^{12} N^2 V^{-4} (6c\alpha^4)^{-3} \exp\left(-\frac{2ME}{\hbar^2\alpha} - \frac{3}{8\alpha}\,\frac{1-c}{c}\,k^2\right), \qquad \ldots\ldots(45)$$

where $$N = \int \phi(\boldsymbol{\rho}) \exp\left(-c\alpha\rho^2\right) d\boldsymbol{\rho}.$$

Choosing the value $c = 1/2$, the probability of process (43) relative to that of (41) is found to be $0{\cdot}1\ N^2\alpha^{3/2}$. The value of N depends on the spin of $^{8}Be^*$, which according to Wheeler (1941) is 0. Thus, taking the $^{8}Be^*$ wave function as

$$\phi(\boldsymbol{\rho}) = (\mu/\pi)^{3/2} \exp\left(-\mu\rho^2\right), \qquad \ldots\ldots(46)$$

the relative probability is of order 20% for reasonable values of $\mu(\sim\alpha)$. More recently, scattering experiments (reviewed by Hornyak *et al.* 1950) indicate that $^{8}Be^*$ has spin 1 or 2; our assumptions would then give $N = 0$. This does not mean that process (43) is forbidden, for slight changes in the model adopted would give non-vanishing values of N. The relative probability should however be much less than the 20% found for spin zero.

The distribution of energy ϵ of the α-particles is found to be

$$P(\epsilon)\,d\epsilon = d\epsilon \int g(v)v^{-1}\,dv, \qquad \ldots\ldots(47)$$

the limits of integration being $v=(2M)^{-1/2}\,|\sqrt{(U/2)} \pm \sqrt{\epsilon}|$, where U is the excitation energy of the ^{8}Be*, v is its velocity and $g(v)\,dv$ its velocity distribution. Figure 7 shows this α-spectrum for $c=1/2$ and $c\to 1$; agreement with experiment is only obtained for the latter case. The angular correlation of the α-particles from this process is shown in Figure 8.

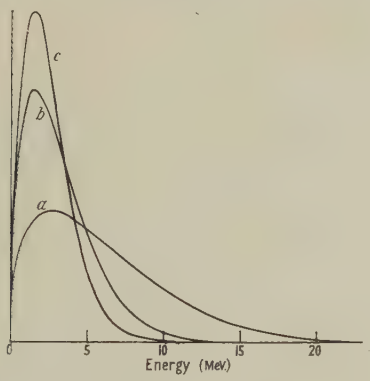

Figure 7. 'Standard' energy spectrum of α-particles from $^{12}C+\pi^-\to{}^8Be^*+{}^1H+3n$; $^8Be^*\to 2\,{}^4He$: a, $\gamma\simeq 0$; b, $\gamma=12$; c, $\gamma=24$.

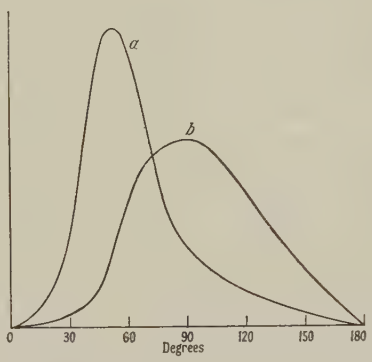

Figure 8. 'Standard' angular correlation of α-particles from $^{12}C+\pi^-\to{}^8Be^*+{}^1H+3n$; $^8Be^*\to 2\,{}^4He$: a, $\gamma\simeq 0$; b, $\gamma=12$.

§ 6. DISCUSSION

In the previous sections the energy spectra of particles emitted from the nuclei ^{3}He, ^{4}He and ^{12}C as a result of π-meson capture have been determined for the meson–nucleon interactions $\psi(\mathbf{r})$ and $\boldsymbol{\sigma}.\nabla\psi(\mathbf{r})$. These were compared in each case with a standard spectrum, which is independent of the meson interaction and depends only on the nuclear wave functions assumed and on the statistical (phase-space) factor. The standard spectrum neglects the antisymmetry properties of the wave functions, which would cause a reduction of intensity at the high-energy end of the spectrum with a corresponding increase of intensity at low energies : such a deviation from the standard is noticed in all other spectra.

In the cases of ^{3}He and ^{4}He the standard matrix element is a constant, independent of the way the kinetic energy is shared amongst the emitted particles, so the standard spectrum is just the statistical one. The dependence of the proton spectra of ^{3}He and ^{4}He (Figures 1 and 2) on the meson interaction is probably not sufficient to enable experiment to distinguish between the two interactions. Observations on the neutrons emitted from ^{4}He, whose spectrum (Figure 3) depends considerably on the meson interaction, would probably be necessary.

In the case of ^{12}C, which was treated on an α-particle model, the standard spectrum (Figure 4) depends on the parameter γ, which represents the degree of binding of the α-particles in the nucleus. (The limit $\gamma=0$, representing such strong binding that the α-particles are no longer distinguishable, gives the statistical spectrum.) γ may also be used to determine the radius of the carbon nucleus. For a nucleus composed of n α-particles, by integrating the square of

its wave function over the coordinates of all but one of the nucleons, the density of nuclear matter is found to be

$$\rho(r) \propto \exp\left(-\frac{4nc\alpha r^2}{n-1+3nc}\right) = \exp\left(-2r^2/R_n^2\right), \qquad \ldots\ldots(48)$$

defining $R_n^2 = (n-1+3nc)/2nc\alpha$. Thus $R_n/R_1 = \{(n-1+3nc)/3nc\}^{1/2}$. If we use the value $c = 1/2$, which gives agreement with the experiments of M.M.R., we find $R_C/R_{He} = 1{\cdot}20$, compared with the value 1·44 obtained from the formula $R_n \propto A^{1/3} \propto n^{1/3}$. This rather poor agreement must be attributed to the fact that gaussian wave functions cannot represent simultaneously both the nuclear radius and the average kinetic energy of the α-particles in the nucleus.

The α-particle energy spectra (Figure 5) from ^{12}C (or ^{16}O) do not distinguish between the two meson interactions. This is not very surprising since the form of the matrix elements (equation (34)) shows that the interaction only affects the momenta of the free nucleons relative to the split α-particle and this can be expected to reflect little in the energy spectra of the other α-particles. The deviation of these α-spectra from the standard spectrum may be considered as due solely to the antisymmetry properties of the wave functions. In the centre-of-mass system of the split α-particle the energy of the proton (or neutron) relative to the total energy in this system has the same spectrum as in the ^4He case (exactly in the case of the standard and pseudo-scalar spectra and approximately in the case of the scalar spectrum). The proton energy spectrum in the usual system (centre of mass of all nucleons at rest) requires the inclusion of integrations over the momenta of the α-particles and is expected to show even less dependence on the meson interaction.

The pseudo-scalar interaction and the standard matrix element give the same distribution of the angle between the two α-particles emitted in the direct disintegration of ^{12}C (Figure 6) and this is independent of the parameter c. The angular distribution due to the scalar interaction depends slightly on c and differs somewhat from the standard.

In § 5 the possibility of the indirect disintegration of ^{12}C involving the 3 MeV. excited state of ^8Be was considered. The (standard) α-particle energy spectrum obtained on this assumption (Figure 7) agrees with the experiments of M.M.R. only for $c \simeq 1$, which is the strong-binding limit of the α-particle model used. Thus the indirect process alone is insufficient to account for the observed energy spectrum which may, however, be reproduced, within the limits of experimental error, by increasing the value of c beyond 1/2 and by assuming a corresponding proportion of indirect splitting. The (standard) angular correlation of the α-particles emitted by this indirect process (Figure 8) depends considerably on the value of c. The difference between the angular distributions of the direct and indirect processes should be sufficient to allow an experiment to determine the relative amounts of the two processes and the corresponding value of c. Preliminary measurements by Rochat (private communication), quoted above, suggest that many of the observed disintegrations follow the indirect process. As indicated in § 5 the simple α-particle model used here is not sufficient to estimate the probability of the indirect process since it gives zero unless the spin of $^8Be^*$ is zero, which is probably not the case. It would be desirable to have an independent estimate of the relative probability of the two processes: this, used in conjunction with the observed energy spectrum, would

determine the value of c required. With this information the angular correlations and the proton and neutron energy spectra could be determined uniquely.

The values of the relative probabilities of emission of the various charged particles cannot be relied upon in the same way as can the spectra since, although these values are independent of the intensity of the meson interaction, and the term $\exp(-2ME/\hbar^2\alpha)$ which appears in the total probabilities is eliminated, the ratio of proton to triton probabilities, for instance, involves a factor $\alpha^{-3} \propto R_{\mathrm{He}}{}^6$ and the radius of the ^{4}He nucleus is not known very exactly.

It is interesting to note that the use of wave functions for ^{3}H and ^{4}He of the type suggested by Irving (1951), which have approximately the correct asymptotic form, leads to nearly the same relative probabilities as (31 *a*). Putting $n=0$ and fixing α in each case by the binding energy (n and α are defined in Irving's paper) and neglecting the meson interaction, the relative probabilities of triton, deuteron and proton emission from ^{4}He are 1 : 20 : 320.

As pointed out by Yamaguchi (1950) it is possible to apply Fermi's (1950) theory of high-energy nuclear events, which Fermi himself describes as the opposite extreme to the perturbation theory approach, to the disintegrations here considered. This theory supposes that energy, here equal to the mass of the π-meson, is suddenly released in the nuclear volume Ω and that statistical equilibrium is reached. This gives the square of the effective matrix element for s emitted particles as $(\Omega/V)^{s-1}$, where V is the normalization volume and momentum is conserved. This is independent of any interaction and may be compared with the standard expression W_0 of this paper, which is an approximation, independent of interaction, to the square of the matrix elements given by first order perturbation theory. The Fermi expression $(\Omega/V)^{s-1}$, being independent of energy, would give purely statistical energy spectra in all cases. In the cases of ^{3}He and ^{4}He therefore, the energy spectra obtained by the two methods agree. It has been shown by M.M.R. that the observed α-spectra of ^{12}C, ^{14}N and ^{16}O do not agree with the corresponding statistical spectra, whereas they may be explained by the perturbation method. The relative probability of proton to triton emission given by Fermi's method depends on $\Omega^2 \propto R^6$ as in the perturbation method, but using $\Omega = 4\pi R^3/3$ with $R = A^{1/3} \times 1{\cdot}4 \times 10^{-13}$ cm. gives equal probabilities of proton and triton emission from both ^{4}He and ^{12}C.

We conclude that for a very light nucleus (^{4}He) the disintegration is practically independent of the details of the nuclear structure but depends on the meson interaction to a certain extent. For slightly heavier nuclei (^{12}C) the disintegration depends strongly on the nuclear structure and only weakly on the meson interaction. The disintegrations of heavy nuclei (^{108}Ag) can, as is well known, be described by the evaporation theory and are independent of both meson interaction and nuclear structure.

APPENDIX

All the matrix elements occurring in this paper can be expressed in terms of integrals of the type

$$I_n = \int O_n \exp\left\{-\sum_{i,j}^{n} b_{ij}\mathbf{r}_i \cdot \mathbf{r}_j - i\sum_{j}^{n} \mathbf{p}_j \cdot \mathbf{r}_j\right\} d\mathbf{r}_1 \ldots . d\mathbf{r}_n. \quad \ldots\ldots (49)$$

Here we have put $\Sigma_1^{n+1} m_i \mathbf{r}_i = 0$ and $\mathbf{p}_j = \mathbf{k}_j - \mathbf{k}_{n+1} m_j/m_{n+1}$ (m_i = mass of ith particle; for He, m_i = nucleon mass M, for C, $m_i = M$ or $4M$). We have omitted the

constant factor due to integration over the centre-of-mass coordinate and require $\Sigma_1^{n+1}\mathbf{k}_i=0$. The equality

$$\int \exp\{-br^2-i\mathbf{p}.\mathbf{r}\}\,d\mathbf{r}=(\pi/b)^{3/2}\exp(-p^2/4b)$$

can be applied successively to the integrations over $\mathbf{r}_1 \ldots . \mathbf{r}_{n-1}$ leaving an integral of the form

$$\int O_n(\mathbf{r}_n)\exp\{-\alpha_n r_n{}^2-i\boldsymbol{\lambda}_n.\mathbf{r}_n)d\mathbf{r}_n$$

and it is obvious that α_n and $\boldsymbol{\lambda}_n$ do not depend on $O(\mathbf{r})$. I_n can be expressed simply in terms of the symmetrical determinant $B=|b_{ij}|$, with cofactors B_{ij}.

$$I_n=\frac{\pi^{3n/2}}{B^{3/2}}\exp\left\{\frac{-1}{4B}\sum_{i,j}^{n}B_{ij}\mathbf{p}_i\cdot\mathbf{p}_j\right\}\left\{\frac{\int O_n(\mathbf{r})\exp(-\alpha_n r^2-i\boldsymbol{\lambda}_n.\mathbf{r})d\mathbf{r}}{\int\exp(-\alpha_n r^2-i\boldsymbol{\lambda}_n.\mathbf{r})\,d\mathbf{r}}\right\}, \qquad \ldots\ldots(50)$$

where $\alpha_n=B/B_{nn}$ and $\boldsymbol{\lambda}_n=\Sigma_1^n B_{ni}\mathbf{p}_i/B_{nn}$.

The final bracket of (50) has the values: 1, standard; $-3/2\alpha_n+\lambda_n{}^2/4\alpha_n{}^2$, scalar; $i\boldsymbol{\lambda}_n/\alpha_n$, pseudo-scalar.

ACKNOWLEDGMENTS

It is a pleasure to express our thanks to Professor H. Fröhlich for suggesting this work and for his continued interest in it, to Dr. K. J. Le Couteur for many helpful suggestions, and to Dr. O. Rochat for useful discussions and communication of his experimental results before publication. We are grateful to the Department of Scientific and Industrial Research for financial support.

REFERENCES

Aamodt, L., Hadley, J., Panofsky, W. K. H., and Phillips, R., 1950, *Phys. Rev.*, **80**, 94, 282.
Bjorkland, R., Crandall, W. E., Mayer, B. J., and York, H. F., 1950, *Phys. Rev.*, **77**, 213.
Bohr, N., and Kalckar, F., 1937, *K. Danske Vidensk. Selsk. Mat.-phys. Medd.*, **24**, 10.
Bruno, B., 1948, *Ark. Mat. Astr. Fys.* A, **36**, No. 8.
Fermi, E., 1950, *Progr. Theor. Phys.*, **5**, 570.
Fermi, E., and Teller, E., 1947, *Phys. Rev.*, **72**, 399.
Hornyak, W. F., Lauritsen, T., Morrison, P., and Fowler, W. A., 1950, *Rev. Mod. Phys.*, **22**, 291.
Irving, J., 1951, *Phil. Mag.*, **42**, 338.
Le Couteur, K. J., 1950, *Proc. Phys. Soc.* A, **63**, 259.
Massey, H. S. W., and Corben, H. C., 1939, *Proc. Camb. Phil. Soc.*, **35**, 84.
Menon, M. G. K., Muirhead, H., and Rochat, O., 1950, *Phil. Mag.*, **41**, 583.
Ruddlesden, S. N., and Clark, A. C., 1949, *Nature, Lond.*, **164**, 487.
Sakata, S., and Tanikawa, Y., 1939, *Proc. Phys.-Math. Soc. Japan*, **21**, 58.
Tamor, S., 1950, *Phys. Rev.*, **77**, 412.
Telegdi, V. L., and Zünti, W., 1950, *Helv. phys. Acta*, **23**, 745.
Wheeler, J. A., 1941, *Phys. Rev.*, **59**, 16.
Yamaguchi, Y., 1950, *Progr. Theor. Phys.*, **5**, 896.
Yang, C. N., 1950 a, *Phys. Rev.*, **77**, 242; 1950 b, *Ibid.*, **77**, 722.

Range–Energy Relation for Protons in Ilford C2 Dry Emulsion

By F. A. EL-BEDEWI
Nuclear Physics Research Laboratory, University of Liverpool

Communicated by H. W. B. Skinner; *MS. received* 21*st March* 1951

ABSTRACT. The range–energy relationship for protons of energies up to 12 MeV. in Ilford C2 dry emulsion has been determined with an accuracy better than 0·5% in energy. The particles were produced by bombarding a thin beryllium foil with deuterons having an energy of 8 MeV. The energy of the incident deuterons was obtained by a method which involves the measurement of the two angles of emission at which the two proton groups of longest range from the reaction $^{9}Be(d, p)^{10}Be$ have the same energy.

§ 1. INTRODUCTION

The range–energy relation for protons in Ilford C2 dry emulsion has recently been measured by Rotblat (1950, 1951) and by Catala and Gibson (1951) by making use of the elastically scattered deuterons and disintegration protons resulting from the deuteron bombardment with various gas targets. The energy of the primary deuterons was determined (Rotblat 1950) by comparing, under the same conditions, the ranges of alpha-particles from polonium, thorium C and thorium C′ with the ranges of alpha-particles scattered from the collision of the deuterons with helium at certain angles of scattering. This work was recently corrected (Rotblat 1951) in the light of a more accurate range–energy relation for particles in air (Bethe 1950) which affects the loss of energy of both the incident and emitted particles in passing through the gas filling the camera.

The present measurements were obtained independently during an investigation of the disintegration products from a thin beryllium foil exposed under vacuum conditions to the deuteron beam from the Liverpool 37 inch cyclotron. Although the results are in agreement with those of previous workers, the method of procedure is sufficiently different to make this report significant. The (d, p) reaction with beryllium is particularly suited for the determination of the range–energy relation for two reasons: (*a*) because of the large variation of the proton energy which can be obtained merely by varying the angle of observation, (*b*) because the Q-values for the two proton groups of longest range have been accurately determined by Buechner and Strait (1949) using a magnetic analyser.

The energy of the primary deuteron beam was determined by a method which involves the measurement of two angles of emission at which these two groups of protons have the same range. The range–energy relation has been obtained for protons having energies up to 12 MeV.

§ 2. EXPERIMENTAL

The camera used in this experiment has been described by Rotblat, Burrows and Powell (1951). The target was a foil of beryllium of thickness 0·325 mg/cm^2 prepared by evaporation. Two exposures were made, one with the foil at an angle of 45° with the deuteron beam for measurements at forward angles and

the other with the foil at 135° for measurements at backward angles. The plates used were Ilford type C2 with an emulsion 200 μ thick. The emulsion was dried by keeping the plates in vacuum for about 2 hours before the experiment as well as throughout the exposure. The plates were examined with a binocular microscope having a 96 × oil immersion objective and 6 × eyepiece. Histograms for the range distribution for 23 different angles ranging from $17\frac{1}{2}°$ to 150° were plotted for all accepted tracks of elastically scattered deuterons, disintegration tritons and protons. About 2,000 tracks were measured for each angle in a small area of width corresponding to a maximum variation of $\pm 30'$ in the angle.

§ 3. RESULTS

A representative spectrum for the disintegration particles at angle 30° is shown in Figure 1. An analysis of the histogram shows that groups 1 and 3 are due to protons emitted in the reaction $^{9}Be(d, p)^{10}Be$, in which the ^{10}Be nucleus

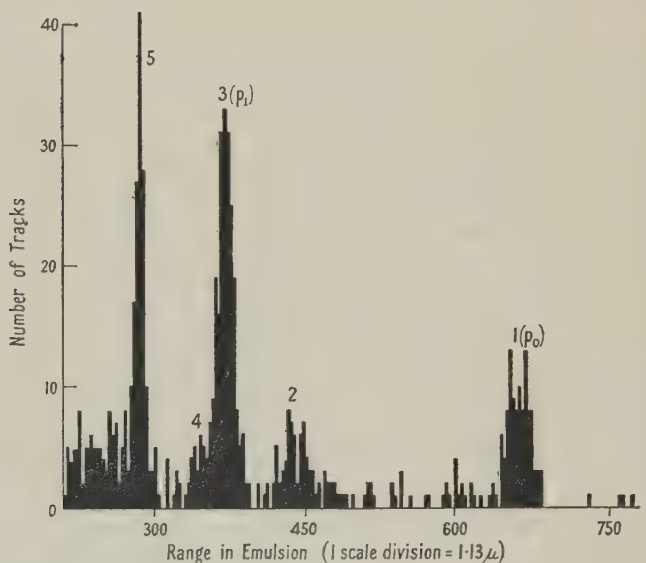

Figure 1. Histogram of disintegration products of beryllium bombarded by 7·7 MeV. deuterons at 30°.

is left in the ground state and first excited state respectively. Groups 2 and 4 are due to protons from the reaction $^{16}O(d, p)^{17}O$ with the residual nucleus formed in the ground state and first excited state. Group 5 is due to tritons from the reaction $^{9}Be(d, t)^{8}Be$ with the ^{8}Be nucleus left in its ground state.

The main target contamination was oxygen in the form of an oxide layer. Since the peaks in the spectrum due to beryllium change position with angle more rapidly than those due to contamination, it was usually possible to separate the two components. With the elastically scattered deuteron group and the proton group p_1 it was found advisable to fit their range distribution with gaussian curves from which the mean range and the half width were determined. In the case of the proton group p_0, the range was so long that it was far from disturbances due to target contamination and the mean range was calculated directly as the weighted mean of the group. These measured ranges are the projections of the true ranges on the plane of the surface of the emulsion.

The true range of a particular group was calculated from the known mean angle of approach of the particles belonging to that group to the surface of the emulsion.

The energies corresponding to these groups can be calculated from the angle of emission if the Q-values and the energy of the primary beam are known. As mentioned before, the two proton groups from beryllium have been magnetically analysed by Buechner and Strait (1949), who give accurate Q-values for these two groups as $Q_0 = 4{\cdot}576 \pm 0{\cdot}012$ MeV. and $Q_1 = 1{\cdot}201 \pm 0{\cdot}007$ MeV. The energy of the incident deuterons was calculated from the fact that the range of protons belonging to the ground state of the reaction at large angles is the same as the range of the protons from the group due to the first excited state at small angles. It was found, for example, that at an angle of 120° the group p_0 had a range of $428{\cdot}8\,\mu$ which was nearly equal to the range of the group p_1 ($429{\cdot}1\,\mu$) emitted at an angle of 17° 30′, i.e. the energy of both groups could be taken to be the same. From the two known equations in Q_0 and Q_1 the proton energy could be eliminated by a simple calculation leading to a second-power equation which could be solved to find the value of the primary deuteron energy at the effective centre of the foil. The problem was more carefully treated by plotting the variation between the range and $\cos\theta$ for the two groups in this small region. By selecting the best line which passes through these points one can find the cosines of the angles of emission for the two groups of protons of the same range, i.e. of same energy. It should be noted that the Be foil is sufficiently thin ($\sim$0·4 cm. air equivalent) for the mean energy of a group of protons to be calculated with sufficient accuracy on the assumption that the nuclear collisions occur on a plane equidistant from both surfaces of the foil. Thus, no correction was necessary for the loss of energy of protons escaping from the foil: this was approximately the same for the two groups since one was measured with the forward exposure arrangement and the other with the backward arrangement. The agreement between the results for different values of the common range are shown in Table 1.

Table 1

Common range (microns)	429	425	420	415	410	405	400
Primary deuteron energy (MeV.)	7·696	7·702	7·705	7·700	7·695	7·700	7·699

From the above results, the mean value of the energy of the deuteron beam at the centre of the foil was taken as 7·70 MeV. and used to determine the energy of the emitted particles. The accuracy of this method depends mainly on the uncertainty in the Q-values of the two proton groups. The energy of the incident deuterons was thus determined with an accuracy of within $\pm 0{\cdot}3\%$.

For the determination of proton energies for constructing the range–energy curve a correction was made at each angle of observation for the loss of energy of a proton in escaping from the foil. The stopping power of the foil material was calculated from the shift in the elastic deuteron group at 30° when the foil was in the forward and backward arrangements. The value adopted was the mean of this value and that given by Livingston and Bethe (1937), namely 0·36 cm. air equivalent for 8 MeV. deuterons. The uncertainty in the stopping power will give rise to a very small error since the energy loss of protons in the foil was only about 0·02 MeV.

The results are shown diagrammatically in Figure 2 (*a*) and (*b*) and representative data from the mean curve are given in Table 2. The experimental points were obtained mainly from the range measurements on the elastically scattered deuterons and the two groups of disintegration protons from the reaction $^{9}Be(d, p)^{10}Be$. A few points between 3·72 and 3·87 Mev. were obtained from the reaction $^{9}Be(d, t)^{8}Be$ the Q-value of which is $4{\cdot}67 \pm 0{\cdot}03$ Mev. (El-Bedewi,

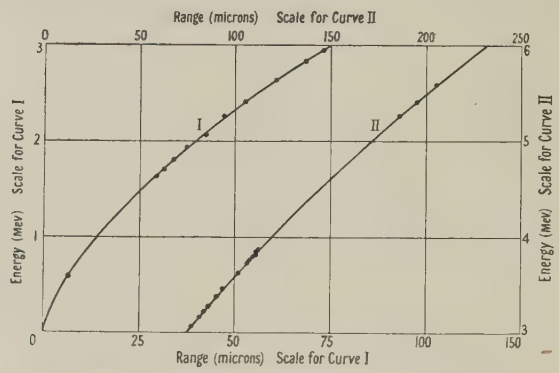
Range (microns) Scale for Curve II
Energy (Mev) Scale for Curve I
Energy (Mev) Scale for Curve II
Range (microns) Scale for Curve I
I
II

Figure 2 (*a*). Range–energy curves for protons. Ilford C2 dry emulsion.

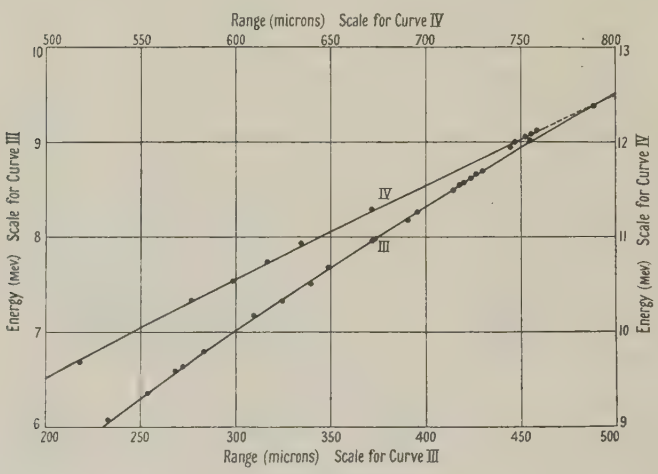
Range (microns) Scale for Curve IV
Energy (Mev) Scale for Curve III
Energy (Mev) Scale for Curve IV
Range (microns) Scale for Curve III
IV
III

Figure 2 (*b*).

Table 2

Range (microns)	Energy (Mev.)	Range (microns)	Energy (Mev.)	Range (microns)	Energy (Mev.)	Range (microns)	Energy (Mev.)
5	0·49	80	3·12	200	5·495	500	9·51
10	0·80	90	3·355	225	5·905	525	9·78
15	1·045	100	3·58	250	6·30	550	10·04
20	1·27	110	3·80	275	6·665	575	10·30
25	1·475	120	4·005	300	7·01	600	10·55
30	1·67	130	4·22	325	7·36	625	10·805
35	1·85	140	4·42	350	7·69	650	11·05
40	2·01	150	4·605	375	8·01	675	11·30
45	2·17	160	4·795	400	8·325	700	11·545
50	2·325	170	4·975	425	8·635	725	11·785
60	2·61	180	5·150	450	8·94	750	12·02
70	2·88	190	5·32	475	9·225	775	12·26

unpublished). The point at 0·584 MeV. was taken from measurements on the protons from the $^{14}N(n, p)^{14}C$ reaction which were recently reported by the author (El-Bedewi 1951). The accuracy at any point above a proton energy of 0·5 MeV. on the range–energy curve is estimated to be better than 0·5% in the proton energy.

ACKNOWLEDGMENTS

The author is very grateful to Dr. J. R. Holt for his generous help and continual interest in the problem and to the Egyptian Government for financial aid during the period in which this work was done.

REFERENCES

Bethe, H. A., 1950, *Rev. Mod. Phys.*, **22**, 213.
Buechner, W. W., and Strait, E. N., 1949, *Phys. Rev.*, **76**, 1547.
Catala, J., and Gibson, W. M., 1951, *Nature, Lond.*, **167**, 551.
El-Bedewi, F. A., 1951, *Proc. Phys. Soc.* A, **64**, 584.
Livingston, M. S., and Bethe, H. A., 1937, *Rev. Mod. Phys.*, **9**, 272.
Rotblat, J., 1950, *Nature, Lond.*, **165**, 387; 1951, *Ibid.*, **167**, 550.
Rotblat, J., Burrows, H. B., and Powell, C. F., 1951, *Proc. Roy. Soc.* A, in the press.

The Differential Cross Section for High Energy Nucleon–Nucleon Collisions and the Mean Square Angle of Scatter

By H. S. GREEN* and H. MESSEL*
School of Theoretical Physics, Dublin Institute for Advanced Studies

MS. received 25th June 1951

ABSTRACT. In an attempt to account theoretically for the lateral and angular development of the penetrating particles in high energy cosmic-ray showers, we have developed a method for deriving the differential from the total cross section, in the laboratory frame of reference. An integral equation is set up for the differential cross section, and solved assuming that the differential cross section in the centre-of-mass frame of reference is of the form $R+S' \cos^2 \bar{\theta}$, where R and S' are functions of the incident and scattered energies only. Using a form of the total cross section derived from the analysis of high-energy cosmic-ray experiments, the mean square angle of scatter in a nucleon–nucleon collision has been calculated and found to be inversely proportional to the energy of the incident particle. The results are compared with experiments.

§ 1. INTRODUCTION AND PRELIMINARIES

Cosmic rays are almost the only reliable source of information on the force between two nucleons whose relative velocity approaches closely to that of light. To frame a tentative theory in these conditions is as difficult as to realize them in the laboratory experiment. It is easy to see that such information —badly needed in the theory of nuclear forces—may well be obtained from investigating the lateral spread of extended air showers, more especially of their nucleon component. A reasonable assumption for the differential cross section that gives the observed lateral spread in agreement with observation up to such high relative energies will probably be fairly correct. The chief requisite for determining the

* Both authors now at Department of Mathematical Physics, University of Adelaide, South Australia.

lateral spread from any assumption for the cross section is the mean square of the angle of scattering after one collision.

The problem of the nucleon cascade differs from the theory of the lateral spread of the electron–photon cascade, developed by Euler and Wergeland (1940 a, b), Molière (1942) and others, in two essential points. In the latter case there is only electromagnetic interaction, which in the collision between nucleons is outweighed by the nuclear force proper, and, for high energy, is even negligible. Secondly, with electrons inelastic scattering may be neglected, while a high-energy nucleon must lose an appreciable amount of energy by meson production in almost every collision.

This paper is concerned with the two chief preparatory steps, the first being the most important: to calculate the differential from an arbitrary total cross section in the laboratory frame and then to infer the probable form of the *differential* cross section from previous work on the nucleon cascade which required only the *total* cross section as a function of the energies and accounted satisfactorily for the vertical distribution of nucleons in the atmosphere, both in number (Messel 1951 a, b, Messel and Ritson 1950, Jánossy and Messel 1951) and in spectral distribution (Messel 1951 c). The first assumption we have made is that at energies greater than 3×10^3 MEV., with which we are mainly concerned, elastic collisions may be neglected, in other words that a meson is always produced even if it does not escape from the nucleus with which the nucleon collides. The second step is merely the computation of the mean square angle of scattering from the differential cross section obtained.

Faced with the problem of finding the differential cross section from a total cross section given in the laboratory frame of reference, we have made the further assumption that the angular dependence will be simplest in that frame of reference in which the mass-centre of the two nucleons is at rest before the collision. More especially we assume that, in this frame, the expansion in powers of the cosine of the scattering angle $\bar{\theta}$ may be terminated at $\cos^2\bar{\theta}$; since it is meaningless to distinguish between the two nucleons after the collision odd powers of $\cos\bar{\theta}$ cannot occur. The differential cross section must then be of the form $R + S'\cos^2\bar{\theta}$, where R and S' depend only on the energy of the incident and scattered particle. It is remarkable that both these functions are uniquely determined by the total cross section and can be expressed in terms of the latter without specializing it. The reduction to the laboratory frame is then obvious.

The most convenient unit of mass for our work is the rest mass of the proton; if, then, the unit of time is so chosen that the velocity of light is unity, the rest energy of the proton ($\sim 10^3$ MEV.) will also be unity. The rest mass of an arbitrary scattered particle in these units will be denoted by m, thus, if the particle is a proton $m = 1$, if it is a π-meson $m = 1/6{\cdot}5$. The momentum and total energy of the particle in the laboratory frame will be denoted by P and U respectively, so that

$$U^2 - P^2 = m^2, \qquad \ldots\ldots(1)$$

and all quantities referring to the centre-of-mass frame are distinguished by a bar, e.g. $\bar{U}$ and $\bar{P}$; since the momentum vector **P** and the energy U together form a covariant four-vector, then

$$\bar{U} = \bar{U}_0 U - \bar{P}_0 P\cos\theta, \qquad \ldots\ldots(2)$$

$$\bar{P}\cos\bar{\theta} = \bar{U}_0 P\cos\theta - \bar{P}_0 U \quad \ldots\ldots(3) \qquad \bar{P}\sin\bar{\theta} = P\sin\theta, \quad \ldots\ldots(4)$$

where $\overline{P}$ and $\overline{U}_0$ are the momentum and energy (which, since $m=1$, is just the coefficient of the transformation) of the incident nucleon in the centre-of-mass system; θ and $\bar{\theta}$ are the scattering angles in the laboratory and centre-of-mass frames respectively. The relations inverse to (2) and (3) are

$$U=\overline{U}_0\overline{U}+\overline{P}_0\overline{P}\cos\bar{\theta} \quad \ldots\ldots(5); \qquad P\cos\theta=\overline{U}_0\overline{P}\cos\bar{\theta}+\overline{P}_0\overline{U}. \quad \ldots\ldots(6)$$

The momentum P_0 and energy U_0 of the incident nucleon are found in terms of $\overline{P}_0$ and $\overline{U}_0$ by substituting $\overline{U}=\overline{U}_0$, $\overline{P}=\overline{P}_0$, and $\bar{\theta}=\theta=0$ in (5) and (6), thus:

$$U_0=\overline{U}_0^{\,2}+\overline{P}_0^{\,2}=2\overline{U}_0^{\,2}-1 \quad \ldots(7); \qquad P_0=2\overline{U}_0\overline{P}_0=2\overline{U}_0(\overline{U}_0^{\,2}-1)^{1/2}. \quad \ldots(8)$$

The requirements of conservation of energy and momentum impose certain restrictions on the energies and momenta of the outgoing particles. The energy of an outgoing particle whose rest mass does not exceed two proton masses cannot exceed the energy of the incident particle in the centre-of-mass system, that is,

$$\overline{U}\leqslant\overline{U}_0. \qquad \ldots\ldots(9)$$

The proof of (9) is given in the Appendix.

The inequality (9) imposes an important restriction on the angle of emission of the scattered particles in the laboratory system. For it follows with the help of (2) that

$$\overline{U}_0U-\overline{P}_0P\cos\theta\leqslant\overline{U}_0, \qquad \cos\theta\geqslant\overline{U}_0(U-1)/\overline{P}_0P. \quad \ldots\ldots(10)$$

The right-hand side of (10) is very nearly $1-U^{-1}$, since $\overline{P}_0\simeq\overline{U}_0$ and $P\simeq U$. Hence the angle of scattering cannot exceed the value $(2U^{-1})^{1/2}$ radians, approximately, where U is the energy of the scattered particle. Scattered particles are limited to a cone which becomes narrower and narrower as their energy increases. Some cosmic-ray photographs show what appears to be a double cone; it is quite plausible that the inner cone be composed of particles from primary collisions, and the outer cone of particles from secondary or tertiary collisions, of nucleons within the nucleus. The latter will naturally have a much lower energy than the former.

We shall repeatedly make use of the Lorentz invariance of certain differentials. For *any* particle, the volume element of momentum space $P^2\,dP\,dc\,d\phi$ divided by the energy U is known to be invariant.* But since $U\,dU=P\,dP$, it follows that $P\,dU\,dc\,d\phi$ is Lorentz-invariant; and, since $d\phi=d\bar{\phi}$,

$$P\,dU\,dc=\overline{P}\,d\overline{U}\,d\bar{c}. \qquad \ldots\ldots(11)$$

Also, if $W(U,c,\phi)\,dU\,dc\,d\phi$ is the probability, in a particular experiment, of finding the particle in question within the limits U, $U+dU$, c, $c+dc$, ϕ, $\phi+d\phi$, this probability must be Lorentz-invariant; thus, if W does not depend on ϕ,

$$W(U,c)\,dU\,dc=\overline{W}(\overline{U},\bar{c})\,d\overline{U}\,d\bar{c}. \qquad \ldots\ldots(12)$$

Dividing (12) by (11) we have further

$$W(U,c)/P=\overline{W}(\overline{U},\bar{c})/\overline{P}. \qquad \ldots\ldots(13)$$

Similarly, if $W(U',c';U'',c'')\,dU'\,dU''\,dc'\,dc''$ is the probability of finding the two nucleons, arising from the same collision, in the specified intervals, $W(U',c';U'',c'')/P'P''$ will be Lorentz-invariant. For our present purpose, we have found it unnecessary to determine $W(U',c';U'',c'')$: on account of the symmetry of this function with respect to the variables U', c'; U'', c'' we require only the function $W(U',c')=\iint W(U',c';U'',c'')\,dU''\,dc''$, which is identical with that defined above.

* c stands for $\cos\theta$ and $\bar{c}$ for $\cos\bar{\theta}$.

In the following determination of the differential cross section for the inelastic scattering of two nucleons, no distinction will be drawn between neutrons and protons. It is, admittedly, likely that the exclusion principle will make the cross section for p–p or n–n collisions somewhat different from that for p–n and n–p collisions. The reason why we do not need to distinguish between neutrons and protons is that the total cross section which we use is averaged over all four types of collisions. The differential cross section derived will therefore be automatically averaged in a similar way.

§ 2. DERIVATION OF DIFFERENTIAL FROM TOTAL CROSS SECTION

Writing $F(U)$ for our total cross section in the laboratory frame of reference, we must have

$$\int W(U,c)\,dc = F(U). \qquad \ldots\ldots(14)$$

Note also that

$$\int F(U)\,dU = 1. \qquad \ldots\ldots(15)$$

It will be convenient to change the integration variable from c to $\overline{U}$, keeping U constant, and to write:

$$\left.\begin{aligned} U &= m\cosh u, \quad \overline{U} = m\cosh\bar{u}, \quad \overline{U}_0 = \cosh v, \quad U_0 = \cosh 2v \\ P &= m\sinh u, \quad \overline{P} = m\sinh\bar{u}, \quad \overline{P}_0 = \sinh v, \quad P_0 = \sinh 2v \end{aligned}\right\}. \qquad \ldots\ldots(16)$$

Then, using relations (2), (5), (9) and (13) we find

$$\int_{m\cosh(v-u)}^{\cosh v} W\left(m\cosh\bar{u},\ \frac{\cosh u - \cosh v\cosh\bar{u}}{\sinh v\sinh\bar{u}}\right)\frac{d(m\cosh\bar{u})}{m\sinh u} = \sinh v\,F(m\cosh u). \qquad \ldots\ldots(17)$$

We assume however, (see § 1) that

$$\overline{W}(\overline{U},\bar{c}) = R(\overline{U}) + S(\overline{U})(\overline{U}\overline{P}\bar{c})^2; \qquad \ldots\ldots(18)$$

so

$$\overline{W}\left(m\cosh\bar{u},\ \frac{\cosh u - \cosh v\cosh\bar{u}}{\sinh v\sinh\bar{u}}\right) = R(m\cosh\bar{u}) + S(m\cosh\bar{u})(m\cosh u - m\cosh v\cosh\bar{u})^2, \qquad \ldots\ldots(19)$$

hence writing

$$R(m\cosh\bar{u}) = r(\bar{u}); \quad S(m\cosh\bar{u}) = s(\bar{u}); \quad F(m\cosh u) = f(u), \qquad \ldots\ldots(20)$$

we get

$$\int_{m\cosh(v-u)}^{\cosh v}\{r(\bar{u}) + m^2 s(\bar{u})(\cosh u - \cosh v\cosh\bar{u})^2\}\frac{d(m\cosh\bar{u})}{m\sinh\bar{u}} = \sinh v\,f(u). \qquad \ldots\ldots(21)$$

The value of u lies between 0 and $2v$; and a further integral equation is obtained by replacing u by $2v-u$ in (21), thus:

$$\int_{m\cosh(v-u)}^{\cosh v}\{r(\bar{u}) + m^2 s(\bar{u})(\cosh(2v-u) - \cosh v\cosh\bar{u})^2\}\frac{d(m\cosh\bar{u})}{m\sinh\bar{u}} = \sinh v\,f(2v-u). \qquad \ldots\ldots(22)$$

Our task is to solve (21) and (22) for $r(\bar{u})$ and $s(\bar{u})$. One may proceed as follows: subtracting (22) from (21), and writing

$$g(u) = \frac{f(u) - f(2v-u)}{4m\cosh v\sinh(u-v)}, \qquad \ldots\ldots(23)$$

one finds

$$\int_{m\cosh(v-u)}^{\cosh v} ms(\bar{u})\{\cosh(u-v) - \cosh\bar{u}\}\frac{d(m\cosh\bar{u})}{m\sinh\bar{u}} = g(u). \qquad \ldots\ldots(24)$$

By differentiating equation (24) twice with respect to u it may then be verified that

$$s(\bar{u}) = -(1/m\sinh\bar{u})\{g''(v-\bar{u})+g'(v-\bar{u})\coth\bar{u}\} = (d/du)\{g'(v-\bar{u})/m\sinh\bar{u})\}. \quad \ldots\ldots(25)$$

One may now substitute this for $s(\bar{u})$ in equation (21) and after a straightforward but lengthy calculation find

$$r(\bar{u}) = -\sinh^2 v(d/d\bar{u})\{m\,g'(v-\bar{u})\sinh\bar{u}\} - \tfrac{1}{2}\sinh v\{f'(v+\bar{u})-f'(v-\bar{u})\}. \\ +\tfrac{1}{2}\cosh v\{f(v+\bar{u})-f(v-\bar{u})\}. \quad \ldots\ldots(26)$$

As a check on the above, we substitute the values found for R and S in (18) and integrate over both $\bar{c}$ and $\overline{U}$; we find the value of the integral to be equal to 1, as it should be, since our probability function $F(U)$ is normalized to 1.

Thus, starting from the general total probability function $F(U)\,dU$ we have without specializing it found the differential probability function $W(U,c)\;dUdc$. It is convenient to express $W(U,c)$ in the centre-of-mass frame of reference, thus using (23), (25) and (26)

$$\overline{W}(m\cosh\bar{u},\bar{c}) = \frac{\sinh^2 v}{4\cosh v}\{f''(v+\bar{u})-f''(v-\bar{u})\} - \frac{\sinh^2 v\coth\bar{u}}{4\cosh v}\{f'(v+\bar{u})+f'(v-\bar{u})\} \\ -\tfrac{1}{2}\sinh v\{f'(v+\bar{u})-f'(v-\bar{u})\} + \left(\frac{\sinh^2 v\,\mathrm{csch}^2\bar{u}}{4\cosh v}+\tfrac{1}{2}\cosh v\right) \\ \times\{f(v+\bar{u})-f(v-\bar{u})\} + \bar{c}^2\sinh^2\bar{u}\sinh^2 v\left[-\frac{1}{4\cosh v\sinh^2\bar{u}}\right. \\ \times\{f''(v+\bar{u})-f''(v-\bar{u})\} + \frac{3\cosh\bar{u}}{4\cosh v\sinh^3\bar{u}}\{f'(v+\bar{u})+f'(v-\bar{u})\} \\ \left.-\frac{2\sinh^2\bar{u}+3}{4\cosh v\sinh^4\bar{u}}\{f(v+\bar{u})-f(v-\bar{u})\}\right]. \quad \ldots\ldots(27)$$

The $W(U,c)$ may be obtained from (27) by using the relations (2), (5), (7), (8) and (13).

We now introduce the special form of $f(\bar{u})$ used by Messel (1951 c)

$$f(\bar{u}) = 20m(U_0-1)^{-5}(\cosh\bar{u}-1)\{U_0+(m-1)-m\cosh\bar{u}\}^3. \quad \ldots\ldots(28)$$

This cross section appears to account for the development of the high-energy nucleon component of the cosmic radiation throughout the atmosphere both from a qualitative and from a quantitative standpoint, and even though it is probably not exact, it is unlikely that, when the true total cross section for high-energy inelastic nucleon–nucleon collisions becomes known, it will differ radically from (28).

In the ultra-relativistic region where $U \simeq P$ and $U_0 \simeq P_0$ the expression given by (27) simplifies a great deal. In the centre-of-mass system in this approximation

$$W(m\cosh\bar{u},\bar{c}) \simeq 30m^3\exp(-5v)\exp 3\bar{u}\,(\exp v - m\exp\bar{u})(1-\bar{c}^2). \quad \ldots\ldots(29)$$

It should be noted that the expression given in (29) is valid either for nucleons or mesons. However, since the cross section (28) has not been checked by seeing whether it can account for the experimentally observed behaviour of the meson component of the cosmic radiation, it should be treated with some caution for mesons.

§ 3. THE MEAN SQUARE ANGLE OF SCATTER

The value of the mean square angle of scatter in a nucleon–nucleon collision is given by

$$\langle\theta^2\rangle = \iint \tan^2\theta W(U,c)\,dU\,dc, \qquad \ldots\ldots(30)$$

where we have replaced θ^2 by $\tan^2\theta$. We prefer to carry out the above integration in the centre-of-mass system. Writing

$$\tan^2\theta = \sin^2\bar{\theta}/\overline{U}_0^2(\cos\bar{\theta}+M)^2, \qquad \ldots\ldots(31)$$

with

$$M = \overline{P}_0\overline{U}/\overline{U}_0\overline{P} \qquad \ldots\ldots(32)$$

$$\langle\theta^2\rangle = \int_1^{\cosh v}\int_{-1}^{1} \frac{1-\bar{c}^2}{\cosh^2 v\,(\bar{c}+M)^2}\{r(\bar{u})+m^2\sinh^2 v\sinh^2\bar{u}\,s(\bar{u})\bar{c}^2\}d(m\cosh\bar{u})\,d\bar{c}. \qquad \ldots\ldots(33)$$

The $\bar{c}$ integration may be carried out immediately, yielding

$$\langle\theta^2\rangle = \int_1^{\cosh v}\frac{r(\bar{u})}{\cosh^2 v}\left\{2M\ln\frac{M+1}{M-1}-4\right\}d(m\cosh\bar{u}) + \frac{\sinh^2 v}{\cosh^2 v}\int_1^{\cosh v} m^2\sinh^2\bar{u}\,s(\bar{u})\left\{\frac{4}{3}-8M^2+2M(2M^2-1)\ln\frac{M+1}{M-1}\right\} \times d(m\cosh\bar{u}). \qquad \ldots\ldots(34)$$

Making use of an ultra-relativistic approximation, and our value of $f(u)$, the integral in (34) yields the simple result

$$\langle\theta^2\rangle = \int_1^{\cosh v} 320m^3\exp 3\bar{u}\exp(-7v)(\exp v - m\exp\bar{u})\,d(\tfrac{1}{2}m\exp\bar{u}), \qquad \ldots\ldots(35)$$

and hence

$$\langle\theta^2\rangle = (4/U_0)(\text{radians})^2. \qquad \ldots\ldots(36)$$

It may be noted that the integrand in (35) is simply the mean square angle of scatter as a function of both the primary and secondary energies.

§ 4. DISCUSSION OF RESULTS

It is perhaps surprising that it is possible to derive from the total cross section in the laboratory frame of reference, not only the total cross section, but also something of the angular distribution in the centre-of-mass frame of reference, and thus also indirectly in the laboratory system. It is, however, a fact that isotropy in the centre-of-mass system is possible only when certain restrictions are imposed upon the total cross section in the laboratory system. This is essentially a consequence of the circumstance that the cross section in the laboratory frame is defined over a much wider range of energies than in the centre-of-mass frame. The differential cross section obtained by our method shows an angular distribution with a diffuse maximum at right angles to the motion of the two incident nucleons in the centre-of-mass system. This characteristic is not a property of the particular form of the total cross section $F(U)$, but is shared by all other reasonable cross sections which are homogeneous (with respect to the energies of the incident and secondary nucleons) and vanish as the momentum goes to zero in the laboratory frame. The differential cross section is negligible for scattering in the backward and forward directions; this, however, is only true in the ultra-relativistic approximation, and it can be seen from formula (27) that at lower energies the contribution from forward and backward scattering increases continuously. It is thus not inconsistent with low-energy laboratory experiments. It is important to notice also that we have excluded completely the consideration of elastic scattering, which is predominant at low energies, and probably contributes significantly to the scattering near 0° and 180° even at very high energies.

The neglect of this scattering is not important for our purposes, as it does not directly contribute to the lateral spread of air showers. Our method is applicable to any kind of inelastic collision between two elementary particles, and is independent of the kind of particle emitted. We have considered the application of the theory to plural meson production in nucleon–nucleon collisions, and with the particular total cross section assumed in formula (28) their angular distribution is the same as for the scattered nucleons.

The mean square angle of scatter given by (36) is applicable to nucleon–nucleon collisions only; what are usually observed experimentally are nucleon–nucleus collisions. Consequently, our present results will only permit us to give a qualitative picture of what is to be expected. It is almost certain that there occurs a cascading effect within the nucleus itself, so that the emitted particles may result from either the primary, secondary, or even tertiary, collisions. The latter particles will have a mean square scattering angle greater than that which we have calculated. We shall give the complete theory of this process shortly.

In the case of the electron–photon cascade, it is well known that the only important source of deflection, giving rise to the lateral and angular spread of the shower, is the multiple coulomb scattering of the shower electrons by the nuclei of the material traversed. This effect gives, in a path length equal to one cascade unit, a mean square angular deflection proportional to $1/E^2$. On this basis the theory of the lateral and angular spread of the electrons and photons in cosmic-ray showers has been developed. On the other hand we find that in a single nucleon–nucleon collision the mean square angle of scattering is inversely proportional to the primary energy. We are thus inevitably led to the conclusion that in considering electrons and photons on the one hand, and nucleons an the other, the nucleons will have a greater lateral and angular spread. Our work above will thus allow us to form the following qualitative picture of air showers as far as *high-energy* particles are concerned. The core of the shower will consist of a mixture of all products of high-energy nuclear collisions, but naturally the electrons generated by the cascade process will predominate. As one passes from the core to the periphery of the shower, the proportion of electrons to penetrating particles will fall. This picture appears to be in good agreement with what has acually been found experimentally (cf. Eidus *et al.* 1950, Cocconi *et al.* 1949, 1950).

ACKNOWLEDGMENTS

The authors wish to express their thanks to Professor E. Schrödinger for the many stimulating discussions on the above work, and for the short proof given in the Appendix.

APPENDIX

We now give a proof of the fact that the energy of an outgoing particle whose rest mass does not exceed two proton masses cannot exceed the energy of the incident particle in the centre-of-mass system. The proof given below is quite general and holds regardless of the number of particles given off.

Let us denote by m_r, $\overline{P}_r$ and $\overline{U}_r$, the mass measured in proton mass units, the absolute value of the momentum, and the total energy, respectively, of the rth particle in the centre-of-mass system.

Since $$\overline{U}_r^2 = \overline{P}_{r,1}^2 + \overline{P}_{r,2}^2 + \overline{P}_{r,3}^2 + m_r^2, \qquad \ldots\ldots(37)$$

we may regard $\overline{U}_r$ as the length of a vector $\overline{\mathbf{U}}_r$ in Euclidean four-space, with the three $P_{r,i}$ and m_r its Cartesian components. The conservation laws tell us that the *vector-sum* of all the $\overline{\mathbf{U}}_r$ lies in the direction of the m axis and that the (ordinary) sum of their absolute values is prescribed, i.e. $2\overline{U}_0$. If one of the $\overline{U}_r$ is longer than half this prescribed total length, it must necessarily contribute more than half to the m component $\Sigma_r m_r$.

REFERENCES

Cocconi, G., and Cocconi-Tongiorgi, V., 1950, *Phys. Rev.*, **79**, 730.
Cocconi, G., Cocconi-Tongiorgi, V., and Greisen, K., 1949, *Phys. Rev.*, **76**, 102c.
Eidus, L. Kh., Alymova, M. M., and Videnskii, V. G., 1950, *Dokl. Akad. Nauk. S.S.S.R.* **75**, 669.
Euler, H., and Wergeland, H., 1940 a, *Asytrophs. Nor.*, **3**, 165; 1940 b, *Naturwissenschaften*, **28**, 41.
Jánossy, L., and Messel, H., 1951, *Proc. Roy. Irish Acad.* A, **54**, 245.
Messel, H., 1951 a, *Proc. Roy. Irish Acad.* A, **54**, 125; 1951 b, *Comm. Dublin Inst. for Advanced Studies*, Series A, No. 7; 1951 c, *Proc. Phys. Soc.* A, **64**, 726.
Messel, H., and Ritson, D. M., 1950, *Proc. Phys. Soc.* A, **63**, 1359.
Molière, G., 1942, *Naturwissenschaften*, **30**, 87.

Nuclear Spin and Magnetic Moment of Rhodium $^{103}_{45}$Rh

By H. Kuhn and G. K. Woodgate
Clarendon Laboratory, Oxford

MS. received 18*th July* 1951

ABSTRACT. The radiation from a hollow-cathode tube containing rhodium was passed four times through an atomic beam of rhodium. Absorption was found in eight lines, four of which showed hyperfine structure doublets of separation 0·023 cm^{-1}. The splitting could be ascribed to the ground state $4d^8\ 5s\ {}^4F_{9/2}$. It was concluded with certainty that the spin of the rhodium nucleus $^{103}_{45}$Rh has the value $I=\frac{1}{2}$. The relative intensities of the components show that the magnetic moment is negative. The observed splitting leads to an estimated value of $\mu=-0{\cdot}10$ nuclear magneton. The values of I and μ indicate a configuration $(5g_{9/2})^6 3p_{1/2}$ for the last seven protons of the rhodium nucleus in the Goeppert-Mayer model.

§ 1. INTRODUCTION

Several investigators (Schüler and Schmidt 1934, Sibaiya 1937, Williams and Granath 1938) have used hollow-cathode tubes to examine lines of the arc spectrum of rhodium, but have been unable to resolve any hyperfine structure. Sibaiya (1937) observed doublet structures in two of the ultra-violet resonance lines, but Williams and Granath (1938) were able to show that self-reversal was the cause of the apparent splitting.

In the present work, an attempt was made at first to resolve hyperfine structures in several rhodium lines with the use of a hollow-cathode tube cooled with liquid air and operated at very low currents. The line 5599 A. and the ultra-violet resonance lines were examined in this way. When this proved unsuccessful, an atomic beam of rhodium was produced and the radiation from the hollow-cathode tube was passed through this beam before it was made to enter the spectrograph and interferometer. The absorption spectrum showed a sufficiently reduced Doppler width to allow doublet structures to be observed in four lines.

The lines investigated with the atomic beam were those arising from a combination of terms of the configuration $4d^85p$ with the two lowest levels $4d^85s\,^4F_{9/2,\ 7/2}$ of the ground term quartet (Sommer 1927).

§ 2. EXPERIMENTAL METHOD

(i) *The Hollow-cathode Discharge Tube*

In Schüler's original design of the cooled hollow-cathode tube and in various modifications which have since been described (Gurewitch 1949, Fowles 1950, Arroe and Mack 1950), the cathode forms the outer wall of the tube and protrudes through the surface of the cooling liquid. The heat conduction along this metal tube leads to a great consumption of liquid air and, unless the tube is made very long, is apt to impair the cooling of the cathode cavity. Also, in this design, the waxed joint between tube and window has to be kept warm by flowing water.

The use of metal–glass seals avoids these drawbacks and allows a very simple design of discharge tube, several modifications of which have been tried out in this laboratory. The type shown in Figure 1 is, apart from a minor modification introduced later, that which was used in the present and earlier work.

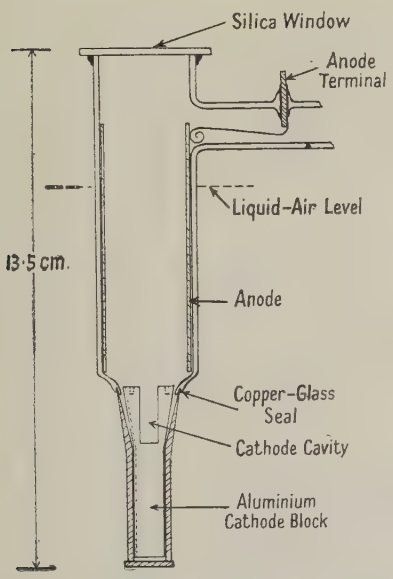

Figure 1. The hollow-cathode discharge tube.

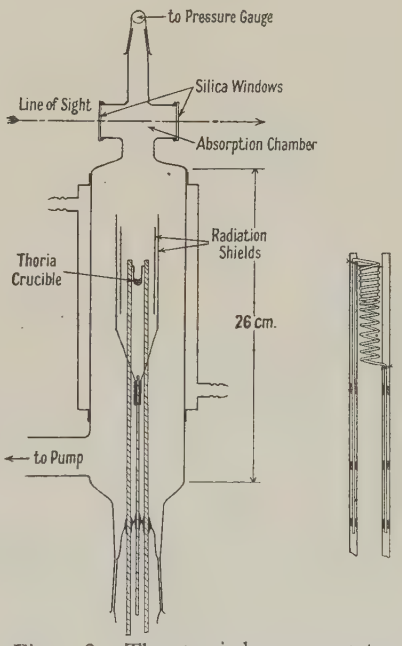

Figure 2. The atomic beam apparatus.

The cathode was an aluminium block which fitted tightly into the copper tube and which had a cavity of 0·5 cm. diameter and 1·5 cm. depth. A sawcut was made down the outside of the block to provide a communicating channel from the small space below the block. Two small screw holes were made in the upper face of the cathode block so that this could be removed from the copper tube by means of threaded rods screwed into the holes. The tight push-fit of the cylindrical cathode used in this work gave adequate thermal contact with the copper tube. The removable cathode block was later modified for other work in the laboratory by substituting a cone fitting for the cylindrical fitting. The

consumption of liquid air when the discharge was switched off was entirely negligible. This type of discharge tube should be especially suitable for use with liquid-hydrogen cooling.

The discharge tube was connected to a liquid-air trap containing a few grains of charcoal, and to a pumping system and reservoirs of rare gases. No provision was made for circulating the carrier gas as the static system remained clean over very long periods. Two short pieces (about 30 mg.) of pure rhodium wire were inserted in the cathode cavity, and the arc lines were excited in an atmosphere of neon at a pressure of 1·2 mm. Hg or of argon at a pressure of 0·6 mm. Hg. Currents from 3 ma. to 50 ma. were passed through the discharge. In argon at a pressure of about 1 mm. Hg the discharge would usually strike at a voltage of about 300 v., and when running at a current of 10 ma. the voltage across the discharge tube was about 175 v.

(ii) *The Atomic Beam Apparatus*

Rhodium has a melting point of about 1,950° c., and below this temperature its vapour pressure is very low. In order to produce an atomic beam of a density sufficient to give absorption in the resonance lines, it was necessary to raise the temperature to about 2,200° c. This demanded the use of refractory crucibles of very high softening point.

A number of experiments were conducted with crucibles of beryllia and of zirconia, but these did not withstand the high temperature. The only refractory material which was found to be satisfactory at the temperatures used was thoria.* In the final experiments thoria crucibles of 1·4 cm. depth, 5 mm. internal diameter, and 7 mm. external diameter were used; a rim projecting outwards about 0·5 mm. fitted into the upper turns of the heating filament and supported the crucible (see Figure 2). The weight of the crucible contributed to the sagging of the filament, but it was found difficult to support the crucible independently. Attempts were made to provide a stand on which the bottom of the crucible could rest; this took the form of a vertical tungsten rod with a flat end, or a wire bent over at the top, but in all cases the crucible was punctured: obviously the thoria became too soft at high temperatures to withstand mechanical pressure. Also the high electrical conductivity of thoria at these high temperatures led frequently to short circuits.

The heating coil was a helix of tungsten wire of 18 turns, inside which the crucible fitted. The diameter of the wire was 0·83 mm. and that of the helix was about 8 mm. The ends of the coil were spot-welded on to two upright tungsten rods. Windings of thin nickel wire assisted in the spot-welds at the extremities of the filament wire; in the hotter region near the helix, platinum was used. In addition, the filament was tied to the uprights at the right-angle bends by means of tungsten wire of 0·2 mm. thickness. In this way the filament was prevented from leaning over when the tungsten began to soften at high temperatures.

However, a sagging of the helix under its own weight and that of the crucible did take place when the tungsten softened. This gave rise to a separation of the turns at the upper part, with a consequent loss of heating efficiency and a short-circuiting of the turns at the lower part of the helix. In order that the separation

* The authors are indebted to Mr. Powell, of Messrs. Johnson, Matthey, for his advice in this matter.

of the turns of the helix should be correct at the highest temperatures used (i.e. after sagging), the helix was initially made with uneven spacings of the turns.

The crucible assembly was surrounded by two coaxial cylindrical radiation shields made of molybdenum foil. The tungsten rod carrying these shields and the two tungsten rods serving as supports and current leads for the heating coil were sealed through a Pyrex ground joint. This was fitted by means of Apiezon wax into the lower end of the Pyrex tube, the details of which can be seen in Figure 2. The Pyrex tube was surrounded by a water jacket.

At a power input of 2,000 watts (40 amp., 50 v.) the rhodium could be evaporated at a rate sufficient to produce absorption. A charge of 0·5 gm. of rhodium lasted for about 30 minutes of evaporation. The pressure in the tube as read on the Penning gauge was maintained below about 2×10^{-4} mm. Hg during evaporation. At this pressure the 'shadow' of the collimating aperture was clearly defined by the rhodium deposit.

The collimation of the atomic beam was determined by the aperture of the crucible (5 mm.), the diameter of the glass neck of the outer tube, which was 2 cm., and the vertical distance, about 10 cm., between the two. According to the formula given by Minkowski and Bruck (1935), the half-value width of the lines should be about one-fifteenth of that in an ordinary gas at the temperature of the crucible. This gives a value of 0·007 cm^{-1} for the line width to be expected, though it must be remembered that the shape of an absorption line due to an atomic beam is different from a normal Doppler distribution. The value of the collimation was chosen in order to match the Doppler width with the instrumental resolving limit (see the next paragraph).

(iii) *The Optical System*

In the final experiments the radiation from the hollow-cathode tube was made to pass four times through the atomic beam: this was necessary when absorption in the weaker lines was studied. Figure 3 shows schematically the

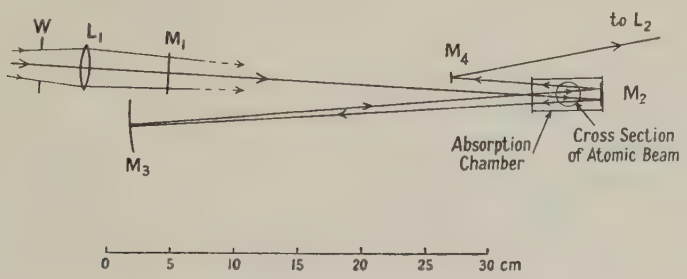

Figure 3. The optical system.

optical arrangement. The light emerging from the window W of the discharge tube was deflected into a horizontal direction by the mirror M_1. The lens L_1 formed an image of the cathode cavity near the window M_2 which was coated with aluminium. A concave mirror M_3 of radius of curvature 37·5 cm. was placed so that the image of the hollow cathode was at its centre of curvature. After the second and third passages through the beam, a second image was formed by M_3 at M_2, slightly displaced laterally from the first. The radiation was then

reflected back through the beam to the mirror M_4 and then to the lens L_2 and to the spectrograph slit.

The numerical aperture of the beam of light passing through the absorption chamber was 1/15. This value was chosen in such a way that the full numerical aperture at the hollow cathode, namely 1/5·5, was used, and the spectrograph (a numerical aperture of 1/30) was filled with light; at the same time, the image of the hollow cathode formed on the slit of the spectrograph was magnified five times.

The spectrograph was a Hilger instrument with quartz–rocksalt–quartz achromats of 150 cm. focal length and 6 cm. diameter. With a quartz Cornu prism, the linear dispersion at 3400 A. was about 20 A/mm.

The high resolution instrument was a Fabry–Perot etalon placed between the collimator and the prism of the spectrograph. The aluminium-coated surfaces of the etalon had a reflectivity of about 81% in the near ultra-violet which corresponds to a theoretical resolving limit of about 0·008 cm^{-1} with a 5 cm. spacer, which was used in most experiments. This value is about the same as the half-value width of the absorption lines caused by the atomic beam. A pure isotope ^{198}Hg lamp, supplied by the General Electric Company, proved most valuable in adjusting the etalon for parallelism of the plates. When used with a rare earth filter, it provides a source which is both more highly monochromatic and more intense than any ordinary source, as for example a cadmium lamp.

Ilford Special Rapid plates were used to photograph the resonance lines of rhodium in the near ultra-violet.

§ 3. RESULTS

In emission, the lines 3434 A., 3692 A. and 3396 A. arising from transitions to the ground term $4d^85s\,^4F_{9/2}$ of rhodium were found to be slightly broader than the lines 3658 A. and 3528 A. which arise from transitions to the slightly higher term $4d^85s\,^4F_{7/2}$, and which showed the expected Doppler width. But even at the lowest current used, 3·5 ma., no structure could be resolved.

With the atomic beam, absorption was observed in eight lines of the arc spectrum of rhodium. In four of these a doublet splitting was clearly resolved, and in the other four no structure, but only a single absorption line was observed. The structures are indicated in the Table.

Transition	Line	Structure	Separation
$4d^85s\,^4F_{9/2}$–$4d^85p\,^4G_{11/2}$	3434 A.	Doublet	$-0{\cdot}022_8 \pm 0{\cdot}001_5$ cm^{-1}
$^4F_{9/2}$	3396 A.	Doublet	$-0{\cdot}023_8$ cm^{-1}
$^4D_{7/2}$	3692 A.	Doublet	$-0{\cdot}023_9 \pm 0{\cdot}002$ cm^{-1}
$^4G_{9/2}$	3502 A.	Doublet	Not measured
$4d^85s\,^4F_{7/2}$–$4d^85p\,^4G_{9/2}$	3700 A.	Unresolved	
$^4F_{7/2}$	3528 A	Unresolved	
$^4D_{5/2}$	3658 A.	Unresolved	
$^2G_{9/2}$	3323 A.	Unresolved	

The negative sign in the values of the separation indicates that the component of lower intensity lay towards longer wavelength. A photometer tracing of the atomic beam absorption in the line 3434 A. is shown in Figure 4, with a tracing of the background superimposed. The two components are marked by arrows.

No attempt was made to achieve great accuracy in the values of the separation, since only a rough estimate of the nuclear magnetic moment could be made. The doublet splitting of the line 3434 A. was measured with a travelling microscope on four plates, that of the line 3692 A. on two plates, and that of the line 3396 A. on only one plate.

The emission line was excited at a current just below that at which self-reversal took place in the hollow cathode. The operating current was usually about 30 ma. in neon at a pressure of 2·0 mm. Hg, or about 17 ma. in argon at a

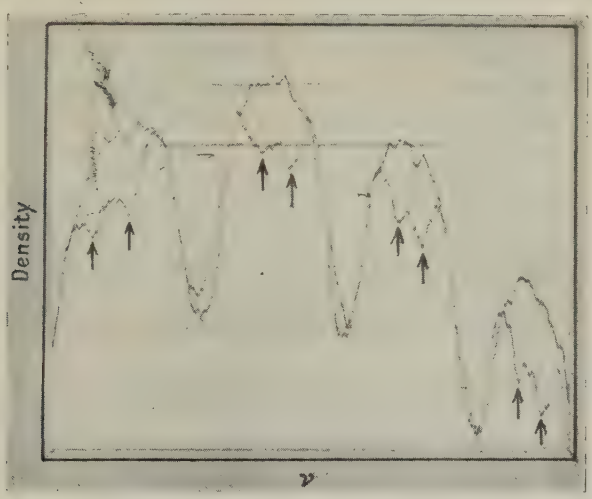

Figure 4.

pressure of 0·3 mm. Hg. At these currents the line was broadened and flattened by self-absorption, but not reversed. The exposure time ranged from about 5 minutes for the strongest line 3434 A., with only two passages through the atomic beam, to about 15 minutes for the weaker lines, with four passages through the beam. The emission line alone was always photographed on the same plate under the same conditions of the discharge as in the exposure with the atomic beam.

§4. DISCUSSION OF THE RESULTS

Rhodium consists of only one stable isotope of atomic number 45 and mass number 103. Hence the observed doublet splittings must be ascribed to hyperfine structure caused by the nuclear spin. In transitions between terms whose J values are all greater than 5/2, a doublet splitting can only be caused by a nuclear spin of $I=\frac{1}{2}$. Any other possible value of I would have caused a structure of four or more components.

Since there are no penetrating electrons in the configuration $4d^8 5p$, the splitting of the terms of this configuration can be expected to be small compared with that of the term $4d^8 5s\,{}^4F_{9/2}$. The validity of this assumption is borne out by the fact that all four lines arising from the combination of the ground term with terms of the $4d^8 5p$ configuration show the same splitting, within the accuracy of the measurements. To this degree of accuracy, the splitting can therefore be ascribed entirely to the ground term $4d^8 5s\,{}^4F_{9/2}$, and is taken to be about 0·023 cm^{-1}.

The fact that the component of longer wavelength is the weaker one shows that the hyperfine structure of the term $4d^85s\,{}^4F_{9/2}$ is inverted. In this term the spin of the s electron points in the same direction as the total angular momentum; the inverted order of the hyperfine structure terms therefore shows that the magnetic moment of the nucleus is negative. The calculated value of the intensity ratio of the two components is 11/9 for all the doublets. This is consistent with the appearance of the photometer tracings, but no actual measurements of intensities were made.

To a first approximation, pure Russell–Saunders coupling can be assumed and the interaction of the nucleus with the d electrons can be neglected. The ratio of the doublet separations of the two terms $^4F_{9/2}$ and $^4F_{7/2}$ arising from the configuration $4d^85s$ is found to be 7 : 4. This explains the fact that no structure was observed in the four lines connected with the term $^4F_{7/2}$.

On the same assumptions, the value of the nuclear magnetic moment can be calculated by the usual approximation methods (see, for example, Kopfermann 1940). The value found was $\mu \simeq -0{\cdot}10_5$ nuclear magneton. An attempt to estimate the effect of the d electrons on this value of μ was made by assuming that the relation between the interval factor $A(^4F_{9/2})$ and the splitting factors a_s and a_d, given by Crawford (1935) for the $4d^25s\,{}^4F_{9/2}$ term of lanthanum, applied also to the $4d^85s\,{}^4F_{9/2}$ term of rhodium. The result of including the influence of the d electrons was a reduction of the numerical value of μ by about 10%. This is of the same order of magnitude as the other uncertainties in this approximate calculation of μ. The final value $\mu \simeq -0{\cdot}10$ n.m. may be taken to be accurate within about 25%.

The comparative ease with which absorption was observed in lines arising from transitions from the state $4d^85s\,{}^4F_{7/2}$ was due to the very high temperature of the atomic beam oven. At a temperature of 2,500° K. the number of atoms thermally excited to the state $^4F_{7/2}$ which is raised by 1,530 cm^{-1} above the ground state $^4F_{9/2}$ is one-third of the number in the ground state. This is an interesting case of some advantage being derived from the use of a high oven temperature, which from other points of view (Doppler width, ease of operation) is regarded as a drawback.

From the theory of nuclear shell structure, Goeppert-Mayer (1950) predicts a spin of either $\frac{1}{2}$ or 9/2 for the rhodium nucleus. Since the experimental value is $\frac{1}{2}$ the configuration $(5g_{9/2})^6 3p_{1/2}$ for the last seven protons is suggested. This is supported by the value of the nuclear magnetic moment $-0{\cdot}10$ n.m. which lies very close to the line $I = l - \frac{1}{2}$ in the Schmidt diagram (Schmidt 1937). Since $I = \frac{1}{2}$, l must have the value 1, and the ground state of the nucleus is a $^2P_{1/2}$ state. This assignment is in disagreement with that quoted by Feenberg and Hammack (1949) as being most preferred, namely

$$(1s)^2(2p)^6(3d)^{10}(4f)^{14}\begin{bmatrix}(5g)^{12}(2s)^1\\(5g)^{13}\end{bmatrix},$$

in which the orbits $(5g)^{13}$ in square brackets refer to the ground state and $(5g)^{12}(2s)^1$ to a metastable state. If the order of these terms is inverted so that $(5g)^{12}(2s)^1$ describes the ground state, the spin $\frac{1}{2}$ is correctly given, but the small value of μ cannot be reconciled with the interpretation of the ground state as an $s_{1/2}$ term. It must therefore be concluded that at $Z = 45$ the 3p orbit is not

pushed upwards as much as is predicted by Feenberg and Hammack, and that the scheme of Goeppert-Mayer gives the better representation of the rhodium nucleus.

ACKNOWLEDGMENT

One of us (G.K.W.) is indebted to the Department of Scientific and Industrial Research for financial support.

REFERENCES

Arroe, O. H., and Mack, J. E., 1950, *J. Opt. Soc. Amer.*, **40**, 386.
Crawford, M. F., 1935, *Phys. Rev.*, **47**, 768.
Feenberg, E., and Hammack, K. C., 1949, *Phys. Rev.*, **75**, 1877.
Fowles, G. R., 1950, *Phys. Rev.*, **78**, 744.
Goeppert-Mayer, M., 1950, *Phys. Rev.*, **78**, 16.
Gurewitch, M., 1949, *Phys. Rev.*, **75**, 767.
Kopfermann, H., 1940, *Kernmomente* (Leipzig : Akademische Verlaggesellschaft), p. 111 ff.
Minkowski, R., and Bruck, H., 1935, *Z. Phys.*, **95**, 274.
Schmidt, T., 1937, *Z. Phys.*, **106**, 358.
Schüler, H., and Schmidt, T., 1934, *Naturwissenschaften*, **22**, 839.
Sibaiya, L., 1937, *Proc. Ind. Acad. Sci.* A, **6**, 229.
Sommer, L. A., 1927, *Z. Phys.*, **45**, 147.
Williams, D. T., and Granath, L. P., 1938, *Phys. Rev.*, **54**, 338.

Slow Neutron Scattering by Ferromagnetic Crystals

By R. G. MOORHOUSE
Department of Natural Philosophy, The University, Glasgow

Communicated by R. E. Peierls; *MS. received* 11*th July* 1951

ABSTRACT. Consideration is made of the predictions of the Bloch spin wave model within its region of approximate validity, for the magnetic scattering of very slow neutrons by a ferromagnetic. It is found that observable peaks of intensity in the angular distribution of scattered neutrons occur due to spin wave absorption. Neutrons are also scattered with phonon absorption and by an analogous calculation it can be shown that similar peaks occur due to this vibrational scattering. A possible method is suggested of differentiating between the two kinds of scattering in order to provide a check of the Bloch model.

§1. INTRODUCTION

Elastic magnetic scattering of slow neutrons by ferromagnetics has been the object of much theoretical study (see, for example, Halpern and Johnson 1939). In fact, in most of the work that has been done it is implicit that the elementary magnetic moments of the ferromagnetic are not changed in direction by the scattering. This is broadly true at low temperatures and for the slow neutrons used, as the neutrons will not be able to supply the exchange energy that the ferromagnetic would gain if an atomic magnetic moment turned out of the direction of magnetization of its domain.

But at higher temperatures, say, approaching half the Curie temperature, measured in absolute units, there will be in each domain a fair number of disoriented magnetic moments. Thus one would expect an effect in which the scatterer gave energy to the neutrons by means of a turn round of atomic magnetic

moment into the direction of domain magnetization. This would result in a loss of exchange energy by the scatterer. The cross section for this effect should increase with temperature and also with the wavelength of the incoming neutrons. If then the incoming neutrons had a wavelength greater than the Bragg reflection wavelength there could be no elastic magnetic scattering and energetic considerations would make an energy transfer from the neutron to the scatterer extremely unlikely. Thus, any magnetic scattering observed would be from the inelastic scattering in which the neutrons gain energy.

The main object of the work presented here is to investigate the order of magnitude and distinguishing features of this effect. The difficulty arises that the problem of ferromagnetism is by no means solved, and thus some doubt is cast on the validity of the wave functions that are used for the initial and final states of the scatterer.

At present the only wave functions that can be used for scattering calculations and that take into account the co-operative nature of ferromagnetism are those of the Bloch (1930) spin wave model. An objection to the spin wave picture is that while the wave functions give a good approximation to the solution of the Schrödinger equation at low temperatures, the problem of finding a wave function to give a good solution near the Curie point has not been overcome. However, for temperatures up to about a third of the Curie point the wave functions of the spin wave picture should be reasonably good.

Thus though the Bloch spin wave model is imperfect, it seems to be the only means, at present, of approaching the problem of inelastic magnetic scattering. Comparison of the results with experiment to investigate the predictions of the Bloch model are a useful further check on its validity.

Perturbation theory, and a simplified model of one electron per atom, are used.

§2. CROSS SECTION FOR MAGNETIC SCATTERING

After Heisenberg had demonstrated that the exchange interaction between atomic electrons provides a suitable mechanism for ferromagnetism, Bloch (1930) was able to give a simple model. Consider a crystal lattice containing one valence s-electron in each atom and with these electrons responsible for the ferromagnetism. Then an approximate eigenfunction of the total Hamiltonian, including the exchange interaction between nearest neighbours, for just one disoriented electron spin in a domain containing N ferromagnetic electrons is (Sommerfeld and Bethe 1933)

$$\Phi = N^{-1/2}(N!)^{-1/2}\sum_{Q}(\pm Q)\sum_{l}\exp(i\mathbf{k}\mathbf{R}_l)\Psi_1(r_1)S_{1/2}(s_1)$$
$$\ldots\ \Psi_l(r_l)S_{-1/2}(s_l)\ \ldots\ \Psi_N(r_N)S_{1/2}(s_N). \qquad \ldots\ldots(2.1)$$

$\mathbf{k}$ is a vector of the form $\mathbf{k}=(2\pi/a)(n_1/N_1,\ n_2/N_2,\ n_3/N_3)$ where a is the side of the unit cell, assumed to be cubic, N_1, N_2, N_3 are large integers with N_1a, N_2a, N_3a the sides of the domain of the crystal considered and n_1, n_2, n_3 is an integral vector. $(\pm Q)$ is the operator of permutation of both the electron space and spin coordinates (r, s), according as the permutation is even or odd. $\mathbf{R}_l$ is the position vector of the lth atom and runs over all the atoms, the spin of the electron on the lth atom being the one that is reversed. Ψ_l is the space wave function of the electron on the lth atom and S the spin wave function, $S_{1/2}$ denoting an electron spin oriented in one direction and $S_{-1/2}$ an orientation

in the opposite direction. The electron wave functions $\Psi_1, \Psi_2 \ldots, \Psi_N$ are equal in shape, but are centred round different origins, namely, the nuclei of the various atoms of the crystal. $N^{-1/2}(N!)^{-1/2}$ is a normalizing factor.

The normalized wave function for no disoriented spins in the domain is

$$\Phi' = (N!)^{-1/2}\sum_Q (\pm Q)\Psi_1(r_1)S_{1/2}(s_1) \ldots \Psi_l(r_l)S_{1/2}(s_l) \ldots \Psi_N S_{1/2}(s_N). \quad \ldots\ldots(2.2)$$

Taking s-electrons instead of d-electrons as carriers of the ferromagnetism is not significant. For the orbital current of the d-electrons in a crystalline ferromagnetic is quenched and the ferromagnetism is wholly due to the spin.

Scattering by a single crystal is investigated where the quantum mechanical scattering unit is the magnetic domain. As the scattering is inelastic the contribution from the different scattering units will superpose incoherently. In a magnetized crystal the scattering unit is the whole crystal.

Suppose now that a neutron beam, taken unpolarized for simplicity and with the neutrons having wavelength greater than the Bragg reflection wavelength, is inelastically scattered, the scatterer going from state Φ to state Φ'. Thus one spin wave of wave vector $\mathbf{k}$ is annihilated. The scatterer is the ferromagnetic domain and perturbation theory is used. Then the scattered wave of the neutron and the domain for the neutron at a large distance r from the scatterer is (Halpern and Johnson 1939), with unit density of incident neutrons,

$$\Psi = \frac{2\pi M}{\hbar^2}\sum_{s'} r^{-1} \exp(i\mathbf{p}'\mathbf{r})\chi_{s'}\Phi'(\Phi', \chi_{s'}, \mathbf{p}'|V|\Phi, \chi_s, \mathbf{p}). \quad \ldots\ldots(2.3)$$

Primes indicate final states. p is the wave number of the neutron, χ_s the spin state of the neutron, M is the neutron mass, $(\hbar^2/2M)(p^2 - p'^2) = E' - E$, E being the energy of the scatterer. For a body-centred cubic lattice, for instance (Sommerfeld and Bethe 1933, eqn. 6.20)

$$E = E_0 + E(\mathbf{k}), \quad E(\mathbf{k}) = 8J(1 - \cos \tfrac{1}{2}k_1 a \cos \tfrac{1}{2}k_2 a \cos \tfrac{1}{2}k_3 a), \quad \ldots\ldots(2.4)$$

J being the positive exchange integral, and it is found for any crystal lattice, when $|\mathbf{k}|a$ is small, that

$$E(\mathbf{k}) = Jk^2a^2, \quad \ldots\ldots(2.5)$$

so that

$$\frac{\hbar^2}{2M}(p^2 - p'^2) = -Jk^2a^2. \quad \ldots\ldots(2.6)$$

V is the energy of interaction between the neutron and the ferromagnetic electrons (Halpern and Johnson 1939)

$$V = e\boldsymbol{\mu}\frac{\boldsymbol{\alpha}_l \times (\mathbf{r} - \mathbf{r}_l)}{|\mathbf{r} - \mathbf{r}_l|^3}, \quad \ldots\ldots(2.7)$$

$\mathbf{r}$ is the position vector of the neutron, $\mathbf{r}_l$ that of the lth electron, $\boldsymbol{\alpha}_l$ is the Dirac matrix vector for the lth electron and $\boldsymbol{\mu}$ is the magnetic moment of the neutron

$$\boldsymbol{\mu} = (e\hbar/2Mc)\gamma\mathbf{s}, \quad \ldots\ldots(2.8)$$

γ being the ratio of the neutron magnetic moment to the nuclear magneton.

$$(\mathbf{p}', \chi_{s'}, \Phi'|V|\mathbf{p}, \chi_s, \Phi) = \int d^3\mathbf{r}_l\, d^3\mathbf{r}[S_{1/2}{}^{\dagger}\Psi_l{}^{*}(\mathbf{r}_l)\boldsymbol{\alpha}_l S_{-1/2}\Psi_l(r_l)]\frac{(\mathbf{r} - \mathbf{r}_l)}{|\mathbf{r} - \mathbf{r}_l|^3}$$
$$\cdot(\chi_{s'}|e\boldsymbol{\mu}|\chi_s)\exp\{i(\mathbf{p} - \mathbf{p}')\mathbf{r}\}[\sum_{j=1}^{M}\exp\{i\mathbf{R}_j(\mathbf{k} - \mathbf{q})\}]N^{-1/2}. \quad \ldots\ldots(2.9)$$

The origin of the vectors $\mathbf{r}$ and $\mathbf{r}_l$ is the centre of atom l (the choice of atom l is, of course, quite arbitrary and immaterial); $\mathbf{q}=\mathbf{p}'-\mathbf{p}$. Equation (2.9) can be evaluated by the method given by Halpern and Johnson (1939). It is then found that the differential cross section per atom for scattering of the neutron into the angle $d\omega_{p'}$ with absorption of the spin wave $\mathbf{k}$ is

$$\left(\frac{2e^2\gamma}{mc^2}\right)^2 \frac{1}{N^2}\frac{1}{16}\frac{p'}{p}d\omega_{p'}DF^2S \qquad \ldots\ldots(2.10)$$

where

$$F=\int\Psi^*(r_l)\Psi(r_l)\exp(-i\mathbf{q}\cdot\mathbf{r}_l)d^3r_l \qquad \ldots\ldots(2.11)$$

$$S=1+e_m^2, \quad \mathbf{e}=(\mathbf{p}-\mathbf{p}')/|\mathbf{p}-\mathbf{p}'|=-\mathbf{q}/|\mathbf{q}| \qquad \ldots\ldots(2.12)$$

and e_m is the component of $\mathbf{e}$ in the direction of magnetization of the domain. $d\omega_{p'}$ is the differential scattering (solid) angle.

$$D=|\sum_j \exp\{i\mathbf{R}_j(\mathbf{k}-\mathbf{q})\}|^2$$

$$D=|\sum_i \exp\{i\mathbf{R}_i(\mathbf{k}-\mathbf{q})\}|^2\,|\sum_f\{\exp i\mathbf{k}_f(\mathbf{k}-\mathbf{q})\}|^2. \qquad \ldots\ldots(2.13)$$

In the first factor on the right-hand side of (2.13) summation is carried out over all the unit cells in the crystal and in the second over all atoms in any one elementary cell; therefore

$$D=\frac{\sin^2(\mathbf{k}-\mathbf{q})_1\tfrac{1}{2}N_1a\sin^2(\mathbf{k}-\mathbf{q})_2\tfrac{1}{2}N_2a\sin^2(\mathbf{k}-\mathbf{q})_3\tfrac{1}{2}N_3a}{\sin^2(\mathbf{k}-\mathbf{q})_1\tfrac{1}{2}a\sin^2(\mathbf{k}-\mathbf{q})_2\tfrac{1}{2}a\sin^2(\mathbf{k}-\mathbf{q})_3\tfrac{1}{2}a}|\sum_f\exp\{iR_j(\mathbf{k}-\mathbf{q})\}|^2. \qquad \ldots\ldots(2.14)$$

Up to now the scatterer has been taken to have only one disoriented electronic spin, that is only one spin wave. On the assumption that there are few spin waves and that they do not interact, the differential cross section per atom for annihilation of a spin wave $\mathbf{k}$, if there are initially $L_\mathbf{k}$ spin waves with wave vector $\mathbf{k}$ is

$$\left(\frac{2e^2\gamma}{mc^2}\right)^2 \frac{L_\mathbf{k}}{N^2}\frac{1}{16}d\omega_{p'}\frac{p'}{p}DF^2S. \qquad \ldots\ldots(2.15)$$

This corresponds to equation (2.10). The approximation of non-interacting spin waves is probably adequate when the proportion of disoriented spins is small. And for temperatures up to about one-third of the Curie temperature the number of wrong spins is small.

In this approximation equations (2.4) and (2.6) still hold.

§3. SCATTERING BY A SINGLE CRYSTAL

For variations of $\mathbf{k}$ or $\mathbf{p}'$ large compared with $2\pi a/N_i$, we may substitute for D the expression

$$(2\pi/a)^3N_1N_2N_3N_f^2\Sigma_\mathbf{n}\delta(\mathbf{k}+\mathbf{p}-\mathbf{p}'-2\pi\mathbf{n}/a). \qquad \ldots\ldots(3.1)$$

N_f is the number of atoms in any elementary cell. Thus $N_1N_2N_3N_f=N$. The summation over $\mathbf{n}$ is over all integral vectors including zero for which $\Sigma_f\exp(2\pi i\mathbf{R}_f\mathbf{n}/a)\neq 0$; that is $2\pi\mathbf{n}/a$ is in the reciprocal lattice. We shall consider the wavelength of the neutron as greater than the Bragg reflection wavelength. It can be shown that for this case scattering with excitation of a spin wave, and the neutron losing energy, does not take place into appreciable angles, for $p'<p$, and k (given by (2.4) with a change of sign on the right-hand side) cannot be large enough for $\mathbf{k}+\mathbf{p}-\mathbf{p}'-2\pi\mathbf{n}/a$ to be zero for $\mathbf{n}\neq 0$. The case of elastic scattering gives rise to a function $\Sigma_\mathbf{n}\delta(\mathbf{p}-\mathbf{p}'-2\pi\mathbf{n}/a)$ and there is no elastic angular scattering for long wavelengths.

The total cross section, for the initial neutron wavelength greater than the Bragg reflection wavelength, is, ignoring the small angle contribution from $\mathbf{n}=0$,

$$\boldsymbol{\sigma}=\sum_{\mathbf{n}\neq 0}\sigma_{\mathbf{n}} \qquad \ldots\ldots(3.2)$$

where

$$\sigma_{\mathbf{n}}=\left(\frac{2e^2\gamma}{mc^2}\right)^2\int d^3\mathbf{k}\int\frac{p'}{p}\,d\omega_{p'}F^2(p-p')$$
$$\delta(\mathbf{k}+\mathbf{p}-\mathbf{p}'-2\pi\mathbf{n}/a)\tfrac{1}{16}(1+e_{\mathrm{m}}{}^2)L_{\mathbf{k}}. \qquad \ldots\ldots(3.3)$$

This follows from equation (2.15) by summing over $\mathbf{k}$ and replacing the summation by an integration:

$$\int\frac{N_1N_2N_3a^3}{(2\pi)^3}\,d^3\mathbf{k}.$$

$L_{\mathbf{k}}$ is the number of spin waves in the scatterer having wave vector $\mathbf{k}$.

The spin waves obey Bose statistics, so the cross section for scattering at an absolute temperature T is given by substituting in (3.3)

$$L_{\mathbf{k}}=1/(\exp\{E(\mathbf{k})/\boldsymbol{k}T\}-1) \qquad \ldots\ldots(3.4)$$

where $\boldsymbol{k}$ is Boltzmann's constant, and $E(\mathbf{k})$ is defined in (2.4). Suppose that ka is small enough for (2.5) to hold. Then from (2.6) and (3.3) the following two relations are fulfilled

$$p'^2=p^2+\alpha k^2 \quad \ldots\ldots(3.5) \qquad\qquad \mathbf{p}'-\mathbf{p}_1=\mathbf{k} \quad \ldots\ldots(3.6)$$

where $\alpha=2JMa^2/\hbar^2\gg 1$, $\mathbf{p}_1=\mathbf{p}-2\pi\mathbf{n}/a$. Then (3.5) and (3.6) give, by elimination of $\mathbf{k}$,

$$(\alpha-1)p'^2-2p_1p'\alpha\cos\theta+(\alpha+1)p_1{}^2-Qp_1{}^2=0 \qquad \ldots\ldots(3.7)$$

where θ is the angle between $\mathbf{p}'$ and $\mathbf{p}_1$ and where

$$p_1{}^2Q=\left(\frac{2\pi}{a}\right)^2\mathbf{n}^2-\frac{4\pi}{a}\,\mathbf{n}\,.\,\mathbf{p}=-\left(\frac{2\pi}{a}\right)^2\mathbf{n}^2-\frac{4\pi}{a}\,\mathbf{n}\,.\,\mathbf{p}_1, \qquad \ldots\ldots(3.8)$$

whence

$$p'=p_1\frac{\alpha\cos\theta\pm\{\alpha^2\cos^2\theta-\alpha^2+1+(\alpha-1)Q\}^{1/2}}{(\alpha-1)}. \qquad \ldots\ldots(3.9)$$

Both the positive and negative signs in the numerator give equally valid solutions. For, take $\mathbf{p}_1$ as polar axis and take the usual coordinates p', θ, ϕ for the end point of the vector $\mathbf{p}'$. To find the possible values of $\mathbf{p}'$, satisfying (3.5) and (3.6), that lie in any plane $\phi=$ constant (which, of course, contains the vectors $\mathbf{p}'$, $\mathbf{p}_1$ and $\mathbf{k}$), first take a z axis perpendicular to the plane, as shown in the Figure. Then construct the surfaces of revolution $z=p'^2$ and $z=p^2+\alpha(\mathbf{p}'-\mathbf{p}_1)^2$. Project the line of intersection of the two surfaces perpendicularly on to the plane $\phi=$ constant. The end point of $\mathbf{p}'$ then moves on this projection in the plane $\phi=$ constant. As every plane $\phi=$ constant is equivalent the end point of $\mathbf{p}'$ moves on the surface of revolution given by rotating the projection round the polar axis. This shows how to each value of θ, ϕ correspond two values of $\mathbf{p}'$. From (3.5) and (3.9)

$$k^2=p_1{}^2(2\alpha\cos^2\theta-2\alpha+2+(\alpha-1)Q\pm 2\cos\theta\,\{\alpha^2\cos^2\theta-\alpha^2$$
$$+1+(\alpha-1)Q\}_{1/2}/(\alpha-1)^2. \qquad \ldots\ldots(3.10)$$

For the sake of definiteness, take now the scatterer as being an unmagnetized crystal of a body-centred cubic lattice. The wave number corresponding to the Bragg reflection wavelength is $2\pi/a\sqrt{2}$. Thus if $p=2\pi\kappa/a$, $\kappa<1/\sqrt{2}$. Taking the vectors of the reciprocal lattice as axes, consider as examples of the two cases $\mathbf{p}=(2\pi/a)\,(\kappa,0,0)$, $\mathbf{p}=(2\pi/a)\,(\kappa/\sqrt{3},\kappa/\sqrt{3},\kappa/\sqrt{3})$.

In Table 1 are given the values of p_1^2 and of Q for the lowest values of $\mathbf{n}$. As will be seen later the higher values are not so important. In the body-centred lattice only those values of $\mathbf{n}$ occur, the sum of whose components is even (see equation (2.14)). Numbers are given for the particular case $\kappa = \frac{1}{2}$.

It is seen that $Q < 1$. Though it is possible for Q to be zero when κ has its limiting value ($1/\sqrt{2}$ in the body-centred case), for smaller values of κ it is seen from Table 1 that $Q \sim 1$. Unless otherwise stated the values of Q in what follows are such that $Q \sim 1$.

The limits of θ are, from (3.10),

$$Q/\alpha \sim \{1 + (\alpha - 1)Q\}/\alpha^2 \geqslant \sin^2\theta \geqslant 0 \qquad \ldots\ldots(3.11)$$

also

$$k^2/p_1^2 = Q/\alpha + O(1/\alpha^{3/2}). \qquad \ldots\ldots(3.12)$$

Now

$$\alpha = \frac{2JMa^2}{\hbar^2} = \frac{J}{\boldsymbol{k}\Theta}\frac{\boldsymbol{k}\Theta}{(\hbar^2/2Ma^2)}, \qquad \ldots\ldots(3.13)$$

where Θ is the Curie temperature. For a body-centred cubic $J/\boldsymbol{k}\Theta = 1/6{\cdot}1$ (Sommerfeld and Bethe 1933). Thus, taking the constants and body-centred lattice structure of iron, $a = 2{\cdot}85$ A., $\Theta = 1{,}043\ 0°$ K., $\alpha = 62$. From (3.12)

$$k^2a^2 \simeq (Q/\alpha)p_1^2a^2 = (4\pi^2Q/\alpha)(ap_1/2\pi)^2. \qquad \ldots\ldots(3.14)$$

Thus the expansion of $E(\mathbf{k})$ (equations (2.4), (2.5)) is certainly valid for $(ap_1/2\pi)^2 \leqslant 1$, for a body-centred cubic.

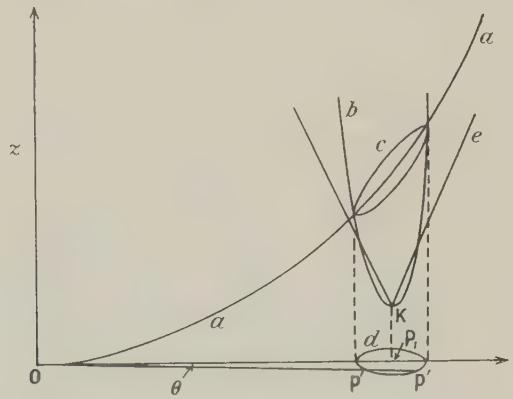

a, paraboloid $z = p'^2$; *b*, paraboloid $z = p^2 + \alpha(\mathbf{p}' - \mathbf{p}_1)^2$; *c*, intersection of A and B ; *d*, projection of C ; *e*, cone for phonon absorption. $(P_1K)^2 = p^2$ $\overrightarrow{OP}_1 = \mathbf{p}_1$ $\overrightarrow{OP}' = \mathbf{p}'$.

To evaluate the cross section (3.3) the values of $L_{\mathbf{k}}$ are needed. For ka small enough it is found, using in turn (2.5), (3.12), (3.13)

$$E(\mathbf{k})/\boldsymbol{k}T = (ap_1/2\pi)^2Q(110/T). \qquad \ldots\ldots(3.15)$$

It is thus evident that at room temperatures or higher and for $(ap_1\,2\pi)^2 \lesssim 1$ a good approximation for $L_{\mathbf{k}}$ is given by

$$L_{\mathbf{k}} = \frac{2M\boldsymbol{k}T}{\hbar^2 p_1^2 Q} = \frac{T}{110}\frac{1}{Q(ap_1/2\pi)^2}. \qquad \ldots\ldots(3.16)$$

In Table 2 values of k^2a^2 and $\sigma_{\mathbf{n}}$ are given, worked out on the assumption that (2.3) and (3.16) are valid. As the crystal is assumed to be unmagnetized e_m^2 is replaced by its average, $\frac{1}{3}$.

This assumption is made only to simplify the formulae. In fact, from the point of view of theoretical prediction it is rather better to have a magnetized

crystal, for then no question arises, such as for instance, the smallness of domain size affecting the theory. For a magnetized crystal the cross sections $\sigma_{\mathbf{n}}$ given below must be multiplied by $\frac{3}{4}(1+n_{\mathrm{m}}^2)$, where n_{m} is the component of $\mathbf{n}$ in the direction of magnetization.

Using (3.3), (3.9), (3.11), (3.16) and (3.17) it follows that

$$\sigma_{\mathbf{n}}=2\left(\frac{2e^2\gamma}{mc^2}\right)^2\int_{\cos\theta}^{1}{}_{(1-\frac{1}{2}Q/\kappa)}\frac{p_1}{p}\frac{2\pi\cos\theta}{12}d(\cos\theta)\left(\frac{T}{110}\right)\frac{1}{Q(ap_1/2\pi)^2}F^2(2\pi\mathbf{n}/a-\mathbf{k}). \quad \ldots\ldots(3.17)$$

The factor 2 in front comes from the fact that to each value of $\cos\theta$ in the range (3.11) correspond two values of $\mathbf{p}'$.

Table 1

$\mathbf{n}$	$\mathbf{p}=(2\pi/a)(\kappa,0,0)$ $\left(\frac{p_1}{2\pi/a}\right)^2$	$\kappa=\frac{1}{2}$	Q	$\kappa=\frac{1}{2}$	$\mathbf{p}=(2\pi/a)(\kappa,\kappa,\kappa)/\sqrt{3}$ $\left(\frac{p_1}{2\pi/a}\right)^2$	$\kappa=\frac{1}{2}$	Q	$\kappa=\frac{1}{2}$
(0, 0, 0)	κ^2	$\frac{1}{4}$	0	0	κ^2	$\frac{1}{4}$	0	0
(1, 1, 0)	$2-2\kappa+\kappa^2$	$\frac{5}{4}$	$\frac{2-2\kappa}{2-2\kappa+\kappa^2}$	$\frac{4}{5}$	$2-2\cdot3\kappa+\kappa^2$	1·1	$\frac{2-2\cdot3\kappa}{2-2\cdot3\kappa+\kappa^2}$	0·77
(1, −1, 0)	$2-2\kappa+\kappa^2$	$\frac{5}{4}$	$\frac{2-2\kappa}{2-2\kappa+\kappa^2}$	$\frac{4}{5}$	$2+\kappa^2$	2·25	$\frac{2}{2+\kappa^2}$	0·88
(−1, 1, 0)	$2+2\kappa+\kappa^2$	$\frac{13}{4}$	$\frac{2+2\kappa}{2+2\kappa+\kappa^2}$	$\frac{12}{13}$	$2+\kappa^2$	2·25	$\frac{2}{2+\kappa^2}$	0·88
(−1, −1, 0)	$2+2\kappa+\kappa^2$	$\frac{13}{4}$	$\frac{2+2\kappa}{2+2\kappa+\kappa^2}$	$\frac{12}{13}$	$2+2\cdot3\kappa+\kappa^2$	3·4	$\frac{2+2\cdot3\kappa}{2+2\cdot3\kappa+\kappa^2}$	0·92
(1, 0, 1)	$2-2\kappa+\kappa^2$	$\frac{5}{4}$	$\frac{2-2\kappa}{2-2\kappa+\kappa^2}$	$\frac{4}{5}$	$2-2\cdot3\kappa+\kappa^2$	1·1	$\frac{2-2\cdot3\kappa}{2-2\cdot3\kappa+\kappa^2}$	0·77
(1, 0, −1)	$2-2\kappa+\kappa^2$	$\frac{5}{4}$	$\frac{2-2\kappa}{2-2\kappa+\kappa^2}$	$\frac{4}{5}$	$2+\kappa^2$	2·25	$\frac{2}{2+\kappa^2}$	0·88
(−1, 0, 1)	$2+2\kappa+\kappa^2$	$\frac{13}{4}$	$\frac{2+2\kappa}{2+2\kappa+\kappa^2}$	$\frac{12}{13}$	$2+\kappa^2$	2·25	$\frac{2}{2+\kappa^2}$	0·88
(−1, 0, −1)	$2+2\kappa+\kappa^2$	$\frac{13}{4}$	$\frac{2+2\kappa}{2+2\kappa+\kappa^2}$	$\frac{12}{13}$	$2+2\cdot3\kappa+\kappa^2$	3·4	$\frac{2+2\cdot3\kappa}{2+2\cdot3\kappa+\kappa^2}$	0·92
(0, 1, 1)	$2+\kappa^2$	$\frac{9}{4}$	$\frac{2}{2+\kappa^2}$	$\frac{8}{9}$	$2-2\cdot3\kappa+\kappa^2$	1·1	$\frac{2-2\cdot3\kappa}{2-2\cdot3\kappa+\kappa^2}$	0·77
(0, 1, −1)	$2+\kappa^2$	$\frac{9}{4}$	$\frac{2}{2+\kappa^2}$	$\frac{8}{9}$	$2+\kappa^2$	2·25	$\frac{2}{2+\kappa^2}$	0·88
(0, −1, 1)	$2+\kappa^2$	$\frac{9}{4}$	$\frac{2}{2+\kappa^2}$	$\frac{8}{9}$	$2+\kappa^2$	2·25	$\frac{2}{2+\kappa^2}$	0·88
(0, −1, −1)	$2+\kappa^2$	$\frac{9}{4}$	$\frac{2}{2+\kappa^2}$	$\frac{8}{9}$	$2+2\cdot3\kappa+\kappa^2$	3·4	$\frac{2+2\cdot3\kappa}{2+2\cdot3\kappa+\kappa^2}$	0·92

Equation (3.17) is not an exact formula for $\sigma_{\mathbf{n}}$, but within the limitations given is a good approximation. It can be seen from the column C in Table 2 how good the approximation for $L_{\mathbf{k}}$ is, and from column A how good the approximation Jk^2a^2 for the energy change is. It is seen, for example, that for $\mathbf{p}=(2\pi/a)(\frac{1}{2},0,0)$ the $\sigma_{\mathbf{n}}$ given is a very good approximation for $\mathbf{n}=(1,1,0)$

$(1,-1,0)$ $(1,0,1)$ $(1,0,-1)$,while for the other values of $\mathbf{n}$ tabulated it holds in order of magnitude.

From column A it is evident that $F^2(2\pi\mathbf{n}/a-\mathbf{k})$ can be replaced by $F^2(2\pi\mathbf{n}/a)$ since $|\mathbf{k}| \ll |2\pi\mathbf{n}/a|$. Various estimates of F have been made by various authors in connection with elastic magnetic scattering of neutrons by iron. If then we take, consistently with the previous assumptions for the lattice constant and the Curie temperature, the form factor to be the same as that for the 3d electrons of iron, we can make use of the previous estimates.

Table 2

	$\mathbf{p}=(2\pi/a)(\kappa,0,0)$				$\mathbf{p}=(2\pi/a)(\kappa,\kappa,\kappa)/\sqrt{3}$			
	A		B	C	A		B	C
$\mathbf{n}$	k^2a^2		$\sigma_{\mathbf{n}}$(barns)	$E(\mathbf{k})/kT$	k^2a^2		$\sigma_{\mathbf{n}}$ (barns)	$E(\mathbf{k})/k$
		$\kappa=\frac{1}{2}$	$\kappa=\frac{1}{2}$	$\kappa=\frac{1}{2}$		$\kappa=\frac{1}{2}$	$\kappa=\frac{1}{2}$	$\kappa=\frac{1}{2}$
$(1,1,0)$	$\frac{4\pi^2}{\alpha}(2-2\kappa)$	$\frac{2}{3}$	$G\sqrt{\frac{4}{5}}$	$\frac{110}{T}$	$\frac{4\pi^2}{\alpha}(2-2{\cdot}3\kappa)$	0·57	$G\sqrt{\frac{1}{1{\cdot}1}}$	$\frac{110}{T}$ 0·8
$(1,-1,0)$	$\frac{4\pi^2}{\alpha}(2-2\kappa)$	$\frac{2}{3}$	$G\sqrt{\frac{4}{5}}$	$\frac{110}{T}$	$\frac{4\pi^2}{\alpha}(2)$	1·3	$G\sqrt{\frac{1}{2{\cdot}25}}$	$\frac{110}{T}$ 2
$(-1,1,0)$	$\frac{4\pi^2}{\alpha}(2-2\kappa)$	2	$G\sqrt{\frac{4}{13}}$	$\frac{110}{T}$ 3	$\frac{4\pi^2}{\alpha}(2)$	1·3	$G\sqrt{\frac{1}{2{\cdot}25}}$	$\frac{110}{T}$ 2
$(-1,-1,0)$	$\frac{4\pi^2}{\alpha}(2-2\kappa)$	2	$G\sqrt{\frac{4}{13}}$	$\frac{110}{T}$ 3	$\frac{4\pi^2}{\alpha}(2+2{\cdot}3\kappa)$	2·1	$G\sqrt{\frac{1}{3{\cdot}4}}$	$\frac{110}{T}$ 3·1
$(1,0,1)$	$\frac{4\pi^2}{\alpha}(2-2\kappa)$	$\frac{2}{3}$	$G\sqrt{\frac{4}{5}}$	$\frac{110}{T}$	$\frac{4\pi^2}{\alpha}(2-2{\cdot}3\kappa)$	0·57	$G\sqrt{\frac{1}{1{\cdot}1}}$	$\frac{110}{T}$ 0·8
$(1,0,-1)$	$\frac{4\pi^2}{\alpha}(2-2\kappa)$	$\frac{2}{3}$	$G\sqrt{\frac{4}{5}}$	$\frac{110}{T}$	$\frac{4\pi^2}{\alpha}(2)$	1·3	$G\sqrt{\frac{1}{2{\cdot}25}}$	$\frac{110}{T}$ 2
$(-1,0,1)$	$\frac{4\pi^2}{\alpha}(2+2\kappa)$	2	$G\sqrt{\frac{4}{13}}$	$\frac{110}{T}$ 3	$\frac{4\pi^2}{\alpha}(2)$	1·3	$G\sqrt{\frac{1}{2{\cdot}25}}$	$\frac{110}{T}$ 2
$(-1,0,-1)$	$\frac{4\pi^2}{\alpha}(2+2\kappa)$	2	$G\sqrt{\frac{4}{13}}$	$\frac{110}{T}$ 3	$\frac{4\pi^2}{\alpha}(2+2{\cdot}3\kappa)$	2·1	$G\sqrt{\frac{1}{3{\cdot}4}}$	$\frac{110}{T}$ 3·1
$(0,1,1)$	$\frac{4\pi^2}{\alpha}2$	$\frac{4}{3}$	$G\sqrt{\frac{4}{9}}$	$\frac{110}{T}$ 2	$\frac{4\pi^2}{\alpha}(2-2{\cdot}3\kappa)$	0·57	$G\sqrt{\frac{1}{1{\cdot}1}}$	$\frac{110}{T}$ 0·8
$(0,1,-1)$	$\frac{4\pi^2}{\alpha}2$	$\frac{4}{3}$	$G\sqrt{\frac{4}{9}}$	$\frac{110}{T}$ 2	$\frac{4\pi^2}{\alpha}(2)$	1·3	$G\sqrt{\frac{1}{2{\cdot}25}}$	$\frac{110}{T}$ 2
$(0,-1,1)$	$\frac{4\pi^2}{\alpha}2$	$\frac{4}{3}$	$G\sqrt{\frac{4}{9}}$	$\frac{110}{T}$ 2	$\frac{4\pi^2}{\alpha}(2)$	1·3	$G\sqrt{\frac{1}{2{\cdot}25}}$	$\frac{110}{T}$ 2
$(0,-1,-1)$	$\frac{4\pi^2}{\alpha}2$	$\frac{4}{3}$	$G\sqrt{\frac{4}{9}}$	$\frac{110}{T}$ 2	$\frac{4\pi^2}{\alpha}(2+2{\cdot}3\kappa)$	2·1	$G\sqrt{\frac{1}{3{\cdot}4}}$	$\frac{110}{T}$ 3·1

$$G=\frac{T}{110}\frac{1}{\alpha}F^2\left(\frac{2\pi}{a}\mathbf{n}\right)$$

Hamermesh (1942) calculated F using Hartree wave functions for free iron atoms. Steinberger and Wick (1949) took into account the Fock exchange integrals of a 3d electron with all other shells and with its own. Values of $F^2(2\pi\mathbf{n}/a)$ are given in Table 3. $N(n^2)$ is the number of values of $\mathbf{n}$ such that $\mathbf{n}^2=n^2$.

It is evident from Table 3 that $\Sigma_{n^2>2}\sigma_{\mathbf{n}}$ is small. For the increase in $N(n^2)$ is more than compensated by the decrease in F^2, while the value of any particular $\sigma_{\mathbf{n}}$ decreases rapidly with increasing $\mathbf{n}$ due to the factor $1/\exp\{E(\mathbf{k})/\boldsymbol{k}T\}-1$ in the integrand. Taking the higher, and probably better, value of Steinberger and Wick for F^2, it is seen from Table 2 and equation (3.17) that the cross section for scattering into a solid angle of $\pi Q/\alpha$ radians around the direction, approximately, of $(\mathbf{p}-2\pi\mathbf{n}/a)$ for $\mathbf{p}=(2\pi/a)(\frac{1}{2}, 0, 0)$ and $\mathbf{n}=(1, 1, 0)$, and $T=400°$ K. is about 1/50. A value of 62 has been used for α. Since $\pi Q/\alpha$ is about 1/25, this corresponds to a differential cross section of approximately 0·5 barn per steradian. Taking, as usual, the structure for iron it is seen that the mean free path for this $\mathbf{n}$-type scattering (with $\mathbf{n}=(1, 1, 0)$, $\mathbf{p}=(2\pi/a)(\frac{1}{2}, 0, 0)$, $T=400°$ K.) is about 580 cm.

Table 3

$\mathbf{n}^2$		2	4	6	8	10	12
$N(n^2)$		12	6	24	12	24	6
$F^2(2\pi\mathbf{n}/a)$	H.	0·23	0·078	0·036	0·014	0·0064	0·0028
	S. & W.	0·36	0·2	0·1	0·048	0·025	0·014

H.=Hamermesh ; S. & W.=Steinberger and Wick.

It is in the high-temperature range that the assumption of non-interaction of spin waves begins to part with reality, so little confidence can be placed on the predictions of (3.17) for T above half the Curie temperature.

The calculations of this section have been carried out for a crystal of 'ideal iron', which has the lattice structure and Curie temperature of iron, but only one ferromagnetic electron per atom. The construction of a model with two spins per atom, which approximates closely to real iron (2.2 spins per atom), is more complicated, though it presents no fundamental difficulties. In such a theory the general features of the present model would be preserved. The peculiar angular distribution of the scattering depends on the energy and momentum equations—equations (3.5) and (3.6). In a two spin per atom model these equations would still hold, but there would be two possible equations corresponding to (3.5). Consider the spin of the two electrons, which will be coupled (Mott and Jones 1936) as quantized in the direction of magnetization. Then one equation (3.5), with a constant α_1, will correspond to electron spin transitions $-1\rightarrow 0$. The other, with constant α_2, will correspond to the electron spin transition $0\rightarrow 1$. Both α_1 and α_2 will be somewhat smaller than α, because they correspond to one energy change while the Curie temperature corresponds to two. Thus with the two spin model there will be the two kinds of scattering (that is, with α_1 and α_2 respectively) superimposed. Decrease in α leads to an increase in the angular range for each part $\sigma(\mathbf{n})$ of the scattering (see equation (3.18)), while leaving the differential cross section unaltered. Thus with the two spin per atom model an increase in the angular spread round the directions $\mathbf{p}-2\pi\mathbf{n}/a$, and an increase in the total cross section, is to be expected.

For neutrons of wavelength greater than the Bragg reflection wavelength elastic nuclear scattering will be small and isotropically distributed. It is due to presence of isotopes and nuclei with spin and is less than 0·25 barn per steradian (Cassels and Latham 1948). This small isotropic background of elastic scattering provides no obstacle to the observation of spin wave peaks.

However, the neutron beam undergoes thermo-vibrational scattering (Weinstock 1944), both through magnetic and through nuclear forces. In fact,

the very slow neutrons considered will be scattered with absorption of phonons in the same way as they are scattered with absorption of spin waves.

In order to gain some insight into this effect, the Debye approximation—that the energy of a phonon of wave vector $\mathbf{k}$ is $\hbar c_1 |\mathbf{k}|$ where c_1 is the constant average sound velocity—is used. In this approximation the difference between transverse and longitudinal sound velocities is neglected for simplicity. The approximation of a sound velocity independent of wavelength holds for $\hbar c_1 |\mathbf{k}| \lesssim \frac{1}{2}\Theta_D$ where Θ_D is the Debye temperature (or $|\mathbf{k}| < \pi/a$ in iron). The effect of phonon absorption can be found by a calculation similar to that just performed, with $(2Mc_1/\hbar)|\mathbf{k}|$ put for αk^2 on the right-hand side of equation (3.5). For example, the only change in finding the scattering angle is that the paraboloid b in the Figure is replaced by the cone e. Thus the maxima that occur due to phonon absorption are centred in the same directions as those due to spin wave absorption.

For the maximum corresponding to $\mathbf{p}=(2\pi/a)(\frac{1}{2}, 0, 0)$, $\mathbf{n}=(1, 1, 0)$ phonon absorption gives a differential cross section of 0·5 barn per steradian (with nuclear vibrational scattering dominating magnetic vibrational scattering). The angular range of the peak is of the same order as the angular range of the corresponding spin wave absorption peak on the one spin per atom model. The Debye approximation holds for the low frequency phonons absorbed to make this peak. But for $\mathbf{p}=(2\pi/a)(\frac{1}{2}, 0, 0)$ $\mathbf{n}=(-1, 1, 0)$ OP_1 (see Figure) is greater than in the preceding example, and thus the cone e (phonon absorption) cuts a very much outside the intersection of b with a. This shows, if the Debye approximation holds, that the phonon peak has a very much greater angular spread than the corresponding spin wave peak. In fact, the Debye approximation is probably beginning to break down for the high-frequency phonons absorbed to make this peak. But it can be qualitatively seen that the peak is much broader and less intense than the corresponding spin wave peak (Table 2).

An increase in the differential cross section of 0·5 barn per steradian, such as is predicted for some spin wave peaks, should be well observable with the neutron fluxes available from piles. Another possibility of observing the effect comes from the fact that (equations (3.12), (3.5)) the energy of the scattered neutrons is approximately $(\hbar^2/2M)(p_1^2+p^2)$. For $p=(2\pi/a)(\frac{1}{2}, 0, 0)$ $\mathbf{n}=(1, 1, 0)$ this is about five times the energy of the incoming neutrons. The different variation with $\mathbf{n}$ of spin wave and phonon peaks (as outlined in the last paragraph) might well serve to distinguish the two. The magnetic properties of spin wave peaks also offer a means of distinction.

For a magnetized crystal and unpolarized neutrons the cross section of Table 2 should be multiplied by $\frac{3}{4}(1+n_m^2)$. This factor varies between $\frac{3}{4}$ and $\frac{3}{2}$, according to the relative orientation of $\mathbf{n}$ and the direction of magnetization. If the Bloch spin wave model were correct, the variation of cross section with the direction of magnetization of the crystal could presumably be observed. This variation with magnetization is characteristic of spin wave absorption, and thus may provide a test of the Bloch model. (A, different, variation occurs also for the magnetic part of the scattering with phonon absorption, but calculation shows this scattering to be almost certainly negligible.)

The above analysis is for monochromatic neutrons, but if the direction of the incoming neutrons, that is the direction of $\mathbf{p}$, is the same as the direction $\mathbf{n}$, a peak will be observed in the direction $\mathbf{p}-2\pi\mathbf{n}$ a even if the neutrons are not

monochromatic. For such an experiment, of course, the neutrons would all have wavelength greater than the Bragg reflection wavelength, both in order that this inelastic magnetic scattering should be of considerable magnitude, and that elastic scattering should be small and isotropic.

§4. CONCLUSION

It has been shown that, assuming the Bloch spin wave model of a ferromagnetic, considerable inelastic magnetic scattering of very slow neutrons in which the neutrons gain energy takes place. The essential reason for this is that for such slow neutrons the temperature of the scatterer is considerably greater than that of the neutrons. Though the total cross section for scattering of this kind is not large, the scattering has a peculiarly limited angular distribution (provided the scatterer is a single crystal and the neutrons are monochromatic), due to the energy momentum relations, and in particular the small 'effective mass' of a spin wave. This limitation results in the differential cross section being large for those angles into which scattering takes place. Considerable nuclear scattering with phonon absorption occurs, and gives peaks centred in the same directions as, though not generally coincident with, the spin wave peaks. In a magnetized crystal the variation of spin wave absorption scattering with direction of magnetization might be used to distinguish it from vibrational scattering.

For two reasons the effect of spin wave and phonon absorption is most important for neutrons of wavelength somewhat greater than the Bragg reflection wavelength. Firstly for neutrons of wavelength less than the Bragg reflection wavelength it can be seen from the mathematical methods of §3, and it is indeed obvious from energy considerations, that this type of scattering is less important. Secondly for wavelengths greater than the Bragg reflection wavelength elastic nuclear scattering is small and isotropic. Thus the peaks of intensity discussed here appear more clearly.

The calculations have been carried out here for iron, but similar, though not so marked, peaks are to be expected for nickel.

ACKNOWLEDGMENTS

The author would like to acknowledge the receipt of a maintenance allowance from the Department of Scientific and Industrial Research during the tenure of which this work was carried out. It is a pleasure to thank Dr. J. M. Cassels for bringing the problem to the author's notice, and Professor R. E. Peierls for his continual help and guidance.

REFERENCES

Bloch, F., 1930, *Z. Phys.*, **61,** 206.
Cassels, J., and Latham, R., 1948, *Phys. Rev.*, **74,** 103.
Halpern, O., and Johnson, M. H., 1939, *Phys. Rev.*, **55,** 898.
Hamermesh, M., 1942, *Phys. Rev.*, **61,** 17.
Mott, N. F., and Jones, H., 1936, *Theory of the Properties of Metals and Alloys* (Oxford : University Press), p. 224.
Sommerfeld, A., and Bethe, H., 1933, *Handbuch der Physik*, Vol. XXIV/2 (Berlin : Springer), p. 601 ff.
Steinberger, J., and Wick, G. C., 1949, *Phys. Rev.*, **76,** 994.
Weinstock, R., 1944, *Phys. Rev.*, **65,** 1.

Antiferromagnetism by the Bethe Method

By J. M. ZIMAN
Clarendon Laboratory, Oxford

MS. received 6th June 1951

ABSTRACT. The Bethe method for order–disorder is applied to a lattice of magnetic dipoles with antiferromagnetic nearest-neighbour interactions. Magnetization and entropy are calculated for all values of temperature and magnetic field, and an anti-parallel ordered phase is found below a definite transition curve. The computed curves agree qualitatively with those observed experimentally with certain paramagnetic salts at low temperatures.

Some recent experiments (Garrett 1951, Kurti 1951, Gorter 1951) on paramagnetic salts at low temperatures have yielded results which may be interpreted according to a theory proposed by Sauer and Temperley (1940). The anomalies in the entropy and magnetic susceptibility are considered to be due to anti-parallel ordering of the lattice of atomic spins, due to magnetic dipole–dipole interactions. The crystal behaves as if it were antiferromagnetic, the anti-parallel state existing when the temperature and external magnetic field have values lying below a certain curve in the H,T plane.

The theory of Sauer and Temperley uses the Bragg–Williams (1934) approximation for the energy. It is well known that better approximations are available to solve order–disorder problems, in particular the method of Bethe (1935), which takes rather more account of local order. Unfortunately, the Bethe method assumes that the ordering of the lattice is due to the interaction of any atom with one or more shells of neighbouring atoms. In the case of dipole–dipole forces this assumption is rather artificial, since the interaction is highly anisotropic, and falls off only as the inverse cube of the distance between the spins, so that a very large number of shells, which would interact among themselves in a complicated way, would be needed. Nevertheless, it is worth considering a very simple model, to see how far it can give results in agreement with experiment.

Let two lattices interpenetrate in such a way that each atom of one lattice has z nearest neighbours on the other. At each lattice point let there be an Ising dipole, i.e. a spin variable S which can only take the values $+1$ and -1. If i and j refer to neighbouring atoms, there is to be an interaction energy $J\mu^2 S_i S_j$, where J is positive, μS_i is to be the magnetic moment of the ith atom, measured along a direction in which there is an external magnetic field H_0. The configuration of lowest energy for such a system is one in which all spins on one lattice point to the right and all on the other lattice point to the left.

This problem has been solved formally by the Bethe method by Firgau (1942). We follow her procedure, but in the more elegant formulation suggested by Weiss (1948). Suppose, as in Figure 1 (*a*), that μS_0 is the moment of a central atom on a site where the dipole points to the right in the lowest-energy state (right-hand site), that is, S_0 takes the value $+1$ when this dipole points to the right. μS_1 is the total moment of the shell of z atoms surrounding S_0; S_1 takes the values $z, z-2, z-4, \ldots . -z$, and its sign is to be positive when all the dipoles of the shell point to the left, as in the diagram, i.e. $S_1 = -\Sigma S_j$, where the sum is over

sites surrounding S_0. Again, H_0 is the field acting on S_0; as usual in the Bethe method, this must be the external field, since the internal field acting on the central atom is taken account of by considering explicitly the interaction between S_0 and the shell S_1. However, H_1 is a hypothetical internal field acting on S_1 alone, and represents the combined effects of the external field and of the neighbours of the shell (apart from the central atom). The positive senses of these fields are indicated in Figure 1 (*a*).

The partition function for this cluster may be written

$$\begin{aligned}(\text{p.f.}) &= \sum_{S_0=\pm 1} \sum_{S_1=-z}^{z} \frac{z!}{[\frac{1}{2}(z+S_1)!\,[\frac{1}{2}(z-S_1)]!} \\ &\quad \times \exp\{-(-\mu H_0 S_0 - \mu H_1 S_1 - \mu^2 J S_0 S_1)/\boldsymbol{k}T\} \\ &= x_0\left(\frac{x}{y}+\frac{y}{x}\right)^z + \frac{1}{x_0}\left(xy+\frac{1}{xy}\right)^z, \qquad \ldots\ldots(1)\end{aligned}$$

where $x_0 = \exp(-\mu H_0/\boldsymbol{k}T)$, $x = \exp(-\mu H_1/\boldsymbol{k}T)$, $y = \exp(-\mu^2 J/\boldsymbol{k}T$.

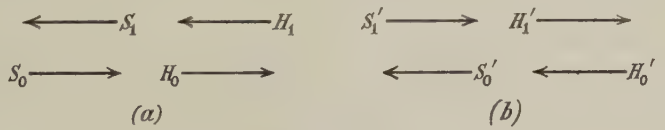

Figure 1 (*a*). Right-hand site. (*b*) Left-hand site.

For atoms on, and surrounding, a left-hand site we define the fields and spins according to the scheme of Figure 1 (*b*), and obtain similarly a partition function:

$$(\text{p.f.})' = \xi_0\left(\frac{\xi}{y}+\frac{y}{\xi}\right)^z + \frac{1}{\xi_0}\left(\xi y+\frac{1}{\xi y}\right)^z,$$

where $\xi_0 = \exp(-\mu H_0'/\boldsymbol{k}T$, $\xi = \exp(-\mu H_1'/\boldsymbol{k}T$.

The average moment of each type of atom may now be determined; thus $\bar{m}_0$, the average value of μS_0, refers to an atom on a right-hand site, and is given by

$$\begin{aligned}\bar{m}_0 &= -\mu x_0 \frac{\partial}{\partial x_0}[\log(\text{p.f.})] \\ &= -\mu\left[x_0\left(\frac{x}{y}+\frac{y}{x}\right)^z - \frac{1}{x_0}\left(xy+\frac{1}{xy}\right)^z\right] \Big/ \left[x_0\left(\frac{x}{y}+\frac{y}{x}\right)^z + \frac{1}{x_0}\left(xy+\frac{1}{xy}\right)^z\right],\end{aligned}$$

and similarly $\bar{m}_1 = (\mu S_1/z)_{\text{av}} = -\dfrac{\mu}{z} x \dfrac{\partial}{\partial x}[\log(\text{p.f.})]$, etc.

But the two lattices are interleaved, and are subject to the same external field. In other words, $H_0' = -H_0$, i.e. $\xi_0 = 1/x_0$.

Moreover, since any two right-hand sites or any two left-hand sites are equivalent, whether considered as occupied by a central atom or by an atom in a shell, they must possess the same average moment. That is, $\bar{m}_0 = \bar{m}_1'$ and $\bar{m}_0' = \bar{m}_1$.

We now have sufficient equations to eliminate the unknown fields H_1, H_1'. The partition function for the whole crystal can be written $(\text{P.F.}) = [(\text{p.f.})(\text{p.f.})']^{N/2(z+1)}$ since there are $\frac{1}{2}N$ sites of each type, but each atom is counted $z+1$ times, being either a central atom of a site or in the first shell of z other sites. By differentiating (P.F.) with respect to T and H_0 all the thermodynamic and magnetic properties may be deduced.

Writing $\theta = \left(\dfrac{x}{y}+\dfrac{y}{x}\right)\Big/\left(xy+\dfrac{1}{xy}\right)$, $\phi = \left(\xi y+\dfrac{1}{\xi y}\right)\Big/\left(\dfrac{\xi}{y}+\dfrac{y}{\xi}\right)$ and using θ and ϕ as parameters, it is possible to find a quartic equation for x_0^2, which may

be solved numerically. In this way a set of simultaneous values of H_0, T, the magnetic moment M, and the entropy S is obtained, and by choosing various values of θ and ϕ any number of such sets may be computed. Isomomentals, isentropics, etc. may then be drawn by numerical interpolation, in an obvious manner. The results of these calculations (for $z=8$) are plotted in Figures 2 and 3. The following points should be observed.

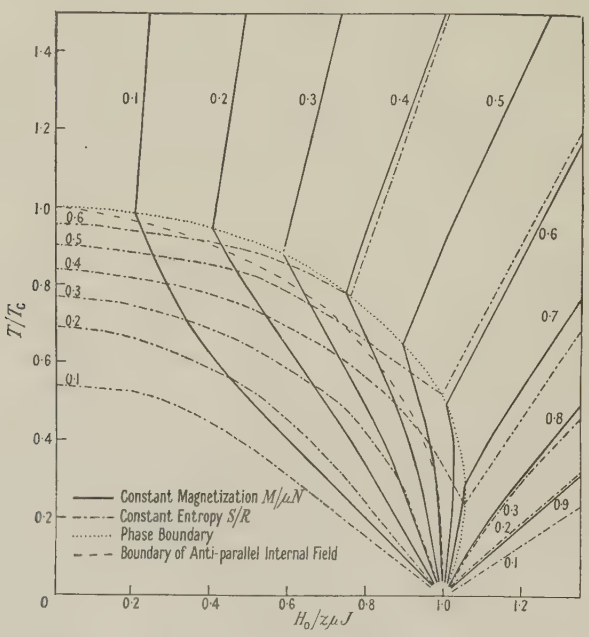

Figure 2.

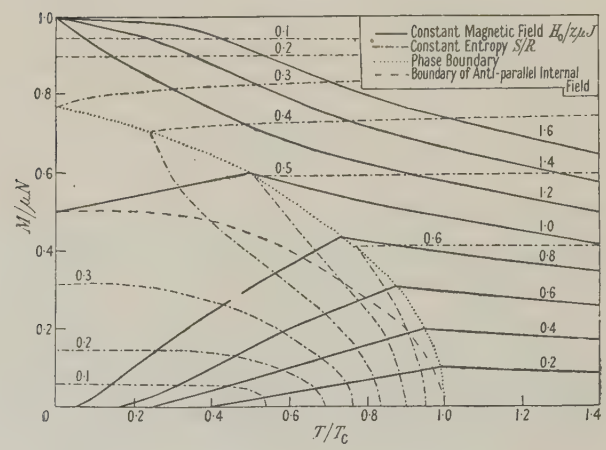

Figure 3.

(*a*) Outside a line labelled 'phase boundary' the equations have only one solution, which is obtained by putting $\xi=1$ *x*. This corresponds to absence of long-range order, so that right-hand and left-hand sites have identical properties; this is the solution quoted by Firgau. Inside the boundary, however, there is an additional solution which has a lower free energy, and corresponds to long-range anti-parallel order. The two solutions join on the phase boundary, but

not smoothly, so that there should be no abrupt change in magnetization or entropy, but jump discontinuities in susceptibility and specific heat should appear as the boundary is crossed. The first-order transition postulated by Sauer and Temperley below $T_C/3$ does not appear.

(*b*) In zero external field there is a Curie point at the temperature T_C where $J\mu^2/\boldsymbol{k}T_C = \frac{1}{2}\log[z/(z-2)]$. At very low temperatures the zero-field susceptibility behaves as

$$\chi_0 = \frac{4N\mu^2}{\boldsymbol{k}T}\exp(-2zJ\mu^2/\boldsymbol{k}T)$$

and the entropy vanishes as $N\boldsymbol{k}\exp(-zJ\mu^2/\boldsymbol{k}T$ (but these formulae do not hold up to the Curie point itself). Above the Curie point the Firgau formula is valid, i.e.

$$\frac{1}{\chi_0} = \frac{\boldsymbol{k}T}{2N\mu^2}\left[z\exp\left\{\frac{T_C}{T}\log\left(\frac{z}{z-2}\right)\right\} - (z-2)\right].$$

(*c*) At zero temperature, when the field reaches the value $z\mu J$, the magnetic moment jumps from zero to its maximum possible value μN. This corresponds to the turning over of all the anti-parallel spins into the direction of the field, which is now stronger than any possible internal field. It is to be noted that the anti-parallel phase extends for a certain distance above the level of this critical field at some temperatures. Although definitely predicted by the equations, this phenomenon does not seem to be physically significant, but is a result of the somewhat artificial model employed. It has been assumed that long-range order, and the definite identification of right-hand and left-hand sites, can be called into action whenever they are required. But the solutions of the equations near the phase boundary correspond to states in which dipoles on both right-hand and left-hand sites have average moments in the same sense, although with different magnitudes. It seems very doubtful whether a state of this kind could subsist in a large crystal, with the quantum-mechanical exchange forces always tending to give mixtures of many states with the same energy total. In any case, as we approach the transition region the Bethe model becomes more and more approximate, and takes no account of the intermediate state, in which long-range order has broken down while there is still a large degree of order over a range of a few lattice distances from any given site. A line has been drawn in the figures showing where the average moment of an atom on a left-hand site vanishes and changes sign. This may well be taken as the limit to the region in which the low-temperature solution is trustworthy. Outside the phase boundary the high-temperature results are also probably correct.

(*d*) These curves differ in other respects from those of Sauer and Temperley. It is not possible, of course, to discuss the effect of the macroscopic shape of the specimen, since only nearest-neighbour forces have been included. But it should be noted that the lines of constant magnetization all tend towards the point $H = z\mu J$, $T = 0$, whereas Sauer and Temperley seem to show the isomomentals sloping more sharply away from the temperature axis, and cutting the transition curve again at a finite temperature.

(*e*) The experimental data are, as yet, somewhat meagre. The only case in which a substantial area of the phase diagram has been obtained is Garrett's study of a single crystal of cobalt ammonium sulphate. His results have been displayed on a diagram equivalent to, and directly comparable with, Figure 2. Such comparison shows very good general agreement for the isomomentals, but the entropy, on our model, seems too dependent on the magnetic field. This is

to be expected, since we have neglected all entropy save that due to the disordering of the magnetic dipole lattice. Our method is also defective in not taking full account of the intermediate-range order, which contributes some negative entropy above the Curie point even in zero field.

Garrett finds no discontinuities of susceptibility or specific heat. We may assume, therefore, that the isomomentals should not meet at an angle, as in our figure, but that they should be replaced by smooth curves in the transition region (i.e. between the phase boundary and the 'boundary of the anti-parallel field'). The boundary of the antiferromagnetic region, according to Garrett's definition, should then lie on the minima of these smoothed isomomentals, that is, somewhere between the two lines enclosing the transition region.

(*f*) The number $\boldsymbol{k}T_C/\mu H_C$, which Garrett finds to be equal to 1·2 for cobalt ammonium sulphate, on our model turns out to be $2z^{-1}\log[z/(z-2)]$, which is slightly less than unity for real lattices. Although this figure may seem to agree a little better with experiment that Sauer and Temperley's value of 2, it is difficult to assign any great significance to this fact. Garrett's salt actually contains two differently oriented dipoles per unit cell, which seriously complicates the analysis. Because of the simplicity of the model, it is not very profitable to discuss precise values of Curie temperatures, zero-field susceptibility, atomic constants, etc. It has already been pointed out by Kurti (1951) that the observed Curie points for substances showing these anomalies indicate that the forces are indeed magnetic dipole interactions (or are at least of that order of magnitude), and our analysis can do no more than support that assertion. We have obtained a rather general phase diagram for antiferromagnetics, to which any substance should conform qualitatively; more exact treatment, taking into account the nature of the forces and the exact crystal structure, must inevitably use more refined mathematical techniques, which go beyond the scope of this paper.

Note added in proof. Since this paper was written, C. G. B. Garrett (*J. Chem. Phys.*, 1951, **19**, 1154) has applied the internal field method to a model almost identical with our own, and obtained a theoretical phase similar to Figure 2. The chief difference is in the shape of the phase boundary, which is shown 'bulging' much further beyond the critical field. Since the Bethe method is an approximation of higher order, it is likely that the exact solution will not show this anomaly at all.

ACKNOWLEDGMENTS

Acknowledgment is due to Dr. G. S. Rushbrooke for his encouragement and advice, and to the Department of Scientific and Industrial Research for a maintenance grant.

REFERENCES

Bethe, H., 1935, *Proc. Roy. Soc.* A, **150,** 552.
Bragg, W. L., and Williams, E. J., 1934, *Proc. Roy. Soc.* A, **145,** 699.
Firgau, U., 1942, *Ann. Phys., Lpz.*, **40,** 295.
Garrett, C. G. B., 1951, *Proc. Roy. Soc.* A, **206,** 242.
Gorter, C. J., 1951, *J. Phys. Radium*, **12,** 281.
Kurti, N., 1951, *J. Phys. Radium*, **12,** 275.
Sauer, J. A., and Temperley, H. N. V., 1940, *Proc. Roy. Soc.* A, **176,** 203.
Weiss, P. R., 1948, *Phys. Rev.*, **74,** 1493.

Asymmetrical Electron Diffraction Effects from Single Crystals of Silver

By D. W. PASHLEY

Physics Department, Imperial College, London

Communicated by G. P. Thomson; MS. received 1st June 1951

ABSTRACT. Silver crystal surfaces which had been prepared by either electrolytic etching or electrolytic polishing were studied by means of the electron diffraction reflection technique. It was found that fine structure effects, in the form of split spots or streaks through spots, gave information concerning the topographies of the various surfaces of the crystals. The fine structure effects showed certain asymmetries which do not immediately follow from the Laue diffraction theory. The possible causes of these asymmetries are discussed, and it is concluded that they were probably due to distortion of the silver crystals, but that some might have also been due to refraction effects.

§1. INTRODUCTION

ELECTRON diffraction reflection patterns obtained from single crystal surfaces are considerably influenced by the topography of the crystal surface. Atomically flat surfaces are characterized by the effects due to refraction of the electrons upon entering and leaving the surface (Thomson and Cochrane 1939, Chapter VIII). With other surfaces, diffraction patterns arise when electrons penetrate through sub-microscopic projections covering the surfaces (Thomson 1931), and the shape and size of such projections can introduce important effects. Firstly, the electrons may be refracted when entering or leaving the projections by certain facets; Miyake (1938) has reported an example of this effect in which the diffraction spots are split up into groups of close subsidiary spots. Similar refraction effects have also been found during high resolution examination of certain oxide smokes (see, for example, Cowley and Rees 1947). Secondly, Laue (1936) has shown that around each reciprocal lattice point due to a crystallite with well-developed facets, there is an intensity region which can be approximated to a number of spikes or 'stachel' perpendicular to each of the well-developed facets. When the usual Ewald sphere construction is applied to such a reciprocal lattice, the spikes cause some of the diffraction spots to be split up into groups of subsidiary spots. If, therefore, a crystal surface is covered by many similarly shaped projections, then such groups of subsidiary spots should occur on electron diffraction patterns from that surface. The effect has been observed several times (Kirchner and Lassen 1935, Brück 1936, Cochrane 1936).

In the present paper, an account is given of the application of electron diffraction to the study of various surfaces of single crystals of silver, with the object of obtaining information concerning their topography, as a preliminary to the study of the growth of chemical compounds on them. Fine structure effects are observed, and these can be partially explained in terms of reciprocal lattice spikes. Some of the results suggest, however, the existence of spikes which are not symmetrical about the centre of the appropriate reciprocal lattice point. The Laue diffraction theory, which predicts the spikes, also predicts

that they should be symmetrical about the centre of the reciprocal lattice point. One of the principal aims of this paper is to report and discuss these asymmetrical effects.

§ 2. THE PREPARATION OF THE SILVER CRYSTALS

Silver crystals were grown by slowly cooling beads of molten silver, of a few millimetres diameter, in a continuously evacuated quartz tube. About half of the specimens consisted of more than one crystal grain, and were therefore rejected. Flat surfaces were ground on those specimens consisting of only one crystal grain, by careful grinding on grade 0 emery paper, and finishing on grade 0000 paper. The surfaces were etched, and the orientation of the crystal axes determined by means of electron diffraction. Flat surfaces could then be prepared parallel to any chosen lattice plane, using a specially designed jig for clamping the crystals during the grinding. Crystals with flat surfaces parallel to the (100), (111), (110) and (311) type lattice planes were prepared, these being the four most closely packed planes.

The final preparation of the surfaces was carried out in one of three ways: (i) 35% nitric acid etching, (ii) electrolytic polishing, or (iii) electrolytic etching. Nitric acid etching was found to be not very controllable, and to leave the surface very uneven, so that only preliminary experiments were carried out with this technique.

The electrolytic polishing was performed according to the method of Shuttleworth, King and Chalmers (1947), and very bright even surfaces could be obtained after about twenty minutes polishing, with a potential of 0·7 v. across the cell. The brown film which formed during the polishing could be easily brushed off during the rinsing of the specimens in distilled water.

Electrolytic etching was carried out in the same bath, using a potential of 0·05 v.; the cell current density was then about 1 ma/cm^2. The etching was usually continued for two hours on each specimen, immediately after the specimen had been prepared on grade 0000 emery paper.

Before examination in the electron diffraction camera, the specimens were always washed in distilled water, alcohol and benzene before being dried.

§ 3. THE ELECTRON DIFFRACTION APPARATUS

Two different electron diffraction cameras were used, one having a cold cathode electron gun and the other a hot filament electron gun; both were fitted with magnetic focusing coils. The electron accelerating potentials were in the range 30–50 kv. and the camera lengths were 40 and 35 cm. respectively. The reflection technique was used exclusively.

§ 4. THE GEOMETRICAL RELATION BETWEEN RECIPROCAL LATTICE SPIKES AND THE POSITIONS OF SUBSIDIARY DIFFRACTION SPOTS

During the analysis of some of the diffraction patterns it became necessary to calculate the positions on the photographic plate of subsidiary spots due to certain reciprocal lattice spikes. A suitable approximate relation has been derived.

Let the crystal surface be cut parallel to a given lattice plane, and let the electron beam direction be inclined at an angle i to this surface (Figure 1 (*a*)). Let the beam also be set off from being perpendicular to a certain reciprocal

plane (yz plane) by the small azimuth angle ϕ. If a point P in that reciprocal lattice plane gives rise to the diffraction spot P′ (Figure 2), with coordinates Y and Z with respect to the undeviated spot as origin, then it can be shown that the coordinates of a spot P_1' due to a spike through P are S and U, where

$$S=\tfrac{1}{2}F\sin\gamma, \quad U=-\tfrac{1}{2}F\tan\beta \qquad \ldots\ldots(1)$$

and

$$F=\frac{(Y^2+Z^2)-2L(Z\sin i-Y\cos i\sin\phi)}{(Z\tan\beta-Y\sin\gamma)-(\sin\gamma\cos i\sin\phi+\sin i\tan\beta-\cos\phi\cos\gamma)L}. \qquad \ldots\ldots(2)$$

β and γ define the direction of the spike, as given in Figure 1 (*b*). The xy plane is parallel to the crystal surface, and the yz plane is parallel to the above-mentioned reciprocal lattice plane containing P; L is the camera length.

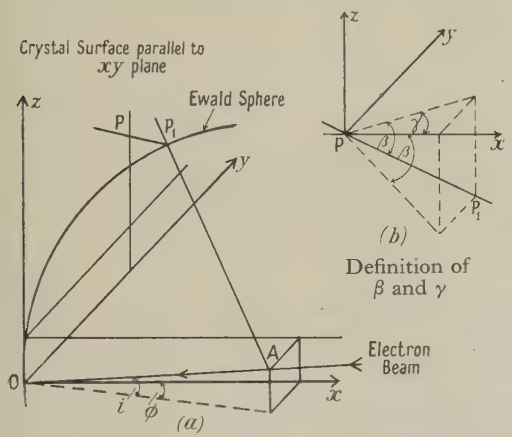

Figure 1. Reciprocal lattice and Ewald sphere construction.

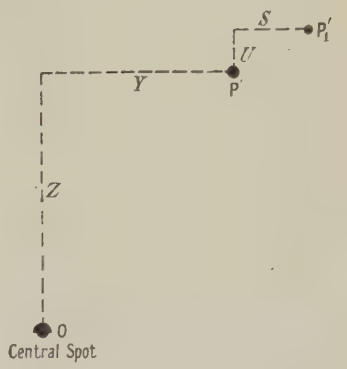

Figure 2. Definition of S and U.

These formulae may be used to calculate the pattern of subsidiary spots due to a given system of spikes, with a given crystal setting relative to the electron beam direction.

§ 5. THE DIFFRACTION PATTERNS FROM THE ETCHED SILVER CRYSTAL SURFACES

35% nitric acid was first used as etching agent, and this produced matt surfaces which gave rise to cross-grating patterns of spots which were sometimes split into groups of subsidiary spots, as previously reported (Pashley 1949). The etching was not very controllable, however, and the surfaces tended to become visually uneven. The electrolytic method of etching was therefore finally adopted, and this was found to produce surfaces which gave rise to cross-grating patterns of spots often having very marked fine structure. Diffuse Kikuchi line patterns were also occasionally obtained, as well as some weak diffuse streaks connecting the cross-grating spots along the [111] directions.

(i) (100) *Surface*

Figure 3 (Plate *) shows a reflection pattern from an electrolytically etched (100) surface of silver, with the beam set along the [011] azimuth. Some of the diffraction spots are resolved into groups of five subsidiary spots. When the

* For Plates see end of issue.

electron beam was set along the [001] azimuth, some of the cross-grating spots were split up into groups of four subsidiary spots. The two groups of spots are illustrated in Figure 4. The subsidiary spots can be accounted for if it is assumed that through each reciprocal lattice point there are spikes along the following crystal directions: [010], [001], [011], [01$\bar{1}$], [120], [1$\bar{2}$0], [102], and [10$\bar{2}$]. Explanation in terms of a refraction effect such as observed by Miyake (1938) does not seem possible in this case.

The angle of incidence of the electron beam with the (100) crystal plane was calculated from formulae (1) and (2), assuming the subsidiary spots C and D (Figure 5), for the (600) spot of Figure 3, to be due to [010] and [001] spikes. ϕ was assumed zero because of the symmetry of the pattern. The values of β and γ for all of the spikes are listed in Table 1.

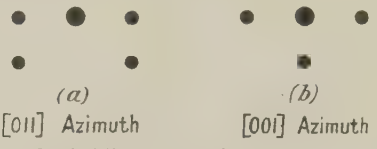

Figure 4. Groups of subsidiary spots observed from etched (100) surface.

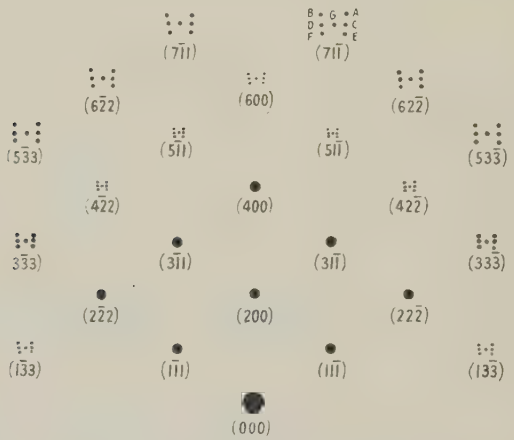

Figure 5. Calculated pattern of Figure 3.

Table 1. Calculated Values of β and γ

Spike	[010]	[001]	[011]	[01$\bar{1}$]	[120]	[1$\bar{2}$0]	[102]	[10$\bar{2}$]
β (deg.)	0	0	0	0	−26·3	+26·3	−26·3	+26·3
γ (deg.)	+45	−45	0	+90	+45	+45	−45	−45

The expected pattern of spots for the proposed system of spikes, calculated according to formulae (1) and (2), is plotted in Figure 5. A comparison with the observed pattern of Figure 3 is given in Table 2. The spots C and D are due to the [010] and [001] spikes, and the spots A, B, E and F to the [120], [1$\bar{2}$0], [102] and [10$\bar{2}$] spikes. The [011] spike gives rise to the spot G.

Although the calculated and observed positions of subsidiary spots agree well, it is noticed that no subsidiary spots with U positive (spots A and B) are observed. It was at first thought that this could be explained by the absence of the [1$\bar{2}$0] and [10$\bar{2}$] spikes; these spikes would be expected to appear, however, since the (102), (10$\bar{2}$), (120), and (1$\bar{2}$0) planes are equivalent and are placed in

symmetrical positions with respect to the surface. A photograph (Figure 6 (Plate)) was therefore taken with $\phi = 4°$, by changing the azimuthal setting of the crystal. Here subsidiary spots due to the Ewald sphere passing both in front and behind reciprocal lattice points are observed, as illustrated in Figure 7. Splitting due to the [120], [1$\bar{2}$0], [102] and [10$\bar{2}$] spikes is thus recorded on one

Table 2. Comparison between Observed and Calculated Positions of the Subsidiary Spots

Subsidiary spot	S (mm.) Obs.	S (mm.) Calc.	U (mm.) Obs.	U (mm.) Calc.	Subsidiary spot	S (mm.) Obs.	S (mm.) Calc.	U (mm.) Obs.	U (mm.) Calc.
(600)A	—	+1·02	—	+0·72	(62$\bar{2}$)A	—	+1·58	—	+1·10
(600)B	—	−1·02	—	+0·72	(62$\bar{2}$)B	—	−1·43	—	+0·99
(600)C	+1·0	+0·97	0	0	(62$\bar{2}$)C	+1·4	+1·49	0	0
(600)D	−1·0	−0·97	0	0	(62$\bar{2}$)D	−1·2	−1·36	0	0
(600)E	+1·0	+0·92	−0·6	−0·65	(62$\bar{2}$)E	+1·4	+1·41	−0·7	−0·99
(600)F	−1·0	−0·92	−0·6	−0·65	(62$\bar{2}$)F	−1·2	−1·30	−0·7	−0·91
(51$\bar{1}$)A	—	+0·68	—	+0·48	(133$\bar{3}$)A	—	+0·95	—	+0·67
(51$\bar{1}$)B	—	−0·65	—	+0·46	(133$\bar{3}$)B	—	−0·83	—	+0·58
(51$\bar{1}$)C	+0·7	+0·66	0	0	(133$\bar{3}$)C	+0·9	+0·96	0	0
(51$\bar{1}$)D	−0·6	−0·63	0	0	(133$\bar{3}$)D	−0·8	−0·83	0	0
(51$\bar{1}$)E	+0·7	+0·63	−0·4	−0·44	(133$\bar{3}$)E	+0·9	+0·97	−0·5	−0·68
(51$\bar{1}$)F	−0·6	−0·60	−0·4	−0·42	(133$\bar{3}$)F	−0·8	−0·84	−0·5	−0·56
(71$\bar{1}$)A	—	+1·79	—	+1·25	(333$\bar{3}$)A	—	+1·08	—	+0·76
(71$\bar{1}$)B	—	−1·70	—	+1·19	(333$\bar{3}$)B	—	−1·00	—	+0·71
(71$\bar{1}$)C	+1·6	+1·68	0	0	(333$\bar{3}$)C	+1·1	+1·07	0	0
(71$\bar{1}$)D	−1·3	−1·60	0	0	(333$\bar{3}$)D	−0·9	−0·93	0	0
(71$\bar{1}$)E	+1·6	−1·57	−1·0	−1·10	(333$\bar{3}$)E	+1·1	+1·05	−0·6	−0·73
(71$\bar{1}$)F	−1·3	−1·50	−1·0	−1·05	(333$\bar{3}$)F	−0·9	−0·91	−0·6	−0·64
(42$\bar{2}$)A	—	+0·70	—	+0·49	(533$\bar{3}$)A	—	+1·73	—	+1·21
(42$\bar{2}$)B	—	−0·63	—	+0·44	(533$\bar{3}$)B	—	−1·49	—	+1·04
(42$\bar{2}$)C	+0·7	+0·69	0	0	(533$\bar{3}$)C	+1·6	+1·66	0	0
(42$\bar{2}$)D	−0·6	−0·62	0	0	(533$\bar{3}$)D	−1·3	−1·44	0	0
(42$\bar{2}$)E	+0·7	+0·66	−0·4	−0·46	(533$\bar{3}$)E	+1·6	+1·59	−1·0	−1·11
(42$\bar{2}$)F	−0·6	−0·60	−0·4	−0·42	(533$\bar{3}$)F	−1·3	−1·38	−0·9	−0·77

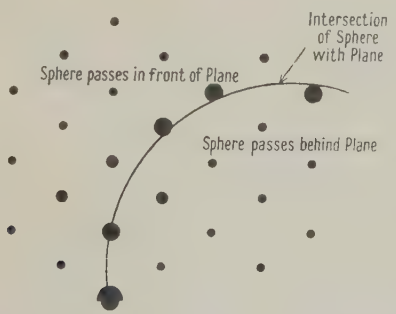

Figure 7. Intersection of Ewald sphere with (011) reciprocal lattice plane, for pattern of Figure 6.

photograph, but still no subsidiary spots with U positive are observed. Occasionally there were signs of subsidiary spots with U positive, for cases where the Ewald sphere passes very close to the reciprocal lattice point; this was more noticeable at the [001] azimuthal setting, because the [102] type spikes were then more nearly perpendicular to the Ewald sphere. All the effects can be explained, therefore, if it is assumed that the [102], [10$\bar{2}$], [120] and [1$\bar{2}$0] spikes

are much longer on the side of the reciprocal lattice point nearer to the origin than they are on the opposite side. It is estimated that the ratio of the lengths of the spikes on the two sides is approximately five to one.

The [010], [001], [011] and [01$\bar{1}$] spikes showed no such asymmetry. This does not necessarily mean that the spikes are symmetrical, since, for the particular case of facets perpendicular to the surface, the spike can be due to the superposition of two asymmetrical spikes, because two parallel facets facing in opposite directions are then possible.

Apart from the asymmetry effects, the patterns from the etched (100) surfaces suggest that the (010), (001), (011), (01$\bar{1}$), (102), (10$\bar{2}$), (120) and (1$\bar{2}$0) facets are well developed during the etching process. A later paper will show how the presence of some of these facets is also indicated by the way in which silver halides orient on the same surfaces.

(ii) (100) *Surface*

When the (110) silver surface was electrolytically etched, the diffraction spots were not split into groups of subsidiary spots but had various shapes. At the [1$\bar{1}$0] azimuthal setting the spots were often diamond shaped, being predominantly streaked down towards the shadow edge. In Figure 8 (Plate) the spots are star shaped, with three sets of streaks through them. At other azimuthal settings other streaked spots were observed. The patterns obtained varied in detail from experiment to experiment, but the spots always had streaks through them, and these streaks were always perpendicular to certain crystal lattice planes. At various times streaks perpendicular to the following lattice planes were observed: (110), (1$\bar{1}$0), (100), (010), (001), (021), (0$\bar{2}$1), (201), ($\bar{2}$01), (210), ($\bar{2}$10), (120), (1$\bar{2}$0), (113) and (11$\bar{3}$).

The streaks were often asymmetrical about the centres of the Laue spots, being stronger on the side nearer to the central spot. The more nearly the streak was perpendicular to the shadow edge, the more was it asymmetrical. Streaks parallel to the shadow edge were symmetrical.

(iii) (111) *Surface*

When the (111) surface was electrolytically etched, two distinct types of surfaces were obtained, according to conditions. If the crystal was cut with its surface accurately parallel (to better than one degree) to the (111) lattice plane, the electrolytic etching gave a bright flat surface very similar to a cleavage face. If the crystal was not so accurately cut, or if the surface was given a previous etch in nitric acid, then a matt surface was obtained.

The bright flat (111) surface gave rise to diffraction patterns such as shown in Figure 9 (Plate). This is similar to a pattern from a cleavage face, and indicates a high degree of surface flatness. Rotation photographs taken from these surfaces showed that the diffraction spots were displaced down by refraction during the entrance and exit of the electron beam from the surface. An inner potential for silver of approximately 20 v. was indicated. This is consistent with the value of 23·2 v. recently obtained by Tull (1951). It is thus concluded that this type of (111) surface contains areas which are atomically smooth, in contrast to other etched surfaces which are usually rough. It would appear that there is a preference for silver to etch with extensive (111) planes as its boundary, since nitric acid etching of the silver crystals caused the appearance of bright flat

patches of about one millimetre in dimension parallel to the (111) lattice planes (Pashley 1949).

The matt (111) surface gave cross-grating patterns of spots which were heavily streaked asymmetrically, as shown in Figure 10 (Plate) for the $[2\bar{1}\bar{1}]$ azimuthal setting; the streaks are in [120] and [102] directions. Occasionally there were signs of the appearance of subsidiary spots, but there is insufficient evidence on this point to allow any definite conclusions to be drawn. At other azimuthal settings, streaks perpendicular to the following lattice planes were observed: (012), (102), (210), (201), (110), (101), (011), (113), (131) and (311); all showed asymmetry.

(iv) (311) *Surface*

When the (311) surface was electrolytically etched, patterns showing fine structure effects were also obtained. Similar subsidiary spots to those observed from the (100) surface were sometimes found, and asymmetrical streaks perpendicular to (110), (311) and (210) type facets were also observed.

§6. THE DIFFRACTION PATTERNS FROM THE ELECTROLYTICALLY POLISHED SILVER CRYSTALS

Electrolytically polished silver crystal surfaces gave rise to diffraction patterns consisting of the following components: (i) cross-grating patterns of spots which were usually diffuse and strongly streaked out towards the shadow edge, these spots were due to the main silver crystal; (ii) weaker spots due to silver which was twinned on the (111) planes of the main silver crystal; (iii) weak sharp ring patterns; (iv) diffuse Kikuchi line patterns. Figure 11 (Plate) shows a typical example, with prominent twin spots present.

The cross-grating patterns were usually quite extensive, and often two Laue zones of spots were considerably overlapped; they must therefore have been due to electron penetration through very small projections on the surface. The breadth of the diffraction spots indicated that the projections were probably no larger than a few atomic dimensions across. The surfaces were certainly not atomically flat, and even when an accurately cut (111) surface was electrolytically polished, the surface was also covered by small projections, despite the fact that electrolytic etching of such surfaces produced atomically flat areas (see §5). It is therefore concluded that the mechanism of electrolytic polishing does not lead to the formation of an atomically flat surface for the particular technique used. The spots were always elongated downwards; this effect has been observed previously (Kranert, Leise and Raether 1944, Raether 1946, Halfawy 1948) and Kranert *et al.* have explained it as due to a smooth crystal surface which is wavy on an atomic scale.

The electrolytically polished silver crystal surfaces thus gave rise to diffraction patterns which also indicated some asymmetrical effects.

The presence of twinned silver suggests that some silver is re-deposited during the electrolytic polishing; this is supported by the fact that electrolytic deposition of silver on to the crystals is also found to lead to twinned growth. The presence of randomly oriented silver on the electrolytically polished surfaces might also be due to re-deposition. The twinned and randomly oriented silver could be removed by less than five minutes' electrolytic etching, and was therefore

confined to a very thin layer on the surface. The re-deposition might be connected with the brown film which formed on the crystal surface during electrolytic polishing and which disappeared when the surface was brushed with water after the crystal had been taken out of the electrolytic cell.

The diffuse Kikuchi line patterns varied in brightness from specimen to specimen.

§ 7. DISCUSSION

Whereas electrolytic polishing caused the silver crystal surfaces to become smooth and flat, the electrolytic etching, with one remarkable exception, produced rough surfaces which were matt in appearance and which were bounded by certain well-developed facets. It is interesting to note that the facets were always of the (100), (110), (210) and (311) types, and that no (111) oblique facets were ever observed, although the octahedral planes are the most closely packed, and might have been expected to be the most stable. Cochrane (1936) observed that prominent (111) type facets were produced on some electrolytically deposited cobalt surfaces, and Kirchner and Lassen (1935) observed well-developed (111) facets on condensed layers of silver. In the present experiments (111) crystal boundaries were only produced when they were parallel to the surface; they then formed large flat patches on that surface. It is also interesting to note that if the (*hkl*) facet occurs on a given surface, all of the crystallographically equivalent facets do not necessarily occur, but only those which make the same angle with the surface as does the (*hkl*) facet.

With the electrolytically etched surfaces there is the difficulty of explaining the observed asymmetrical effects. These effects were of two distinct types: the subsidiary spots, shown in Figures 3 and 6, which were due to asymmetrical reciprocal lattice spikes, and the asymmetrical streaks as shown on Figures 8 and 10.

Asymmetrical intensity regions around a reciprocal lattice point of silver are inconsistent with the Laue diffraction theory for an undistorted lattice. The intensity of a point (h_1, h_2, h_3) in the reciprocal lattice is proportional to $I_{h_1h_2h_3} = LL^*SS^*$ where $L_{h_1h_2h_3} = \sum_{l,m,n} \exp 2\pi i(lh_1 + mh_2 + nh_3)$

and $$S_{h_1h_2h_3} = \sum_g f_g(\theta) \exp 2\pi i(h_1g_1 + h_2g_2 + h_3g_3).$$

(l, m, n) are the coordinates of the origins of the unit cells in the crystal lattice, and (g_1, g_2, g_3) the coordinates of the individual centres within the unit cell, referred to the cell origin. $f_g(\theta)$ is the atomic scattering factor of those centres. LL^* for $h_1 = h_1' + \alpha$, $h_2 = h_2' + \beta$, $h_3 = h_3' + \gamma$ is equal to LL^* for $h_1 = h_1' - \alpha$, $h_2 = h_2' - \beta$, $h_3 = h_3' - \gamma$ provided h_1', h_2', h_3' are integers. LL^* is therefore symmetrical about each reciprocal lattice point. Although SS^* can, in the general case, be asymmetrical about certain reciprocal lattice points, this is not always so, and for the case of the face-centred cubic structures (e.g. silver) SS^* is symmetrical about all allowed reciprocal lattice points. In the present experiments, there should thus be complete symmetry of the Laue spikes about each allowed reciprocal lattice point. The following explanations have therefore to be considered: (i) refraction effects; (ii) a change in crystal structure near the surface, such that the cell structure factor S can cause asymmetry; (iii) crystal imperfections and distortions.

Although asymmetrical reciprocal lattice spikes do not appear to have been previously observed, one-sided streaks through diffraction spots have been, and Yamaguti (1935) considers the streaks to be due to refraction occurring as electrons enter and leave surface projections via certain facets. He does not explain, however, why refraction gives rise to streaks instead of subsidiary spots, as would be expected. Figure 12 shows the subsidiary spots which would be expected to appear on Figure 10 due to refraction at the (120) and (102) facets. The refraction displacements are very sensitive to the angle of incidence of the electrons with the facet which causes them, so that small variations in the angle of incidence would tend to cause the subsidiary spots to streak along [120] and [102], and perhaps coalesce to give a continuous streak. The variation in angle of incidence could perhaps be caused by facets with wavy surfaces, or might also be caused by a mosaic crystal which gives rise to facets which are rotated through small angles with respect to one another. The diffraction patterns indicate that the angular range due to this latter cause is less than one degree. It must also be remembered that a slightly convergent electron beam is used. It might therefore be possible to overcome the objection that separate subsidiary spots should be observed if refraction effects are appreciable.

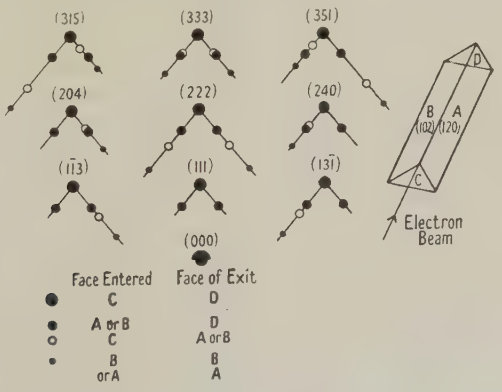

Figure 12. Subsidiary spots due to facet refraction, for pattern of Figure 10.

In the present experiments there are three further objections to the explanation that the observed asymmetrical streaks are due to refraction: (i) Although predominantly one-sided, the streaks pass through the diffraction spots; the shorter upward part of the streak cannot be explained by refraction. (ii) Except in special cases, most of the electron beam should enter and leave the crystal via facets which make large angles with the beam direction. Only a small part of the beam would thus be expected to suffer refraction, and streaks as strong as those observed would not be expected. Miyake (1938) only obtained strong subsidiary spots due to facet refraction when he set his beam several degrees off azimuth, so that much of the electron beam passed through the appropriate facets. (iii) A combined effect due to refraction at two different surfaces, one during entrance and one during exit, would be expected to occur. No such effects are observed.

Refraction cannot, therefore, entirely explain the observed asymmetrical streaks, but it might contribute strongly; thus the asymmetrical streaks which pass through the Laue spots (see Figures 8 and 10) might be due to the

superposition of a streak arising from a Laue spike and a streak due to refraction. That the streaks on Figure 10 can be entirely due to asymmetrical spikes, which are tangential to the Ewald sphere, does not seem very likely, since such long spikes would be expected to give rise to prominent subsidiary spots at certain azimuthal settings, and no such spots were observed.

The cell structure factor S, as previously mentioned, can sometimes introduce asymmetry into the reciprocal lattice, but not with a face-centred cubic structure. If, however, the lattice structure near the surface were changed (e.g. to a hexagonal lattice) then asymmetry might result. The change would have to be such as to introduce no extra reciprocal lattice points, and for this reason an explanation on these lines is considered unlikely.

The final effect to be considered is that of crystal distortion. If a crystal lattice is distorted, then the symmetry of LL^* is no longer maintained. A simple example to consider is that of a crystal (Bravais lattice) with one set of plane spacings changed so that the distance between the nth and $(n+1)$th plane from the surface is given by $af(n)$, where a is the normal spacing of the set of parallel planes, and $f(n)$ is some arbitrary function. Consider a rectangular block of crystal with the crystal axes parallel to the edges of the block, and let the (001) plane spacings be modified. Then the Laue factor may be written as

$$L = \sum_{l,m} \exp 2\pi i(lh_1 + mh_2) \sum_{n} \exp 2\pi i f(n)h_3 ;$$

$f(n)$ is arranged so that the spacings of the (001) planes near the surface are larger than normal, and other parallel planes gradually approach the normal value as n increases. It can be shown (unpublished work by Mr. Skwirzynski) that the spike due to the (001) facets will be asymmetrical, being much longer on the side nearer the origin of the reciprocal lattice. A qualitative picture of the result is given by considering that the gradual increase of the crystal spacings causes a gradual decrease of the corresponding reciprocal lattice distances, so that the diffraction spots are streaked on the side nearer to the central spot. The change in plane spacing may be regarded as a non-linear stretch of the crystal lattice along a direction perpendicular to the particular crystal planes.

An increase of the spacings of the planes parallel to and near to a surface facet would therefore cause the spike due to that facet to become asymmetrical. An important result which follows from the theory is that the reciprocal lattice should contain a plane across which the asymmetry should reverse in direction. This reciprocal lattice plane is perpendicular to the direction along which the crystal lattice is stretched, and passes through the origin. The spikes on either side of this reversal plane will be longer on the side pointing towards the plane. The reciprocal lattice will still be symmetrical about its origin.

In order to apply these calculations to the explanation of the observed case of the asymmetrical (210) type spikes, it is necessary to choose a unit cell with no structure factor (Bravais lattice) so that two of the principal crystal axes are in the (210) plane and the third perpendicular to it. All of these conditions cannot be fulfilled simultaneously, and the third crystal axis has to be chosen (for example) as the $[1\bar{1}0]$ axis (referred to the cubic frame). The other two axes are the $[1\bar{2}1]$ and [001], both lying in the (210) plane, and the unit cell only contains one atom (Figure 13). This means that the crystal is stretched along the $[1\bar{1}0]$ axis, which is not perpendicular to the (210) planes, so that the (210) planes are also displaced parallel to one another during the stretching.

This type of distortion should lead to the (110) reciprocal lattice plane being a plane of reversal for the asymmetrical (210) spikes. Since this plane of reversal is not observed on the diffraction photographs, non-linear stretching along the $[1\bar{1}0]$ crystal axis does not supply a sufficient explanation of the asymmetry. Other stretching directions which can be considered by this simple treatment also do not fit as regards reversal of the asymmetry. The treatment of a non-linear stretch in any general direction is more difficult to deal with, since the stretching would have to be resolved into its three components along the principal crystal axes, and a triple summation evaluated. This would not lead to a simple rule for the plane of reversal.

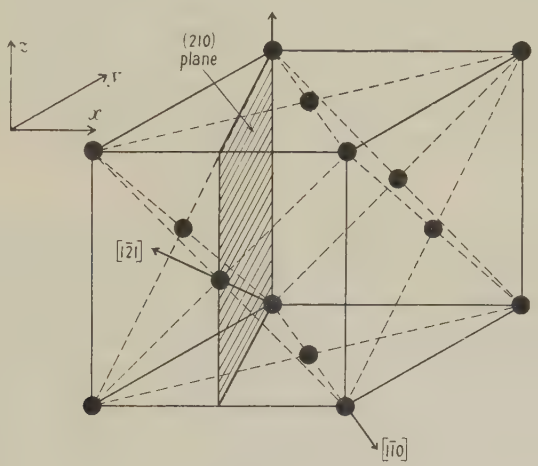

Figure 13.

The important result of these considerations is that lattice distortion can cause the Laue spikes to become asymmetrical about the centre of the reciprocal lattice point, and it seems reasonable to suppose that a certain distortion, not necessarily a simple stretch, would probably lead to the observed asymmetry. It is not easy to decide which distortion has to be chosen, because each choice, which is to a large extent a matter of guesswork, would have to be checked for such details as the occurrence or otherwise of planes of symmetry reversal in the reciprocal lattice, and for the non-appearance of extra reciprocal lattice points.

Summarizing the conclusions which follow from the above discussion, we can offer the following explanation of the asymmetrical effects: (i) the asymmetrical spikes are due to facets on the surface, the asymmetry arising from lattice distortion; (ii) the asymmetrical streaks observed on many of the diffraction photographs are due to the superposition of effects due to the refraction of electrons upon entering and leaving the crystal surface via certain facets, and effects due to Laue spikes arising from the same facets. It is possible that the asymmetry effects observed with the electrolytically polished surfaces are also due to crystal distortions near the surface.

No explanation of the asymmetry in terms of dynamical interaction or other effects such as absorption has so far proved to be satisfactory.

If a change in crystal spacings near the surface is sufficient to account for the observed asymmetry, then this could possibly arise if, during the electrolytic treatment of the crystals, some foreign atoms should become adsorbed at the

surface, and pack between the first few atomic layers. It is well known, for example, that silver readily dissolves oxygen. Any such adsorbed atoms, particularly if they are of low atomic weight, would otherwise be difficult to detect by electron diffraction.

It is interesting to note that asymmetrical effects in the form of streaks through spots have been observed during x-ray studies in aluminium–copper mixtures (Preston 1938a, b, Guinier 1938). Preston (1938a) has suggested that this asymmetry arises from a varying lattice parameter accompanied by a varying structure amplitude.

Laue (1937) has stated that the appearance or otherwise of subsidiary spots (due to reciprocal lattice spikes) around a normally forbidden spot should give some information concerning the fine structure of the facets. With the present experiments, the spikes were so short that it is considered that any spike surrounding a forbidden spot would be too weak to observe. No conclusions can therefore be drawn about the finer details of the facets.

ACKNOWLEDGMENTS

The author is indebted to Sir George Thomson and Dr. W. Cochrane for their guidance and advice throughout the progress of the work. He also wishes to express his gratitude to Dr. M. Blackman, without whose advice and help the treatment of the asymmetrical effects associated with crystal distortions would not have been possible.

REFERENCES

Brück, L., 1936, *Ann. Phys., Lpz.*, **26,** 233.
Cochrane, W., 1936, *Proc. Phys. Soc.*, **48,** 723.
Cowley, J. M., and Rees, A. L. G., 1947, *Proc. Phys., Soc.*, **59,** 287.
Guinier, A., 1938, *C. R. Acad. Sci., Paris*, **206,** 1641.
Halfawy, M., 1948, *Electroplating*, March, 205.
Kirchner, F. and Lassen, H., 1935, *Ann. Phys., Lpz.*, **24,** 113.
Kranert, W., Leise, K. H., and Raether, H., 1944, *Z. Phys.*, **122,** 248.
von Laue, M., 1936, *Ann. Phys., Lpz.*, **26,** 55 ; 1937, *Ibid.*. **29,** 211.
Miyake, S., 1938, *Sci. Pap. Inst. Phys. Chem. Res., Tokyo*, **34,** 565.
Pashley, D. W., 1949, *Metal Industry*, **75,** 557.
Preston, G. D., 1938 a, *Proc. Roy. Soc.* A, **167,** 526 ; 1938 b, *Phil. Mag.*, **26,** 855.
Raether, H., 1946, *Optick I*, **2,** 2.
Shuttleworth, R., King, R., and Chalmers, B., 1947, *Metal Treatment*, **51,** 161.
Thomson, G. P., 1931, *Proc., Roy. Soc.* A, **133,** 1.
Thomson, G. P., and Cochrane, W., 1939, *Theory and Practice of Electron Diffraction* (London : Macmillan).
Tull, V. F. G., 1951, *Proc. Roy. Soc.* A, **205,** 219.
Yamaguti, T., 1935, *Proc. Phys. Math. Soc. Jap.*, **17,** 443.

Field Dependence of the Dielectric Constant*

By J. J. O'DWYER†
Department of Theoretical Physics, University of Liverpool

Communicated by H. Fröhlich; MS. received 13th June 1951

ABSTRACT. A very general calculation has been made by Fröhlich giving the dielectric constant of a material in terms of the spontaneous fluctuations of the electric moment of the material which would occur in a field-free region. This calculation is now extended one step further so as to include the first term in the field dependence of the dielectric constant. By way of illustration the general theory is applied to Kirkwood's model for a dipolar liquid. (In order to preserve continuity of argument it has been found necessary to reproduce much of Fröhlich's work.)

§1. INTRODUCTION

ATTEMPTS to set up a theory of the field dependence of the dielectric constant of a material have nearly always related to water, since the most obvious practical application of this saturation effect is that of finding the field strength in the neighbourhood of ions in an electrolyte. Debye (1928) attempted to estimate this effect by applying Mosotti's hypothesis, but the experiments of Malsch (1928) showed a very much smaller effect for water than that anticipated by Debye's estimate. More recently Booth (1951) has given a treatment of the saturation effect using Kirkwood's analysis, and has applied the results to water. This application, however, contains a mistake, as has been pointed out elsewhere.

In the following paper Fröhlich's (1949) calculations for the dielectric constant are extended so as to include the first term of the field dependence. A general method is developed for dealing with this correction term, which is then applied to Kirkwood's (1939) model of a dipolar liquid.

§2. CALCULATIONS

2.1. *Preliminaries*

Following Fröhlich we consider an infinite, homogeneous, isotropic dielectric which is not permanently polarized. This is split up into equal regions, each of which is just large enough to have the same dielectric properties as a macroscopic specimen. A spherical region containing a large number of these smaller regions is then considered, and the dielectric constant calculated in terms of the spontaneous fluctuations of the large sphere embedded in its own medium. The particles of the sub-regions inside the sphere will be treated according to classical statistical mechanics, but the outside will be considered as a continuous dielectric of macroscopic dielectric constant

$$\epsilon = \epsilon_s + f(E) \qquad \ldots\ldots(1)$$

where ϵ_s is the field independent static dielectric constant.

* Based on *E.R.A. Report* L/T 258.
† Now at National Standards Laboratory, Sydney, Australia.

Suppose that the large spherical region consists of a number of charges e_i, each of which can be described in terms of its displacement $\mathbf{r}_i$ from its position in the ground state of the whole system. If we put

$$X=(\mathbf{r}_1, \mathbf{r}_2, \ldots, \mathbf{r}_i, \ldots), \quad dX=d\mathbf{r}_1\, d\mathbf{r}_2 \ldots d\mathbf{r}_i \ldots$$

then the average value of the projection of the moment of the sphere in the direction of the macroscopic field will be

$$M_E=\frac{\int M(X)\cos\theta \exp\{-U(X,E)/kT\}\,dX}{\int \exp\{-U(X,E)/kT\}\,dX} \qquad \ldots\ldots(2)$$

where $U(X, E)$ is the potential energy of the system in the configuration X in the presence of a field E, $M(X)$ is the moment of the sphere in terms of the charge displacements, and θ is the angle between $\mathbf{M}(X)$ and $\mathbf{E}$.

2.2. *The Cavity Field*

The potential energy is given by Fröhlich as

$$U(X,E)=U(X)-\frac{3\epsilon_s}{2\epsilon_s+1}M(X)E\cos\theta \qquad \ldots\ldots(3)$$

where $U(X)$ is the energy in the absence of a macroscopic field, and the second term represents the interaction of the cavity field with charges of the spherical region. This second term will not be correct for our case as the dielectric constant of the medium is now a variable function depending on the field strength. If it is assumed that equation (1) can be written as

$$\epsilon=\epsilon_s\{1+\delta E^2\} \qquad \ldots\ldots(4)$$

where δ is a small constant, then the first order approximation to the cavity field can be obtained by expansion of the potential in spherical harmonics. The cavity field will, of course, consist of a uniform and a non-uniform part, and it can be shown that the latter is of a smaller order than the correction in the former. In fact to a first order the cavity field is

$$\mathbf{G}=\{3\epsilon_0/(2\epsilon_0+1)\}\mathbf{E}_\infty \qquad \ldots\ldots(5)$$

where $\mathbf{E}_\infty$ is the macroscopic field at a great distance from the cavity and

$$\epsilon_0=\epsilon_s\left\{1+\delta\left(\frac{3\epsilon_s}{2\epsilon_s+1}E_\infty\right)^2\right\}.$$

We may then give the potential energy as

$$U(X,E)=U(X)-\frac{3\epsilon_0}{2\epsilon_0+1}M(X)E\cos\theta. \qquad \ldots\ldots(6)$$

2.3. *The Fundamental Equation*

In view of (6) we make the expansion

$$\exp\{-U(X,E)/kT\}$$
$$=\exp\{-U(X)/kT\}\left[1+C\frac{M(X)E}{kT}\cos\theta + \frac{C^2}{2}\frac{M^2(X)E^2}{k^2T^2}\cos^2\theta+\frac{C^3}{6}\frac{M^3(X)E^3}{k^3T^3}\cos^3\theta+\ldots\right], \qquad \ldots\ldots(7)$$

where

$$C=3\epsilon_0/(2\epsilon_0+1) \qquad \ldots\ldots(8)$$

varies very slowly with E compared with the term of which it is the coefficient. Substituting (7) into (2) and noting that terms of the form

$$\int M^n(X)\cos^n\theta \exp\{-U(X)/kT\}\,dX$$

will vanish if n is odd (they are proportional to an odd power of the moment in the **E** direction in the absence of a macroscopic field) we find

$$M_E = \frac{(C/kT)\int M^2(X)E\cos^2\theta \exp\{-U(X)/kT\}\,dX + (C^3/6k^3T^3)\int M^4(X)E^3\cos^4\theta\exp\{-U(X)/kT\}\,dX}{\int\exp\{-U(X)/kT\}\,dX + (C^2/2k^2T^2)\int M^2(X)E^2\cos^2\theta\exp\{-U(X)/kT\}\,dX}$$

retaining only terms of order up to E^3. Expanding the denominator by the binomial theorem

$$M_E = \frac{CJE}{kT}\int M^2(X)\cos^2\theta\exp\{-U(X)/kT\}\,dX + \frac{C^3JE^3}{6k^3T^3}\int M^4(X)\cos^4\theta\exp\{-U(X)/kT\}\,dX - \frac{C^3J^2E^3}{2k^3T^3}\left[\int M^2(X)\cos^2\theta\exp\{-U(X)/kT\}dX\right]^2 \quad \ldots\ldots(9)$$

where

$$1/J = \int\exp\{-U(X)/kT\}. \quad \ldots\ldots(10)$$

Since the field **E** may have any direction relative to $\mathbf{M}(X)$, we must average over all values of θ. This gives

$$M_E = \frac{1}{3}C\frac{E}{kT}\overline{M^2} + \frac{1}{90}C^3\frac{E^3}{k^3T^3}\{3\overline{M^4} - 5(\overline{M^2})^2\}, \quad \ldots\ldots(11)$$

where $\overline{M^2}$ and $\overline{M^4}$ are the mean square and fourth power respectively of the spontaneous polarization of a sphere of the dielectric embedded in a large specimen of the same material.

Equation (11) is the basic result from which we calculate the dielectric constant. Before proceeding to special cases, it is necessary to develop equation (11) further and show that, in the general case, it does lead to a polarization which is directly proportional to the volume.

2.4. *Discussion of* $\overline{M^2}$

Suppose now that the large sphere is composed of N units (molecules or other groups of atoms) in such a way that each unit has on the average the same polarization in an external field. Let us suppose also that each unit contains the same number, k, of elementary charges which in each case can be arranged in a similar way relative to each other and relative to their surroundings. Let $x_j = (\mathbf{r}_{j1}, \mathbf{r}_{j2}, \ldots \mathbf{r}_{jk})$, denote the whole set of displacements in the jth unit, and $\mathbf{m}(x_j)$ the electric dipole moment of this unit. Then

$$\mathbf{M}(X) = \sum_{j=1}^{N}\mathbf{m}(x_j) \text{ and } M^2(X) = \sum_{j=1}^{N}\mathbf{m}(x_j)\mathbf{M}(X). \quad \ldots\ldots(12)$$

Hence by definition $\overline{M^2} = \sum_{j=1}^{N} J\int \mathbf{m}(x_j)\mathbf{M}(X)\exp\{-U(X), kT\}\,dX. \quad \ldots\ldots(13)$

In the jth term of this summation the integration is carried out firstly over the the whole spherical region except the jth unit, and subsequently over this unit. This gives Fröhlich's result

$$\overline{M^2} = \sum_{j=1}^{N}\int \mathbf{m}(x_j)\,\mathbf{m}^*(x_j)\,p(x_j)\,dx_j, \quad \ldots\ldots(14)$$

where we have put $\mathbf{m}^*(x_j) = \dfrac{\int \mathbf{M}(X) \exp\{-U(X)/kT\}\, dX_j}{\int \exp\{-U(X)/kT\}\, dX_j}$, ...(15)

$$p(x_j) = \frac{\int \exp\{-U(X)/kT\}\, dX_j}{\int \exp\{-U(X)/kT\}\, dX} \qquad \text{.....(16)}$$

It will be seen that $\mathbf{m}^*(x_j)$ represents the average moment of the whole sphere for a fixed set x_j of displacements of the jth unit leading to a moment $\mathbf{m}(x_j)$, and $p(x_j)$ is the probability of finding the jth unit with this particular set of displacements.

Practically all terms in the summation (14) will be equal. The quantity $\mathbf{m}^*(x_j)$ represents the average moment of the large spherical region when the jth unit is fixed with a moment $\mathbf{m}(x_j)$. Now by a simple theorem in electrostatics the same moment $\mathbf{m}^*(x_j)$ is contained in any other sphere surrounding the jth unit, provided only that this sphere is sufficiently large to be treated macroscopically. Hence $\mathbf{m}^*(x_j)$ differs from $\mathbf{m}(x_j)$ because of short range interaction, and is independent of the position of the jth unit provided that it is not too near the surface of the sphere. The number of units for which this will not hold can be made very small compared with the total, so we may write

$$\overline{M^2} = N\overline{\mathbf{m} \cdot \mathbf{m}^*} \qquad \text{.....(17)}$$

where $$\overline{\mathbf{m} \cdot \mathbf{m}^*} = \int \mathbf{m}(x_j)\, \mathbf{m}^*(x_j)\, p(x_j)\, dx_j, \qquad \text{.....(18)}$$

where j may refer to any of the units except those near the surface of the sphere. In view of the above interpretation of $\mathbf{m}^*$ equation (18) may be written somewhat differently. Using (15) and (16), together with the fact that short range interaction determines $\mathbf{m}^*$, we may write

$$\overline{\mathbf{m} \cdot \mathbf{m}^*} = \frac{\int \mathbf{m}(x_j)\mathbf{M}(X_1) \exp\{-U(X_1)/kT\}\, dX_1}{\int \exp\{-U(X_1)/kT\} dX_1}, \qquad \text{.....(19)}$$

where j again may refer to any of the units except those near the surface and $X_1 = (x_h, x_{h+1}, \ldots . x_j, \ldots . x_{m-1}, x_m)$ denotes the set of displacements of any set of units so chosen as to include the jth and all those units in short range interaction with the jth, but subject to no other restrictions.

2.5. *Discussion of* $\{3\overline{M^4} - 5(\overline{M^2})^2\}$

We may write $$\overline{M^4} = \sum_{k=1}^{N} \sum_{l=1}^{N} \overline{\{\mathbf{m}(x_k) \cdot \mathbf{M}(X)\}\{\mathbf{m}(x_l) \cdot \mathbf{M}(X)\}},$$

in virtue of equation (12) so that

$$3\overline{M^4} = 3 \sum_{k=1}^{N} \sum_{l=k}^{k+\eta} \overline{\{\mathbf{m}(x_k) \cdot \mathbf{M}(X)\}\{\mathbf{m}(x_l) \cdot \mathbf{M}(X)\}} + 3 \sum_{k=1}^{N} \sum_{l=1,\, k+\eta+1}^{k-1,\, N} \overline{\{\mathbf{m}(x_k) \cdot \mathbf{M}(X)\}\{\mathbf{m}(x_l) \cdot \mathbf{M}(X)\}}, \qquad \text{.....(20)}$$

the averages being over all configurational coordinates. The first double summation in (20) accounts for the case in which l refers to a unit which has at least one unit in common short range interaction with the kth (there are assumed to be η such units excluding the kth itself), while the second double summation covers all other cases.

To perform the average of the second term of (20), we divide the large sphere into two regions 1 and 2, such that region 1 includes all units from 1 to s including the kth and all units in short range interaction with it, and region 2 includes all

units from $s+1$ to N including the lth and all units in short range interaction with it. Then let $X_1=(x_1, \ldots . x_k, \ldots . x_s)$ and $X_2=(x_{s+i}, \ldots . x_l, \ldots . x_N)$ denote the set of configurational coordinates as shown, and we may write for the potential energy in the absence of a field

$$U(X)=U(X_1, X_2)=U(X_1)+U(X_2) \qquad \ldots\ldots(21)$$

if a small term (surface interaction energy between regions 1 and 2) be ignored. Also

$$\mathbf{M}(X)=\mathbf{M}(X_1)+\mathbf{M}(X_2). \qquad \ldots\ldots(22)$$

Using (22) in the second term of (20) yields four terms of which two vanish on averaging to give

$$\begin{aligned}
&3\sum_{k=1}^{N}\sum_{l=1,k+\eta+1}^{k-1,N}\overline{\{\mathbf{m}(x_k)\,.\,\mathbf{M}(X)\}\{\mathbf{m}(x_l)\,.\,\mathbf{M}(X)\}}\\
&\quad=3\sum_{k=1}^{N}\sum_{l=1,k+\eta+1}^{k-1,N}\big[\overline{\{\mathbf{m}(x_k)\,.\,\mathbf{M}(X_1)\}\{\mathbf{m}(x_l)\,.\,\mathbf{M}(X_2)\}}\\
&\qquad+\overline{\{\mathbf{m}(x_k)\,.\,\mathbf{M}(X_2)\}\{\mathbf{m}(x_l)\,.\,\mathbf{M}(X_1)\}}\big]\\
&\quad=4N(N-\eta-1)\overline{(\mathbf{m}\,.\,\mathbf{m}^*)^2}, \qquad \ldots\ldots(23)
\end{aligned}$$

since on using (21) in the averaging we find

$$\overline{\{\mathbf{m}(x_k)\,.\,\mathbf{M}(X_1)\}\{\mathbf{m}(x_l)\,.\,\mathbf{M}(X_2)\}}=\overline{(\mathbf{m}\,.\,\mathbf{m}^*)^2}$$

and

$$\begin{aligned}
&\overline{\{\mathbf{m}(x_k)\,.\,\mathbf{M}(X_2)\}\{\mathbf{m}(x_l)\,.\,\mathbf{M}(X_1)\}}\\
&\quad=\overline{\{\mathbf{m}(x_k)\,.\,\mathbf{m}(x_l, x_{l+r})\}\{\mathbf{m}(x_l)\,.\,\mathbf{m}(x_k, x_{k+r})\}}\\
&\quad=\tfrac{1}{3}\overline{\{\mathbf{m}(x_k)\,.\,\mathbf{m}(x_k, x_{k+r})\}\{\mathbf{m}(x_l)\,.\,\mathbf{m}(x_l, x_{l+r})\}}\\
&\quad=\tfrac{1}{3}\overline{(\mathbf{m}\,.\,\mathbf{m}^*)^2}
\end{aligned}$$

where $\mathbf{m}(x_k, x_{k+r})$ denotes the total moment due to the jth unit and all those in short range interaction with it.

To perform the average of the first term of (20) we write

$$\mathbf{M}(X)=\mathbf{m}(x_k, x_{k+\eta})+\mathbf{M}(X-x_k, x_{k+\eta}) \qquad \ldots\ldots(24)$$

where $(x_k, x_{k+\eta})$ denotes the set of coordinates $(x_k, x_{k+1}, \ldots . x_{k+\eta})$ and $(X-x_k, x_{k+\eta})$ denotes the set of all other coordinates. Using (24) in the first term of (20), and performing the summation over l, we obtain four terms of which two vanish on averaging to give

$$\begin{aligned}
&3\sum_{k=1}^{N}\sum_{l=k}^{k+\eta}\overline{\{\mathbf{m}(x_k)\,.\,\mathbf{M}(X)\}\{\mathbf{m}(x_l)\,.\,\mathbf{M}(X)\}}\\
&\quad=3\sum_{k=1}^{N}\overline{\{\mathbf{m}(x_k)\,.\,\mathbf{m}(x_k, x_{k+\eta})\}m^2(x_k, x_{k+\eta})}\\
&\quad+3\sum_{k=1}^{N}\overline{\{\mathbf{m}(x_k)\,.\,\mathbf{M}(X-x_k, x_{k+\eta})\}\{\mathbf{m}(x_k, x_{k+\eta})\mathbf{M}(X-x_k, x_{k+\eta})\}}\\
&\qquad\qquad\qquad\qquad\qquad\qquad\qquad\qquad\qquad\qquad\qquad\qquad\qquad\qquad\qquad\qquad\ldots\ldots(25)
\end{aligned}$$

The second term of (25) can be simplified by performing the following averages

$$\begin{aligned}
&3\sum_{k=1}^{N}\overline{\{\mathbf{m}(x_k)\,.\,\mathbf{M}(X-x_k, x_{k+\eta})\}\{\mathbf{m}(x_k, x_{k+\eta})\,.\,\mathbf{M}(X-x_k, x_{k+\eta})\}}\\
&\quad=3\sum_{k=1}^{N}\overline{\{\mathbf{m}(x_k)\,.\,\mathbf{M}(X-x_k, x_{k+\eta})\}\{\mathbf{m}^*(x_k)\,.\,\mathbf{M}(X-x_k, x_{k+\eta})\}}\\
&\quad=\sum_{k=1}^{N}\overline{\{\mathbf{m}(x_k)\,.\,\mathbf{m}^*(x_k)\}M^2(X-x_k, x_{k+\eta})}\\
&\quad=N\overline{\mathbf{m}\,.\,\mathbf{m}^*}(N-\eta-1)\,\overline{\mathbf{m}\,.\,\mathbf{m}^*}. \qquad \ldots\ldots(26)
\end{aligned}$$

Then using (23), (25) and (26) in (20) we have finally

$$3\overline{M^4}-5(\overline{M^2})^2 = 3\sum_{k=1}^{N}\overline{\{\mathbf{m}(x_k)\,.\,\mathbf{m}(x_k,x_{k+\eta})\}m^2(x_k,x_{k+\eta})} - 5N(\eta+1)(\overline{\mathbf{m}\,.\,\mathbf{m}^*})^2 \qquad \ldots\ldots(27)$$

and the expression (27) varies linearly with the volume of the macroscopic sphere considered. Further analysis of the first term of (27) requires the help of an explicit model.

2.6. *The Dielectric Constant*

Returning to equation (8), we write

$$C=\frac{3\epsilon_0}{2\epsilon_0+1}\simeq\frac{3\epsilon_s}{2\epsilon_s+1}, \qquad \ldots\ldots(28)$$

introducing an error which can be shown to be at least an order of magnitude smaller than the correction being calculated. Since

$$\epsilon-1=\frac{4\pi}{E}\frac{M_E}{V} \qquad \ldots\ldots(29)$$

by definition and Fröhlich gives

$$\epsilon_s-1=\frac{4\pi}{3V}\frac{3\epsilon_s}{2\epsilon_s+1}\frac{\overline{M^2}}{kT}, \qquad \ldots\ldots(30)$$

we have on inserting (28), (29) and (30) in (11)

$$\epsilon=\epsilon_s+\frac{4\pi}{V}\frac{1}{90}\left(\frac{3\epsilon_s}{2\epsilon_s+1}\right)^3\frac{E^2}{k^3T^3}\{3\overline{M^4}-5(\overline{M^2})^2\}, \qquad \ldots\ldots(31)$$

where by virtue of (27) the correction term in (31) is independent of the volume of the macroscopic sphere chosen.

§ 3. SPECIAL CASES

Equation (31) will be applied to two cases in which (27) can be calculated with the help of a detailed model.

3.1. *Assembly of Non-Interacting Dipoles*

In this case it is easily seen that (27) becomes

$$3\overline{M^4}-5(\overline{M^2})^2=-2N\mu^4 \qquad \ldots\ldots(27\,a)$$

where there are N dipoles each of moment μ, and (31) gives

$$\epsilon=\epsilon_s-\frac{4\pi}{45}\left(\frac{3\epsilon_s}{2\epsilon_s+1}\right)^3\frac{E^2}{k^3T^3}N_0\mu^4 \qquad \ldots\ldots(31\,a)$$

where there are N_0 dipoles per unit volume. (A simple direct calculation verifies this result.)

3.2. *A Dipolar Liquid (Kirkwood's Formula)*

An attempt to extend Kirkwood's formula for polar liquids can be made as follows. The liquid will be considered as a continuous medium of dielectric constant n^2 containing dipoles of moment $\boldsymbol{\mu}$ (different from the vacuum moment $\boldsymbol{\mu}_v$, but connected with it by

$$\boldsymbol{\mu}_v=3\boldsymbol{\mu}/(n^2+2), \qquad \ldots\ldots(32)$$

for the case of spherical molecules). This amounts to assuming that the molecular polarizability is due to electronic displacement. If, in addition, we assume that the main part of the dielectric saturation is due to dipole orientation and not to electronic displacement then (31) will become

$$\epsilon=\epsilon_s+\frac{4\pi}{V}\frac{1}{90}\left(\frac{3\epsilon_s}{2\epsilon_s+1}\right)^3\frac{E^2}{k^3T^3}\{3\overline{M^4}-5(\overline{M^2})^2\}. \qquad \ldots\ldots(31\,b)$$

Here ϵ_s is calculated from the specialized Kirkwood formula given by Fröhlich, viz.

$$\epsilon_s-n^2=\frac{3\epsilon_s}{2\epsilon_s+n^2}\frac{4\pi N_0\mu^2}{3kT}(1+z\,\overline{\cos\gamma}), \qquad \ldots\ldots(33)$$

where z is the average number of nearest neighbours and $\overline{\cos\gamma}$ is the average of the cosine of the angle between neighbouring dipoles. It is assumed in the derivation of (33) that only nearest neighbours make any contribution to $\mathbf{m}^*$.

When calculating the average of the first term of (27) on the Kirkwood model we may, to a good approximation, take η to refer to nearest neighbours only. Then

$$\overline{\{\mathbf{m}(x_k)\,.\,\mathbf{m}(x_k,x_{k+\eta})\}\mathbf{m}^2(x_k,x_{k+\eta})}$$
$$=\overline{\mu^4(1+z\cos\gamma)(z+1+2z\cos\gamma+\tfrac{1}{2}z(z-1)\cos\gamma')} \qquad \ldots\ldots(34)$$

where $\overline{\cos\gamma'}$ is the average of the cosine of the angle between dipolar directions of two nearest neighbours of a given molecule. For the second term of (27) we have at once

$$(\overline{\mathbf{m}\,.\,\mathbf{m}^*})^2=\mu^4(1+z\,\overline{\cos\gamma})^2 \qquad \ldots\ldots(35)$$

so using (34) and (35) in (27) and applying the result to (31*b*) we find for the extension of the specialized form of Kirkwood's formula

$$\epsilon=\epsilon_s-\frac{4\pi N_0}{90}\left(\frac{3\epsilon_s}{2\epsilon_s+n^2}\right)^3\frac{\mu^4E^2}{k^3T^3}[2(z+1)$$
$$+(7z^2+z)\,\overline{\cos\gamma}-6z^2\,\overline{\cos^2\gamma}+5z^2(z+1)(\overline{\cos\gamma})^2$$
$$-\tfrac{3}{2}z(z+1)\,\overline{\cos\gamma'}(1+z\,\overline{\cos\gamma})]. \qquad \ldots\ldots(31\,c)$$

§ 4. APPLICATION TO EXPERIMENTAL WORK

Since there is some experimental work available on the subject it seems desirable to apply the results of (31*c*) to a calculation of the dielectric constant of water. Using the model of Bernal and Fowler (1933) in which each water molecule has four nearest neighbours at the vertices of a regular tetrahedron, and the bond between neighbouring molecules is directed along the O–H bond of one molecule towards the oxygen ion of the other, we find by elementary trigonometry $\overline{\cos\gamma}=\frac{1}{3}$, $\overline{\cos^2\gamma}=\frac{1}{3}$, $\overline{\cos\gamma'}=\frac{1}{27}$, which gives

$$\epsilon\simeq\frac{14\pi}{3}\left(\frac{n^2+2}{3}\right)^2\frac{\mu_v^2N_0}{kT}-9\pi\left(\frac{n^2+2}{3}\right)^4\frac{\mu_v^4N_0}{k^3T^3}E^2, \qquad \ldots\ldots(31\,d)$$

where (32) has been used, and the approximation $3\epsilon_s/(2\epsilon_s+n^2)\simeq 3/2$ made on account of the high dielectric constant of water.

Substituting numerical values: Avogadro's number $=6\times10^{23}$, molecular weight $=18$, $k=1{\cdot}4\times10^{-16}$, $\mu_v=1{\cdot}9\times10^{-18}$ and $n^2=1{\cdot}77$ we find

$$\epsilon\simeq\frac{19{,}000}{T}-11\frac{E^2}{T^3}, \qquad \ldots\ldots(31\,e)$$

or at room temperature ($T \simeq 300°$ K).

$$\epsilon \simeq 63 - 4{\cdot}3 \times 10^{-12} E^2 \qquad \ldots\ldots (31f)$$

where E is now in volts per cm.

If we define the incremental dielectric constant as $\partial D/\partial E$, then for water at room temperature

$$\partial D/\partial E = 63 - 12{\cdot}9 \times 10^{-12} E^2. \qquad \ldots\ldots (36)$$

On the basis of Debye (1928) theory, Malsch (1927) calculated that he should obtain about 14% decrease in the incremental dielectric constant of water at room temperature in a field of 100,000 volts per cm., but in his initial experiments he failed to detect any effect. In later experiments (Malsch 1928) he found that the dielectric constant did, in fact, saturate according to a law of the form of (36), and he measured a 0·7% decrease in the incremental dielectric constant of water at room temperature, in a field of 250,000 volts per cm. The present theory predicts a decrease of 1·2% in the incremental dielectric constant at this field strength. This agreement must be regarded as satisfactory in view of the approximate nature of the theory and the scarcity of relevant experimental work.

ACKNOWLEDGMENTS

The author wishes to express his sincere thanks to Professor H. Fröhlich who suggested this problem and offered much helpful advice. Thanks are also due to the Commonwealth Scientific and Industrial Research Organization of Australia and to the British Electrical and Allied Industries Research Association for research grants.

REFERENCES

Bernal, J. D., and Fowler, R. H., 1933, *J. Chem. Phys.*, **1**, 515.
Booth, F., 1951, *J. Chem. Phys.*, **19**, 391.
Debye, P., 1928, *Polar Molecules*, (New York : Dover Publications (reprinted 1939)).
Fröhlich, H., 1949, *Theory of Dielectrics* (Oxford : University Press).
Kirkwood, J. G., 1939, *J. Chem. Phys.*, **7**, 911.
Malsch, J., 1927, *Ann. Phys. Lpz.*, **84**, 841; 1928, *Phys. Z.*, **29**, 770.

LETTERS TO THE EDITOR

Approximate Solution of a Transient Heat Flow Problem

The theoretical solution of a geophysical heat conduction problem has been obtained by approximate operational methods; it is thought that the results and the procedure used may be helpful in other types of 'diffusion' problems with analogous boundary conditions.

The problem is that of measuring the thermal constants of an infinite medium of low conductivity by the following method. A thermal 'probe' is inserted into the medium containing a source of heat and some form of thermometer, and a record obtained of temperature within the 'probe' versus elapsed time. The thermal constants are to be evaluated from this record.

A similar method has been used before (Hooper and Lepper 1950), but the simplifying assumptions made in the theory are too extreme for the present problem. The practical restrictions on the latter are: (i) the probe cross section must be circular and its outside diameter of the order of 4 cm. or greater, (ii) thermal contact resistance at the boundary between probe and external medium is likely to be high, and must be taken into account.

By using both 'large time' and 'small time' approximate solutions for the temperature in the probe it becomes possible to measure the contact resistance under the conditions of the experiment and to eliminate its effect.

The problem, basically, is that of solving the heat equation for an infinite region bounded internally by a (hollow) circular cylinder with the standard contact resistance boundary condition at the probe surface (Carslaw and Jaeger 1947 a, pp. 17–18), i.e. $-K_2\partial\theta_2/\partial\rho=H(\theta_1-\theta_2)$ and zero initial temperature.

The differential equation and boundary conditions have been subjected to the Laplace transformation and large and small time approximate solutions (Carslaw and Jaeger 1947 b, Goldstein 1932) obtained for a number of probe arrangements.

Examination of the possibilities shows that a hollow metal probe with constant heat flux across the inner surface is both experimentally practicable and convenient for calculation of results.

With the simplifying assumptions that the probe wall is perfectly conducting and that heat flow is entirely radial, the following results are obtained :

Large times (in the limit $a\to b$, $H\to\infty$, this solution reduces to one given by Carslaw and Jaeger (1947 a, p. 283)) : $(T=h_2^2t/b^2 \gg 1)$

$$\theta_1(t)\simeq\frac{aQ}{2K_2}\left[\ln 4T-\gamma+\frac{2K_2}{bH}+\frac{1}{2T}\left\{\ln 4T-\gamma+1-\frac{\alpha h_2^2}{bK_2}\left(\ln 4T-\gamma+\frac{2K_2}{bH}\right)\right\}+\mathrm{O}\left(\frac{1}{T^2}\right)\right].$$

Small times : $(T=h_2^2t/b^2 \ll 1)$

$$\theta_1(t)\simeq\frac{2aQ}{\alpha b}\left[t-\frac{H}{\alpha}t^2+\frac{16H^2}{15\sqrt{\pi\alpha}}\left(\frac{h_2}{K_2}\right)t^{5/2}+\mathrm{O}(t^3)\right],$$

where $\theta_1(t)$ is the probe temperature, t is the time, K_2, h_2^2 the thermal conductivity and diffusivity of the external medium, H the 'outer conductivity' at probe surface (a measure of the contact conductance), Q the heat flux (constant) across inner surface of probe, a, b the internal and external probe radii, $\alpha=(b^2-a^2)\delta_1c_1/b$, where δ_1, c_1 are the probe density and specific heat, γ is Euler's constant$=0{\cdot}57722\ldots$

Correction for finite probe conductivity is not difficult and may be necessary unless the probe walls can be made thin.

An upper limit can be placed on the error introduced by finite probe length. Restrictions are not particularly severe if temperature measurement is made at the centre; in the writers' work, for example, a length/diameter ratio of about 20 is expected to reduce the error from this cause well below the experimental error.

In order to determine thermal constants, two experiments will be made. From the results of a 'large time' experiment a plot of θ_1 against log t will enable the values of K_2 and $(\log h_2^2+2K_2/bH)$ to be determined to a first approximation. From the results of a 'small time' experiment, H can be determined roughly by rectification of the initial curve. Then a first approximation to h_2^2 can be obtained and, if necessary, the original value of H improved using further terms of the small-time series.

If $2K_2/bH$ is sufficiently small, then it is obvious that this term can be neglected and the small-time solution will not be required.

Experimental work using these results is in its early stages, and a full report on both theoretical and practical aspects will be made later.

Department of Physics,
University of Western Ontario,
London, Ontario, Canada.
25th September 1951.

J. H. Blackwell.
A. D. Misener.

Carslaw, H. S., and Jaeger, J. C., 1947 a, *Conduction of Heat in Solids* (Oxford : University Press); 1947 b, *Operational Methods in Applied Mathematics*, 2nd edition (Oxford : University Press), Ch. XIII.
Goldstein, S., 1932, *Proc. Lond. Math. Soc.*, **34**, 51.
Hooper, F. C., and Lepper, F. R., 1950, *Amer. Soc. Heat. Vent. Eng. J.*, August, 129.

Observations on the Interactions of μ-Mesons Underground

During the course of experiments on penetrating bursts carried out in Holborn Underground Station, at a depth equivalent to 60 metres of water, the results of which are described elsewhere (George and Trent 1951), we have made some observations on the behaviour of penetrating particles traversing large thicknesses of lead.

The apparatus, shown in the Figure, consisted of a number of counter trays separated by lead screens of various thicknesses. The events recorded were coincidences between one of the groups of tray T (a, b, c, d, e in figure), the centre counter of tray M, and one or more of the counters of tray B. In order to record which of the groups of counters of T and which of the counters of B were discharged in any coincidence, these counters and counter groups were connected to a 25-channel hodoscope of orthodox design.

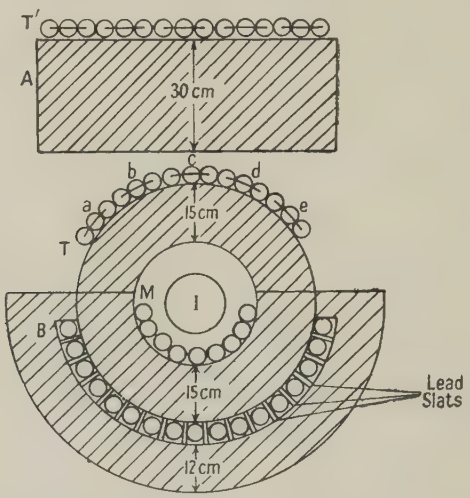

Our results may be separated into two groups, firstly those in which a single counter or counter group was discharged in each bank, and secondly, events in which the discharge of a single counter group in T and the centre counter in M was accompanied by the discharge of two or more counters of B.

In the first case the large majority of coincidences could be explained in terms of the passage of a single, undeviated particle through the apparatus. A small proportion of cases, however, were such that explanation in terms of a single, undeflected particle was not possible. These events could be explained either as a result of the production by a penetrating particle of one or more knock-on electrons in the centre portion of the apparatus, or else by the penetrating particle suffering large angle scatter.

From considerations of geometry, and from some subsidiary experiments on the production of knock-on electrons, we conclude that a large proportion of these events may be due to scatter, and further, the angular distribution of this scatter is such that it could not be due to coulomb interaction alone. We therefore conclude that nuclear scatter is occurring, and assuming that the particles observed are μ-mesons, the cross section deduced is 2×10^{-28} cm^2 per nucleon. On the other hand, the results may be explained by the presence of a small proportion ($\sim1\%$) of particles with nuclear geometric collision cross section, or by deviations of the μ-meson spectrum from the form assumed for the purpose of calculating the contribution due to coulomb scatter, viz. $N(E)dE=dE/(E+E_0)^3$, where E_0 equals $1{\cdot}2\times10^{10}$ ev.

This result is not strictly comparable with the results obtained at sea level by various other workers, and in any case, with the exception of the work of Amaldi and Fidecaro (1951), most other results on the scattering of mesons appear to have been carried out by means of cloud chambers, with consequent very different conditions of geometry, etc. Our results do not compare well with those of Amaldi and Fidecaro, who obtained a

considerably smaller cross section in their experiments with an apparatus similar to ours. Nevertheless, the figure of 2×10^{-28} cm^2 per nucleon appears reasonable in view of the values obtained by cloud-chamber workers (Sahiar, private communication).

With regard to the events in which two or more counters were discharged in bank B, simultaneously with a single counter in banks T and M, our conclusions remain substantially as suggested previously (George and Trent 1949), i.e. that groups, primarily pairs, of penetrating particles are produced with a cross section of 5×10^{-29} cm^2 per nucleon. We have, however, been able to ascertain more accurately the contribution due to knock-on electrons produced in the lead A, by introducing lead slats between the counters of bank B and noting the reduction in the number of coincidences with two or more counters discharged in B. From these later results we conclude that these events may not all be explained in terms of knock-on electrons, but that pairs of penetrating particles are produced, with a cross section having a lower limit of about 4×10^{-29} cm^2 per nucleon.

Further, as a result of the absence of a transition effect when an additional 30 cm. of lead was inserted at A in the telescope, the tray T being moved to position T′ for this purpose, we conclude that at least one of the penetrating particles is either strongly absorbed, as would be a π-meson, or else is generally of low energy (about 200 to 300 MeV.).

The results of further work on these phenomena are in process of publication.

Birkbeck College,
London.
2nd October 1951.

E. P. George.
P. T. Trent.

Amaldi, E., and Fidecaro, G., 1951, *Phys. Rev.*, **81**, 339.
George, E. P., and Trent, P. T., 1949, *Nature, Lond.*, **164**, 838; 1951, *Proc. Phys. Soc.* A, **64**, 733.

Nuclear Spin of $^{53}_{24}$Chromium

Previous observations (Bleaney 1950) of the paramagnetic resonance spectrum of the chrome alums have failed to reveal any hyperfine structure. This is due partly to the low abundance (9·4%) of the single odd isotope of chromium, mass 53, and partly to its presumably small nuclear moment. By using a crystal of potassium chromium selenate alum, diluted with the corresponding aluminium alum, and grown from heavy water, we have managed to reduce the line width sufficiently so that a small satellite line on either side of the main line due to the even isotopes could be observed. If this is ascribed to

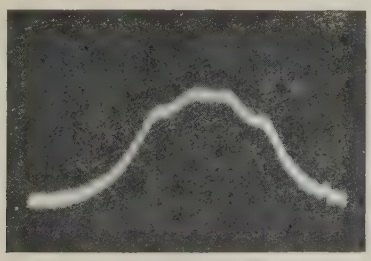

Hyperfine structure of $^{53}_{24}$Cr in the electronic transition $M=\frac{1}{2}\longleftrightarrow-\frac{1}{2}$ of dilute potassium chrome selenate alum.

the expected hyperfine structure of ^{53}Cr, the overall splitting ($\simeq$50 gauss) is of the expected order of magnitude, but the nuclear spin could not be determined owing to intermediate lines being obscured by the strong line of the even isotopes. Relative intensity measurements suggested that the spin is 3/2, but the accuracy was insufficient to be certain.

These measurements have been repeated on a sample of chromium enriched in the isotope 53. Four lines are clearly visible in the photograph of the spectrum shown in the figure, confirming the value 3/2 for the nuclear spin. Fitting the spectrum to the usual Hamiltonian

$$\mathscr{H}=g\beta\mathbf{H}.\mathbf{S}+D\{S_z^2-S(S+1)\}+A\,\mathbf{S}.\mathbf{I}$$

with $S=3/2$, the values of the constants are found to be

$$g=1\cdot976\pm0\cdot002, \quad |2D|=0\cdot21 \text{ cm}^{-1}, \quad |A|=0\cdot0018_5\pm0\cdot0001 \text{ cm}^{-1}.$$

In a crystal containing ordinary water instead of heavy water the value of $|2D|$ was $0\cdot19$ cm^{-1}, while g was unaltered. $2D$ is the electronic splitting in zero magnetic field.

An estimate of the nuclear magnetic moment of ^{53}Cr can be obtained by comparison with the spectrum of the isoelectronic ion V^{++} (Bleaney, Ingram and Scovil 1951). In each case the configuration is $3s^23p^63d^3$, ^4F, and Abragam and Pryce (1951) have shown that hyperfine splitting should be zero except through admixture of the state $3s3p^63d^34s$ by configurational interaction. Quantitative calculation of this admixture is not possible from first principles, and one writes $A=-2\gamma\beta\beta_N\langle 1/r^3\rangle\kappa$, where κ is an empirical coefficient. It turns out that the values of the product $\{\langle 1/r^3\rangle\kappa\}$ vary by not more than 20% for the four ions V^{++}, Mn^{++}, Co^{++} and Cu^{++}. Physically this means that the contribution to the magnetic field at the nucleus due to configurational interaction is constant to this accuracy. If this holds also for Cr^{+++}, one obtains the value $0\cdot45\pm0\cdot1$ n.m. from the ratio of the hyperfine structures of Cr^{+++} and V^{++}, using the known magnetic moment of ^{51}V (Knight and Cohen 1949). The empirical data which justify this method are somewhat scanty, and the result should be accepted with some reserve. The sign is not determined, but is expected to be negative (Schawlow and Townes (1951) predict $-0\cdot67$ n.m.).

The magnitude of the hyperfine structure in zero magnetic field is of interest in work on adiabatic demagnetization below $0\cdot01°$ K. Since the crystalline electric field splits the electronic levels ($\pm3/2$) away from the levels ($\pm1/2$) by about $0\cdot3°$ K., they must be treated separately. The hyperfine structure splits the former into four equally spaced doublets with an overall separation of $0\cdot011_9°$ K. The splitting of the ($\pm1/2$) levels is more complicated. There are two singlets at $-0\cdot0060$ and $+0\cdot0046$, and three doublets at $-0\cdot0055$, $+0\cdot0041$ and $+0\cdot0020$, these values being in degrees Kelvin relative to the position of the unsplit line.

The authors wish to record their gratitude to Dr. P. F. D. Shaw, who converted the chromium to the desired chemical form, and to the Director and the Electromagnetic Separator Group of the Atomic Energy Research Establishment, Harwell, who supplied the enhanced chromium 53. Our measurements show that the sample provided contained at least 97% of the isotope 53.

The Clarendon Laboratory,
Oxford.
6th October 1951.

B. Bleaney.
K. D. Bowers.

Abragam, A., and Pryce, M. H. L., 1951, *Proc. Roy. Soc.* A, **205**, 135.
Bleaney, B., 1950, *Proc. Roy. Soc.* A, **204**, 203.
Bleaney, B., Ingram, D. J. E., and Scovil, H. E. D., 1951, *Proc. Phys Soc.* A, **64**, 601.
Knight, W. D., and Cohen, V. W., 1949, *Phys. Rev.*, **76**, 1421.
Schawlow, A. L., and Townes, C. H., 1951, *Phys. Rev.*, **82** 268.

Interference in the Directional Correlation of Conversion Electrons

Two previous communications (Gardner 1949, 1951, denoted hereinafter by I and II) have investigated the directional correlation between the two conversion electrons successively ejected from an atom whose nucleus undergoes transitions A→B→C in cascade. In I both nuclear transitions were assumed to be pure electric multipole in character; in II pure electric–pure magnetic and pure magnetic–pure magnetic cascades were considered. It was also remarked in II that, to the approximation imposed by the initial assumptions, cascades with either or both transitions a mixture of electric and magnetic multipoles could be treated by taking just a weighted mixture of the appropriate pure cascades, there being no interference terms. The absence of interference terms was also noticed by Fierz (1949) in treating conversion-γ correlation in the approximation

of I and II. The present note shows that this non-appearance of interference terms in c-c and c-γ correlations derives essentially from two assumptions, namely, that the conversion electrons are ejected from an initial s-state, and that a non-relativistic treatment of internal conversion is justified. If either (or both) of these assumptions be disallowed the correlation formula will, in general, contain interference terms.

In I and II the final-state total wave function ψ_A is expressed as a linear combination of the final-state nuclear wave function ψ_C (subsequently dropped as a constant) and the final-state electron wave functions ψ_1, ψ_2, the coefficients of the various terms in this expansion being the familiar products of Wigner (Clebsch–Gordan) coefficients for the vector addition of angular momenta. Now if the transition A→B is a mixture of electric and magnetic multipoles ψ_1 breaks down into 'electric' and 'magnetic' parts, ψ_1^{E} and ψ_1^{M}; similarly with ψ_2 if B→C is a mixture. Hence ψ_A must be written as a mixture, say $\alpha\psi_A^{\mathrm{E}}+\beta\psi_A^{\mathrm{M}}$, so that in using the formula $I(\theta)\sim\sum_{M_A}\int\psi_A^*\psi_A\,d\tau$ for the relative angular distribution of the two electrons (see I and II) we have the following product to consider:

$$(\alpha^*\psi_A^{*\mathrm{E}}+\beta^*\psi_A^{*\mathrm{M}})(\alpha\psi_A^{\mathrm{E}}+\beta\psi_A^{\mathrm{M}})=|\alpha\psi_A^{\mathrm{E}}|^2+|\beta\psi_A^{\mathrm{M}}|^2+\alpha^*\beta\psi_A^{*\mathrm{E}}\psi_B^{\mathrm{M}}+\alpha\beta^*\psi_A^{\mathrm{E}}\psi_B^{*\mathrm{M}}.$$

The first two terms on the right-hand side are the pure multipole terms, fully discussed in I and II; it is the second two—the cross terms—which would give rise to interference effects, but which vanish in the above approximation. To see this one can use the expansion of ψ_A^{E} as a linear combination of the ψ_1^{E}, ψ_2^{E}, the expansion of ψ_A^{M} as a linear combination of the ψ_1^{M}, ψ_2^{M}, and the corresponding complex conjugate expansions for $\psi_A^{*\mathrm{E}}$ and $\psi_A^{*\mathrm{M}}$. On substituting these expansions in $\psi_A^{*\mathrm{E}}\psi_A^{\mathrm{M}}$ and $\psi_A^{\mathrm{E}}\psi_A^{*\mathrm{M}}$, and multiplying out, the general term in the resulting expression is found to contain a factor of the type:

$$\sum_{\alpha',\,\beta'} C^{c\gamma}_{a'\alpha'b'\beta'}C^{c'\gamma'}_{a'\alpha'b'\beta'}$$

where, in the notation of I and II, the C's are Wigner vector addition coefficients, a', b', c, c' are angular momenta and α', β', γ, γ' their magnetic components. In particular the c, c' are the orbital angular momenta of an ejected electron associated with a magnetic 2^l-pole and an electric 2^{l+1}-pole respectively. (This is the only type of mixture of practical interest.) If c, c' are different the above sum of products of Wigner coefficients vanishes by their familiar orthogonality property (see, for example, Racah 1942); that is to say $\psi_A^{*\mathrm{E}}\psi_A^{\mathrm{M}}$ and $\psi_A^{\mathrm{E}}\psi_A^{*\mathrm{M}}$ vanish since every term in their expansions vanishes. Now for electrons initially in an s-state the non-relativistic theory of internal conversion predicts $c=l-1$ (from the magnetic 2^l-pole) and $c'=l+1$ (from the electric 2^{l+1}-pole). In the relativistic treatment, however, there are in general two alternative values of orbital angular momentum available to an electron associated with a particular (electric or magnetic) multipole, according to whether or not 'spin-flip' occurs. Therefore one has to consider two values for c and two values for c', and as these four values are not all different the interference terms do not all vanish. Again, suppose we remove the restriction to s-electrons, and consider conversion electrons ejected from an initial p-state, say. Each electron then has an initial orbital angular momentum which can in general combine in three possible ways with that which it acquires from the nucleus, so, even in the non-relativistic treatment, there are three alternative values for c and three for c'; and since these are not all different, not all the interference terms vanish. When considering specific experimental examples one must, as always, bear in mind the operation of any special selection rules which may prohibit a common value of c and c' and so prevent interference.

The inadequacy of the non-relativistic theory for calculating magnetic internal conversion coefficients, even at relatively low energies, has been pointed out by Drell (1949) who gives a semi-relativistic treatment (neglecting higher powers than the first of $h\nu/mc^2$). In conversion correlation the error is probably not as serious since one has here to deal with a ratio of two matrix elements which are affected more or less equally by the first-order relativistic correction. Fully relativistic calculations for conversion correlation in pure multipole cascades are being carried out by M. E. Rose and collaborators at the Oak Ridge National Laboratory, Tennessee; interference effects are being investigated by S. P. Lloyd at the Princeton Institute. I am indebted to Professor Drell, Dr. Rose and Dr. Lloyd for correspondence; also to Professor Racah who kindly sent me the manuscript of his forthcoming paper (Racah 1951) dealing with the general angular correlation problem (all kinds of particles, with or without interference).

In conclusion, this opportunity is taken to correct an earlier statement concerning a paper by Berestetzky (1948). The treatment of internal conversion in that paper is completely non-relativistic, and not, as erroneously reported in II, semi-relativistic in the sense of Drell's calculations.

Division of Atomic Energy,
National Research Council of Canada,
Chalk River, Ontario.
30th August 1951.

J. W. GARDNER*.

* N.R.L. Postdoctoral Fellow.

BERESTETZKY, V., 1948, *J. Exp. Theor. Phys. U.S.S.R.*, **18**, 1057.
DRELL, S. D., 1949, *Phys. Rev.*, **75**, 132.
FIERZ, M., 1949, *Helv. Phys. Acta*, **22**, 489.
GARDNER, J. W., 1949, *Proc. Phys. Soc.* A, **62**, 763; 1951, *Ibid.*, **64**, 238.
RACAH, G., 1942, *Phys. Rev.*, **62**, 438; 1951, *Ibid.*, in the press.

Theoretical Discussion of the Beta Decay of ^{32}P

The apparent contradiction between the empirically second forbidden *ft* value of ^{32}P and its allowed shape beta spectrum has not yet been explained. The beta spectrum has been measured by Siegba n (1946), Langer and Price (1949), Agnew (1950) and Warshaw, Chen and Appleton (1950), and there can be little doubt that the spectrum has the allowed shape for energies greater than about 250 kev. Below this energy, Agnew and Warshaw *et al.* have reported a marked excess of electrons over the number predicted for an allowed spectrum; this, however, may be due to a second low energy spectrum with an end point at about 250 kev. and an intensity about 1 or 2% of the main transition.

None of the second forbidden correction factors are capable of explaining the shape of the ^{32}P spectrum. The only correction factors which do so are those for the allowed transitions, for first forbidden transitions with unit change of spin on the tensor and polar vector interactions, and for first forbidden transitions with no spin change on the axial vector and pseudoscalar interactions. Since no gamma-rays are observed, the transition must be to the ground state of ^{32}S, and since this has spin zero and the spin change in the transition is not more than 1, the spin of ^{32}P must be 0 or 1. Since the transition must be either allowed or first forbidden, some mechanism such as an additional selection rule is necessary to explain the long lifetime.

According to the shell model, neutron and proton levels are filled in the order $s_{1/2}$, $p_{3/2}$, $p_{1/2}$, $d_{5/2}$, $s_{1/2}$, $d_{3/2}$, . . . (this ordering of the $s_{1/2}$ and $d_{3/2}$ levels is necessary to explain the observed spins of odd nuclei). The shell model interpretation of the decay of ^{32}P is therefore that a $d_{3/2}$ neutron is transformed into a $s_{1/2}$ proton; this involves no parity change, and consequently the transition cannot be first forbidden and must be allowed.

It has been shown (Pursey 1951) that for single particle transitions involving an orbital angular momentum change of two units, and a total angular momentum change of one unit the matrix elements $\int\boldsymbol{\sigma}$ and $\int\beta\boldsymbol{\sigma}$ (which are usually classed as allowed) are of order $(v/c)^2$, where v is of the order of the nucleon velocities. Since according to the shell model the decay of ^{32}P is of this type, this may account for the long half-life of the transition. The correction factor for the transition, assuming the tensor interaction, is the same as C_{1T} given by Konopinski and Uhlenbeck (1941) if $\int\boldsymbol{\alpha}$ is replaced by $\int\beta\boldsymbol{\sigma}$ and $\int\boldsymbol{\sigma}\times\mathbf{r}$ by $\int\beta\boldsymbol{\alpha}\times\mathbf{r}$. If the magnitudes of the matrix elements $\int\beta\boldsymbol{\sigma}$ and $\int\beta\boldsymbol{\alpha}\times\mathbf{r}$ are assumed to be $(v/c)^2$ and $v\rho/c$ respectively, where $\rho=(1/274)A^{1/3}$ is the nuclear radius in units of the Compton wavelength of the electron, then the theoretical lifetime depends only on the sign of the cross term in the correction factor and on one parameter $x=v/c\rho$ which may be chosen to fit the observed lifetime. Good fits are obtained by taking $x=12$ $(v/c=0{\cdot}14)$ if the cross term is negative and $x=5{\cdot}5$ $(v/c=0{\cdot}064)$ if the cross term is positive. These values of the ratio of v/c to ρ are rather larger than those usually taken : the writer's work on the ratio of $\int\boldsymbol{\alpha}$ to $\int\mathbf{r}$ (Pursey 1951) suggests, however, that they are not excessive. The theoretical spectra for both values of x used are experimentally indistinguishable from allowed spectra. A similar explanation of the transition is, of course, possible using the axial vector interaction.

Sherwin (1951) has measured the angular correlation between the electron and neutrino emitted from ^{32}P, and found it to be given approximately by $(1+\cos\theta)$. From the theoretical work of Greuling and Meeks (1951) it is clear that this angular correlation is consistent only with allowed transitions with no spin change on the polar vector interaction, and with first forbidden transitions with no spin change on the axial vector interaction; it is not consistent with the explanation of the spectrum shape and lifetime given above. The spectrum shape, lifetime and angular correlation can all be explained by assuming that the transition is allowed, and that the interaction is mainly tensor or axial vector with an admixture of about 1% of polar vector; this explanation, however, seems very artificial.

A direct measurement of the spin of ^{32}P would be of great value. If the spin is greater than 1, then it is impossible to explain the shape of the spectrum on the present theory of beta decay. If it is 1, then the lifetime and the spectrum shape can both be explained simply and naturally on the basis of the shell model, but Sherwin's angular correlation measurements are in contradiction with the theory given by Greuling and Meeks. If the spin is 0, the angular correlation can be explained, but the shell model level scheme breaks down, and the problem of reconciling the lifetime and spectrum shape remains unsolved unless the interaction is assumed to contain an admixture of the polar vector interaction so small as to be unobservable in any other experiment.

The writer wishes to express his gratitude to the Department of Scientific and Industrial Research for financial assistance during the course of this work.

Department of Natural Philosophy,
University of Glasgow.
2nd October 1950.

D. L. Pursey.*

* Now at Physics Department, King's College, London.

Agnew, H. M., 1950, *Phys. Rev.*, **77**, 655.
Greuling, E., and Meeks, M. L., 1951, *Phys. Rev.*, **82**, 531.
Konopinski, E. J., and Uhlenbeck, G. E., 1941, *Phys. Rev.*, **60**, 308.
Langer, L. M., and Price, H. C., Jr., 1949, *Phys. Rev.*, **76**, 641.
Pursey, D. L., 1951, *Phil. Mag.*, **42**, 1193.
Sherwin, C. W., 1951, *Phys. Rev.*, **82**, 52.
Siegbahn, K., 1946, *Phys. Rev.*, **70**, 127.
Warshaw, S. D., Chen, J. J. L., and Appleton, G. L., 1950, *Phys. Rev.*, **80**, 288.

The G.L.E.E.P. as an Absolute Standard of Thermal Neutron Density

The Graphite Low Energy Experimental Pile at Harwell has been calibrated for use as a standard of thermal neutron density. It can be used within the range 10 neutrons/cm^3 to 2×10^4 neutrons/cm^3, the density being known throughout the range to $\pm5\%$. We have considered as thermal neutrons those with energies below the cadmium 'cut-off', i.e. below about 0·4 ev.

We have made an absolute measurement of the density of thermal neutrons at the centre of the pile in terms of the current from an ion chamber permanently situated 1 metre from the centre. The pile is normally operated only at low powers, with small temperature variations, and with a constant amount of absorbing material in the pile. Thus the neutron density distribution remains constant with time, and the chamber current provides a measure of density at the centre.

The ion chamber is of the boron-coated type (Rossi and Staub 1949), and the ion current from the chamber flows through a wire-wound 100 MΩ resistor, kept in a temperature-controlled cabinet. Resistances of down to 5 MΩ can be selected from the resistor. The voltage produced across the resistor is balanced using a potentiometer, any out of balance being observed by means of a directly coupled amplifier. The potentiometer reads from 1 to 100 volts with an accuracy better than 0·01 volt. Chamber currents between 0·01 and 20 microamperes can therefore be measured, corresponding to the density range quoted previously.

Now if σ is the absorption cross section of an element for neutrons of velocity v, and these neutrons have a density ρ, then the total number of thermal neutrons absorbed per second by the element is $\int\rho v\sigma\,dv$, where the integral extends over the whole thermal

velocity range. If the element follows a $1/v$ cross-section law in the thermal region, then $\sigma=\sigma_0 v_0/v$, where σ_0 is the cross section at some standard velocity v_0. Thus the total rate of absorption of thermal neutrons by the element is $\sigma_0 v_0 \int \rho \, dv$.

It is apparent, therefore, that an absolute determination of the total thermal neutron density in the pile can be made by a measurement of the neutron absorption cross section of an element and a determination of its rate of absorption of thermal neutrons, provided the element follows a $1/v$ law in the thermal region.

The element chosen for the absolute density determination was sodium. This has only one stable isotope, and absorption of thermal neutrons leads always to the 14·9 hr. activity of ^{24}Na. In addition, sodium follows a $1/v$ law in the thermal region, and a measurement of the absolute β-activity acquired by a sample of sodium was used as a measure of the rate of absorption of thermal neutrons. The sodium was used in the form of carbonate, neutron absorption by carbon and oxygen being negligible. A measurement of the activity acquired by a similar sample irradiated inside a cadmium box enabled us to allow for the effect of neutrons with greater than thermal velocities, both in the determination of the rate of absorption of thermal neutrons and in the measurement of cross section.

The determination of the absolute β-activity of the sodium was made using a liquid counter which had previously been calibrated for ^{24}Na. The calibration was made using a sodium sample whose absolute β-activity had been determined by both a defined solid angle and a coincidence method (Putman 1950). The two methods gave calibrations which agreed to better than 1%.

The absorption cross section of sodium at 2,200 m/sec. was obtained by comparison with that of boron using a swing method (Colmer and Littler 1950), a value of 710 barns at 2,200 m/sec. being assumed for boron.

Another measurement of absolute thermal neutron density has been made by a determination of the absolute β-activity of a sample of manganese irradiated in the B.E.P.O. (Price 1951), combined with a measurement in the G.L.E.E.P. of the neutron absorption cross section of manganese at 2 200 m/sec. The manganese used was in the form of sulphate, and the β-activity was determined by a defined solid angle method.

The conditions under which the B.E.P.O. is used are such that the neutron density distribution varies appreciably with time. Instead of expressing the density in terms of ion chamber current, therefore, a manganese foil was calibrated in terms of absolute thermal neutron density. This foil was irradiated in the B.E.P.O. under conditions known with respect to those used for the irradiation of the manganese sulphate, and the activity of the foil was measured on a Geiger–Müller counter, using a standard uranium foil for checking the counter sensitivity. Other manganese foils and Geiger–Müller counters were then standardized for measurement of absolute thermal neutron density.

A comparison of the sodium and manganese density measurements was made by irradiating some of the standardized manganese foils in the G.L.E.E.P. The absolute density of thermal neutrons determined by the two methods agreed to better than 2%.

The neutron density is checked periodically by measuring the radioactivity of other manganese foils irradiated in the centre of the G.L.E.E.P. against that of a radium standard. No significant change in the density has been observed during the past eighteen months.

In addition to making the density measurement, we have used the method described by Anderson *et al.* (1947) to determine the mean velocity of the thermal neutrons in the G.L.E.E.P. This was found to be about 2,690 m/sec. at a pile temperature of 300° K.

We would like to express our thanks to Miss A. M. Wildblood, who carried out the β-counting of ^{24}Na for us.

Atomic Energy Research Establishment,
Harwell, Didcot, Berks.
12th September 1951.

D. J. Littler.
E. E. Lockett.
B. T. Price.

Anderson, H. L., Fermi, E., Wattenberg, A., Weil, G. L., and Zinn, W. H., 1947, *Phys. Rev.*, **72**, 16.
Colmer, F. C. W., and Littler, D. J., 1950, *Proc. Phys. Soc.* A, **63**, 1175.
Price, B. T., 1951, *A.E.R.E. Report* R/M.7.
Putman, J. L., 1950, *Brit. J. Radiol.*, **23**, 46.
Rossi, B., and Staub, H. H., 1949, *Ionization Chambers and Counters: Experimental Techniques* (New York: McGraw-Hill).

Obituary Notices

LESLIE JOHN COMRIE

The death of Dr. L. J. Comrie, F.R.S., in London on 11th December 1950 at the age of fifty-seven has removed an original and independent figure from the ranks of British scientists.

Leslie John Comrie was born on 15th August 1893 at Pukekohe, Auckland, New Zealand. He was educated at Auckland Grammar School and Auckland University College, where, after a promising career, he graduated M.A. in 1916, with First Class Honours in Chemistry. He served in the First World War with the New Zealand Expeditionary Force, incurring severe wounds, with consequent amputation of a leg. It was doubtless this incapacitation, together with the handicap of increasing deafness, that caused him to reconsider his career, for after the war he remained in Britain as a New Zealand Expeditionary Force Scholar, studying astronomy and computation at St. John's College, Cambridge, where he was an Isaac Newton Student from 1920 to 1923. In 1923 a thesis, devoted to the history and detailed examination of methods of predicting the occultation of stars by planets, gained him the degree of Ph.D.

Two years in America followed, the first as Assistant Professor of Mathematics and Astronomy at Swarthmore College, Philadelphia, the second as Assistant Professor of Astronomy at Northwestern University, Evanston, Illinois. In 1925 he was appointed Deputy Superintendent of H.M. Nautical Almanac Office, Greenwich, and in 1926 entered upon his duties there. He was no stranger to Greenwich, having already, in 1920, spent two months at the Royal Observatory as part of the conditions of his Isaac Newton studentship. In 1930 he became Superintendent, a post which he held until 1936. Without delay he used the opportunity to embody in the next issue of the *Nautical Almanac*, for 1931, certain changes which he had without doubt considered for some years, notably the use of a standard equinox. The *Almanac* of 1931, breaking away from the tradition of almost a hundred years, incorporated, among other radical changes, the new ephemerides.

Comrie's imagination, essentially direct and pragmatic, had been captured, from his first contact with calculating machines, by their unexplored possibilities. He saw that with the rapid improvement in calculating machines many accepted procedures, legacies from the pre-machine era, were wasteful in time and effort and should be superseded or re-drafted in the newer idiom. He reconsidered such processes as interpolation, numerical integration and subtabulation from first principles, and devised simple and powerful repetitive techniques, requiring the minimum of copying and capable of being mastered and understood by operators of only moderate mathematical training. His ingenious mind ever busied itself with inventing methods for turning the latest devices, such as transfer levers, split keyboards or twin machines, to practical use. It was characteristic of him, for example, to harness together National Accounting Machines in order to build up and print tabular values from differences of high order, or to use punched cards and the Hollerith machine, as he did in 1928 with E. W. Brown's *Tables of the Moon*, to sum large numbers of harmonic terms. His methods, severely simple and simply described are explicit in the prefaces or introductions to the various tables published under his editorship, notably in *Interpolation and Allied Tables*, reprinted from the *Nautical Almanac* for 1937.

In 1936 he resigned from the Superintendentship and began a new and independent venture, the founding on business lines of a computational firm, the now celebrated Scientific Computing Service Limited. This, at the time, was a bold step, though soon justified by increasing success, by requests for computational help on a large scale by the universities, by industry and by Government departments. With the outbreak of the Second World War the demand, official and unofficial, for such services was extraordinarily accelerated. The office in Bedford Square served as training ground for many computers, who entered with moderate qualifications and passed out as experts. By 1944 the staff numbered thirty; and after the war, with the business now firmly established and enlarged, Comrie found the need of an assistant manager, of similar interest and authority in all matters concerning computation. This was Dr. J. C. P. Miller, who now succeeds him.

Comrie had now for many years been recognized as an authority of international reputation on mathematical tables. He had been the first Director of the Computing Section of the British Astronomical Association, Secretary to the Mathematical Tables

Committee of the British Association, 1930-36, member of the Committee on Mathematical Tables of the National Research Council, Washington; and from 1948 to 1950 he was a member of the Mathematical Tables Committee of the Royal Society. He was elected a Fellow of the Royal Astronomical Society as early as 1919, and served on its Council from 1929 to 1932. He was also a Fellow of the Royal Statistical Society, and of the Physical Society. He was an active member of the International Astronomical Union, attending all its conferences from 1928 onwards, and was elected President, in 1932, of its Commission on Ephemerides. His native country recognized him by honorary fellowships, of the Astronomical Society of New Zealand in 1933 and of the Royal Society of New Zealand in 1945. In March 1950 he was elected a Fellow of the Royal Society, but lived only ten months to enjoy this culminating honour.

His papers, though they number about a hundred, represent only a small part of his work. A proportion of these, mostly appearing in the *Monthly Notices of the Royal Astronomical Society*, are on astronomical matters, but the larger proportion (often appearing in such journals as the *Office Machinery Users' Association Transactions*) deal with table-making and the application of various types of machine to problems of computation. Of great importance are his reviews and notes on errata in existing mathematical tables, a characteristic example being the article in *Mathematical Tables and Aids to Computation*, 1 (1945), pp. 391–399, on Jahnke and Emde's *Tables of Functions*. His erudition in this field was immense.

The tables for which he was personally responsible bear on every page the marks of his exacting standards, imposed not least upon himself. First, by rigorous systematic checking and counterchecking, the values must be impeccably accurate; they must also be interpolable with the maximum of convenience, readable with the maximum of ease, and typographically elegant. No one can doubt, perusing, for example, the third and fourth enlarged editions of *Barlow's Tables*, issued in 1930 and 1941, or, perhaps most conspicuously, the new *Six-Figure Mathematical Tables* in two volumes, logarithmic and natural, published by Chambers in 1948, that such aims have been achieved to the full. These last tables call for special mention; they resulted from the decision of the publishing firm, on the centenary of the old tables in 1944, to take the advice of a modern expert in regard to their re-issue. They are rightly described in the Editor's preface as " one of the greatest of all British table-making enterprises ".

In character Comrie was intolerant of imprecision, direct and outspoken to a degree sometimes startling, though this was really a concomitant of his essential simplicity and singlemindedness. The writer of the present notice was never a fellow committee-man with him; but it is no secret that his abruptness of manner in delivering an opinion, his refusal to use any of the ordinary arts of compromise, did not always meet with a favourable response. This was, however, only one side of the man, reflecting his inveterate honesty.

Perhaps one who was bound to Comrie by ties of friendship, of birth in New Zealand at about the same period, and of similar service and similar though less severe experience in the First World War, may conclude on a specially personal note. Comrie as a young man, before departing for France and suffering so severely, was physically vigorous and energetic, a good rifle shot and tennis player, pursuits in which his qualities of precision and decisiveness found a ready outlet. It is more than probable that the disabilities that permanently precluded such active outlets produced a certain frustration, which in its turn was overcome by the unremitting energy which Comrie poured into everything that concerned astronomy, machines, tables and computation; for, as has already been stated, the amount of work he did in his lifetime cannot by any means be summed up in terms of publications. Not least was the help he unobtrusively and willingly gave to others in the field, of which a fitting memorial exists in the *Index of Mathematical Tables* of Fletcher, Miller and Rosenhead, 1945, already classical. New Zealanders visiting London, and astronomers and computers from America and Europe can testify to the warm hospitality he gave them, ably seconded by his wife; but very few knew of his many acts of secret and private generosity, some of which have only come to light since his death. The picture that lingers most in the mind is of Comrie as host, cut off by deafness, it is true, from the cross-currents of conversation, but himself sitting quietly happy at the evident enjoyment of his guests. It is a question whether, in giving full rein to his proclivities, he did not drive himself too hard along a single track; but his work is of great, permanent and visible value, and he has set standards, in all that concerns table-making and computation, that can hardly be surpassed.

A. C. AITKEN.

LEONARD GEORGE GRIMMETT

I WORKED as assistant to L. G. Grimmett for 18 months, 1934–35, in the Physics Department of the Radium Beam Therapy Research at The Radium Institute, London. I have had as transient a contact with many others, yet they have passed out of my recollection and interest. In contrast, Grimmett made a lasting impression. I have always felt a surge of pleasure on meeting him again, or on hearing of his exploits, and was very grieved to learn of his sudden death from heart failure on 27th May 1951 in Houston, Texas. He had a unique and admirable personality.

The two pillars of Grimmett's career were his love of science and of music; he was a pianist of the first rank. On leaving the Holloway County Secondary School he paid the expenses of a physics degree course at King's College from his earnings in restaurant and theatre bands. He made a voyage as ship's pianist to Buenos Aires. Undoubtedly this double life was a heavy strain. To me he deplored that, at a time when he was engaged in this struggle, his Professor was completely discouraging, believing that a degree could not be taken in this eccentric fashion. Nevertheless it was taken (in 1926), and so well that he was encouraged to do three years' research. In 1930 he became Assistant Physicist at the Westminster Hospital Radium Annexe, working under Professor H. T. Flint, and together they developed one of the earliest hospital physics departments. Grimmett was a pioneer in the development of radium beam units for the treatment of malignant disease; a two-gramme unit designed by him in the early 1930's is still in use. Methods of auxiliary physical measurements, such as those of dose distribution round these units, which are now routine, also claimed his attention.

He collaborated with Dr. F. G. Spear (1932) in an early quantitative study of the influence of gamma-ray intensity on the inhibition of cell division in tissue cultures (Spear and Grimmett 1933). This work caught the eye of Professor McLennan, Chairman of the Executive Committee of the Radium Beam Therapy Research, who persuaded him to join that body. He served it, and the Radiotherapeutic Research Unit of the Medical Research Council which assimilated it, until 1944.

Grimmett excelled in the design of apparatus; he was an artist in temperament. The common view that if a scientific apparatus works it is satisfactory was foreign to him. It must not only work but be well designed, elegant, and properly finished. Furthermore, each stage in its development must reach the same standard. It was not sufficient that the drawing should be adequate for the mechanic's use; the penmanship must be excellent also. He saw everything in a big way. The idea of improving the collimation of a radium beam by fitting a solid gold nozzle to the teleradium unit was typical, and he made it a reality (Flint, Grimmett, Rock Carling and Cade 1934). He spent time and money without inhibition or fear to get the results he wanted. He supplied most of the ingenious ideas for the 5-gramme radium unit (later 10 grammes), with pneumatic transference of the radium (Grimmett 1937), replicas of which have been installed in hospitals all over the world. He was one of the first to realize the importance of the total absorption of radiation by a patient (now known as 'volume dose'), as distinct from the absorption in the malignant growth itself. He tackled its measurement practically by the construction of a full-size human shape of parallel celluloid sheets with narrow air gaps which formed ionization chambers (Grimmett 1942).

He believed in the need for higher voltages in x-ray therapy, and in 1939 began the design of what ultimately became the first high pressure Van de Graaff generator to operate in Britain. Harassed by the war, the work was moved from the bombed Radium Institute to the Imperial College of Science and then to the Hammersmith Hospital, advancing slowly, since each stage must reach perfection without short cuts. Concurrently he supervised the physical side of a long clinical experiment which compared the relative merits of radium beam and 200 kv. x-ray treatments, with the fields of both types arranged to have closely matched dose distributions. At Hammersmith he built up a fine team and a magnificently equipped physical laboratory.

Then in 1944 he disappeared from his usual scenes, reappearing briefly from time to time from Paris, or wherever else his service for the British Council, UNESCO, and UNO had taken him. Finally it was reported that he had settled in Houston, Texas, where he was developing a radiobiological research laboratory in the really big way which suited his temperament.

Grimmett's career might suggest the dominant, aggressive personality, yet he was kind, gentle, always soft-spoken, and quite imperturbable except in sympathy for others. As we walked down Regent Street in 1934 we passed seedy, out-at-elbow violinists playing in the gutter. He was filled with distress—" I know this kind of man; I have played with them. They are good musicians displaced by the 'Talkies' ". He declined to assist in the atom bomb development. " The M.R.C. were approached ", he said, " but I asked them to squash the idea "; then, with a wry grin in oblique explanation, " I don't mind killing Germans in odd ones ".

Grimmett showed that, with few initial advantages other than talent, courage and tenacity, he could be a ' 20th century ' adventurer in the best sense, and at the same time make substantial contributions to human welfare. All who knew him will miss him greatly, and feel deep sympathy with his widow.

JOHN READ.

Flint, H. T., Grimmett, L. G., Rock Carling, F., and Cade, S., 1934, *Brit. Med. J.*, 14 April.
Grimmett, L. G., 1937, *Brit. J. Radiol.*, **10**, 105; *Ibid.*, 1942, **15**, 144.
Spear, F. G., and Grimmett, L. G., 1933, *Brit. J. Radiol.*, **6**, 387.

JOHN R. LOOFBOUROW

Dr. Loofbourow, who had been a Fellow of the Physical Society since 1941, died in Boston, Massachusetts, on 22nd January 1951. At the time of his death he was a professor of biophysics at the Massachusetts Institute of Technology, where he was in addition Executive Officer of the Biology Department and Chairman of the Faculty.

Loofbourow, the son of John Wilson and Henrietta Loofbourow, was born in Cincinnati, Ohio, on 1st November 1902. He was educated at the University of Cincinnati, where he obtained the degree of Bachelor of Arts in 1923. He served as an instructor in Physics there from 1925 to 1929, and as a research associate for the following six years. In 1936 the University of Dayton in Ohio awarded him the honorary degree of Doctor of Science, and he became professor of Biology at that institution. From 1935 to 1940 he was a research professor at the Institution Divi Thomae in Cincinnati, and in 1940 he was called to the Massachusetts Institute of Technology, where he was made an associate professor of biophysics.

During the war years Dr. Loofbourow was Executive Secretary of the Radar Division of the National Research Committee. He served as a special adviser to the Atomic Energy Commission in 1947 and 1948, in which year he was awarded the Presidential Certificate of Merit.

Dr. Loofbourow was a Fellow of the American Association for the Advancement of Science, the American Physical Society, the American Academy of Sciences, the New York Academy of Sciences, the Optical Society of America, the Beta Theta Pi. He was also a member of the Chemical Society, the Faraday Society and the Biochemical Society of England, as well as the Physical Society.

Dr. Loofbourow's untimely death from a heart complication was tragically followed by that of his wife, a practising physician, from the same cause within ten days. They are survived by a son, John W. Loofbourow.

Professor Loofbourow was a frequent contributor to the literature of biophysics, specializing in the field of absorption spectroscopy, particularly in the ultra-violet region. At the time of his death he was engaged in important work on the purines and pyrimidines, and was engaged in developing new techniques for absorption studies at extremely low temperatures. With Professor Richard C. Lord and the undersigned, he was the author of the text *Practical Spectroscopy* published in 1948.

With his unassuming and friendly manner, breadth of interest, and complete grasp of his subject, Professor Loofbourow had won a host of friends among both colleagues and students. As a member of a committee on improving educational methods and as Chairman of the Faculty he had contributed much to the academic community. His tolerance and quiet competence left a deep impression on all who came in contact with him, and contributed greatly to the present feeling of loss among his colleagues, students, and many friends.

GEORGE R. HARRISON.

EDWARD MALLETT

EDWARD MALLETT, born in 1888, was educated at Southend High School and University College, London. He served an apprenticeship with Messrs. Crompton & Co., Chelmsford, and entered the Post Office Engineering Department through a Civil Service competition in 1909. Following a short period of training, he was posted to the West Section of the Scotland District and remained there until the outbreak of war in 1914. He was interested in the Territorial Army and as a result, as soon as war was declared, was posted to the 52nd Lowland Divisional Signals and saw service in the Middle East area of hostilities, finally leaving the Service with the rank of Captain.

After the war, Mallett was posted to the Transmission Section of the Engineer-in-Chief's Office, and here his grasp of electrical fundamentals combined with his abounding energy found outlet in dealing with the problems of telephone transmission, which was then entering into a new phase due to the introduction of the thermionic valve. There is no doubt that Mallett, had he remained in the Post Office service, would have had a brilliant future, but a friendship made during the war years turned his energies in another direction and he left the Post Office service in 1920. It was during this period of service in the Post Office that he carried out his researches into the vibrational modes of a circular diaphragm which led to the work for which he was eventually granted his doctorate.

In September 1921 he joined the academic staff of the City and Guilds College, South Kensington, as Assistant Professor of Electrical Engineering, which post he held until September 1932.

During these eleven years he was developing and expanding the 'light current' engineering section of the department. A considerable expansion was taking place under the direction of Professor Fortescue, and Mallett, with his active and fertile mind, backed by his considerable experience in the Post Office Engineering Department, found scope for developing the instruction and research in electrical communication.

He had an intuitive engineering sense and considerable academic skill, and these combined produced a lecturer of inimitable style and a research worker capable of producing results from the minimum of apparatus. He was extremely popular with both staff and students and joined in many of their social activities.

The title of Reader was conferred on him in 1927 by the University of London, and from that date until his death he remained a member of the Board of Studies in Electrical Engineering. He was for several years Secretary to the Board of Studies, acquiring an intimate knowledge of the activities of the Board and of the University, which knowledge served them well over the period of his long membership.

In addition to these activities he still found time to write several papers on a variety of subjects of interest to the communications engineer which he presented to the Institution of Electrical Engineers and to the Physical Society.

In July 1926 he was awarded the Degree of D.Sc.(Eng.) as an Internal Student of University College, London, the thesis title being *Forced Oscillations, Electrical and Mechanical*. He was frequently consulted by outside bodies and the University on electrical engineering matters, and in 1929 he produced his textbook on Telegraphy and Telephony which became, and still is, a valuable foundation for students of electrical communication.

It was at the height of his academic activities that he left the City and Guilds College to become Principal of Woolwich Polytechnic but, although he became more and more immersed in administrative studies, he never lost contact with the College or the University of London.

As Principal of Woolwich Polytechnic he was intensely interested in the University aspect of the Polytechnic but at the same time took a very active interest in the large non-university side of Polytechnic activities. He was a keen believer in the National Certificate Course for part-time and evening students, and had a place in his heart for the craftsman, ensuring that he was provided with proper shops and tools. It was during his Principalship that the Sandwich Course in Engineering was started, and this eventually developed into the Engineering Degree Course of today. This was soon followed by Degree Courses for B.Sc. (Chemistry, Physics, Mathematics), and the full-time School of Art Course.

The Polytechnic Union came into being during his time. He saw that the union of the diversified clubs and societies of the Polytechnic into one corporate whole could be of great value to the students and members, and the passing of time has proved him correct. The

success of the Union in all its aspects is a tribute to him: he gave it a free, unfettered hand, and held it in high esteem.

Extensions to the Polytechnic were made during his time, and future developments were being planned by him when his fatal illness intervened.

He was a member of the Institution of Civil Engineers, the Institution of Electrical Engineers, the Institute of Physics and the Physical Society (since 1921), and a Fellow of University College.

Edward Mallett, D.Sc.Eng. (Lond.), M.Inst.C.E., M.I.E.E., F.Inst.P., Fellow of University College, London, died on the 10th December 1950. C. R. URWIN.

HANTARO NAGAOKA

Professor Hantaro Nagaoka, who had for nearly forty years occupied a worthy place among the few Honorary Fellows of the Physical Society, died on 10th December 1950 at the age of 85. In the English-speaking world his name is probably most familiar in connection with 'Nagaoka's formula' for the calculation of inductance, and indeed his work on the subject has been of great value to workers in the radio field and to physicists concerned with precision measurements of inductance. For example, in addition to his formulae he published, with S. Sakurai, tables which give, with very little computation, values for the self-inductance of single layer coils, and for the mutual inductance of coaxial circles to six-figure accuracy. This work, however, is hardly representative of his main interest; he was essentially an all-round physicist in the Rayleigh, Kelvin, J. J. Thomson tradition, and one who could refer to physics as 'the Study of Nature'.

He was born in 1865 and was of honourable lineage. He graduated in physics at the Tokyo Imperial University in 1887, a time when, as he recalled later, the library in the physics department occupied but a single shelf six feet wide, and the only periodical available was the *Philosophical Magazine*. Nevertheless he must have immediately embarked upon experimental research in magnetism, for papers published by him in 1888, 1889 and 1890 are discussed in some detail by Ewing in his *Magnetic Induction in Iron and Other Metals*. Among other things Nagaoka showed that in certain circumstances the magnetization of nickel is reversed by torsion, an effect so surprising that both Kelvin (then W. Thomson) and Weiss had it confirmed in their own laboratories. Sixty years later Nagaoka remarked that the reason why still remained quite unknown. He continued his work in Tokyo for six years, took his doctorate in 1893, and then proceeded to Germany, where he studied for three years, attending lectures by Helmholtz, Boltzmann, Planck and others, and working on magnetostriction. During this time he visited the Physikalisch-Technische Reichsanstalt and was received by Lindeck who, having recently translated Ewing's book into German, knew of his work. Lindeck asked him when he had left Ewing's laboratory at Cambridge, and when he learnt that the work had been done several years earlier in Japan was sufficiently impressed to show him the laboratory in detail. Nagaoka with a pleasant touch of humour said later that he realized then that a bit of good work is a much better introduction than a distinguished visiting card.

Returning to Japan, he was appointed Professor of Physics at his old university, and for the next fifty years and more he flourished as an active and versatile leader of physics in Japan, occupying positions of increasing responsibility and influence, which in view of his own sentiment mentioned above need not be set out in detail here.

Much of his early work was done on geophysics with Professor A. Tanakadate who was at that time Director of the Physical Institute of the university; a little later he returned to magnetism and with Professor K. Honda investigated the magnetostrictive properties of nickel-steels of various nickel contents; they showed that changes of volume, as well as of length, occur. The geophysical work included the determination of g at Tokyo, comparisons of g at Tokyo and Potsdam, and a systematic study of the elasticity of rocks in relation to the propagation of seismic waves through the earth's crust. His interest in geophysics remained with him until the end of his life, but round about 1900 he seems to have been strongly attracted by two widely different scientific developments: atomic physics arising from the discoveries of the electron, X-rays and radium on the one hand, and wireless communication on the other. His interest in the atom ultimately gave rise to a very considerable body of detailed work on spectroscopy, hyperfine structure and

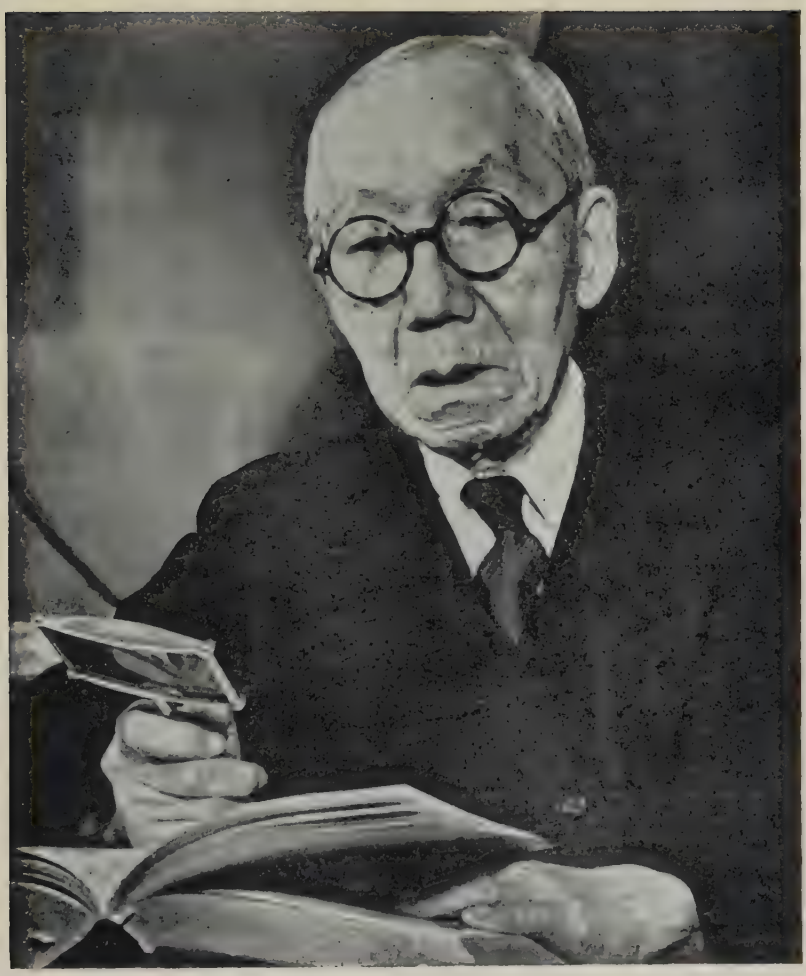

Photograph by Shigeru Tamuru

HANTARO NAGAOKA
(1865–1950)

DR. F. B. YOUNG, O.B.E.

(enlarged from a small group photograph)

the Zeeman effect, carried out with Dr. T. Takamine. His interest in ' wireless ' seems to have led to his work on formulae for inductance calculation, already mentioned, and to a consideration of the effect of the ionosphere, familiar to him from its association with terrestrial magnetism which he had investigated earlier, on radio communication. He foresaw that the solar eclipse of 1914 would provide an opportunity of testing the Kennelly–Heaviside theory, if the ionized layer arises from the photoelectric effect of solar radiation. He made a calculation of the effect that should be observable on suitable wireless signals. Unfortunately the first world war prevented the making of the observations, but the detailed observations made in the U.S.A. at the eclipse of 1925 showed that the idea was sound although, in the light of later information, Nagaoka's original calculation was of course only the first rough approximation.

It is estimated that Nagaoka published in all some 300 papers, and it will be realized from what has been said that they are so diverse in character that they do not lend themselves to brief effective description. What does stand out very clearly is his life-long devotion to physical science: we see him as mathematical physicist, an experimenter—he devised a magnetograph, a silica pendulum for gravity determinations and spectroscopic devices—a patient observer—he himself is said to have made fifty determinations in the gravity survey that he organized—and an original thinker. On this last point it must be noted that he had the honour of being the first to suggest a planetary structure for the atom. Rutherford in *Radioactive Substances and their Radiations* wrote " This type of ' Saturnian ' atom was first suggested in 1904 by Nagaoka, who investigated mathematically the stability of an atom composed of a central attracting mass surrounded by rings of rotating electrons. He showed that such a system was stable if the attractive force was large and the electrons in rapid motion ". When it is remembered that it was in this year also that J. J. Thomson was still investigating the model consisting of electrons inside a positively charged sphere, the originality of the conception can be better appreciated. It was spectroscopy rather than radioactivity that was in Nagaoka's mind; his aim was to account for the discrete spectral lines characteristic of the atom, and he thought that they might be associated with vibrations of the electrons in and perpendicular to the plane of the ring. We now know that the vital key to the problem was still missing, and that Bohr was to find it some years later, but Nagaoka's contribution commands our respect.

Nagaoka came to occupy an eminent position in the scientific life of Japan. He was elected a member of the Imperial Academy in 1905, became Director of the Institute of Physical and Chemical Research in Tokyo (now the Scientific and Research Institute) in 1926 and was among the first recipients of ' Bunkwa Kunsho ', a medal of great distinction, in 1937. He was President of the Imperial Academy in 1939 and 1948. He visited England on two or three occasions, was awarded an honorary degree at Cambridge, and read papers in London before the Physical Society. He was elected an Honorary Fellow of the Society in 1912. That this tribute to an outstanding fellow worker in the new school of physics then rapidly rising in Japan has survived the shock of two world wars may serve as a welcome reminder that physics still stands as a co-operative human enterprise.

L. H.

FRANK BENNETT YOUNG

It is recorded with regret that Frank Bennett Young died on 29th January 1951. He was a Fellow of the Physical Society from 1916 to the time of his death, and a founder Fellow (1920) and life member of the Institute of Physics.

He was born in 1877 in Bristol where he received his early education. In 1896 he went to the Borough Road College, Isleworth, where he was awarded a scholarship enabling him to spend a year at Jena University. In 1899 he obtained the B.A. degree of London University. At this time he became interested in science from a philosophical point of view and began to study physics, returning to Bristol to teach physics in a Higher Grade School. During this period he attended evening classes at University College, Bristol, before the foundation of the University. It was there he met Professor Chattock who had an important influence on his career. His enthusiasm for research in physics increased and he spent all his spare time (evenings, week-ends and holidays) on research under Chattock's guidance.

His published papers at this time included " The field at the point of an electrified needle " (*Phil. Mag.*, 1907, **13,** 542) and " Critical phenomena of ether " (a study of the opalescent phenomena near the critical point) (*Phil. Mag.*, 1910, **20,** 793). On the foundation of the University of Bristol he took advantage of one of its early ordinances which permitted him in 1910 to present these publications for the degree of B.Sc. by research. In 1915, soon after the outbreak of the 1914–18 war, (Prof.) A. M. Tyndall obtained for him the job of localizing shrapnel bullets in the body by x-rays at the Bristol Royal Infirmary, a problem quite beyond the medical man of that day. This was the first time a physicist had entered its doors to give service.

In 1916 he joined the Admiralty, for anti-submarine research under the Board of Invention and Research (W. H. Bragg and Rutherford were on the controlling committee). He worked in Admiralty research establishments at Aberdour (Fife), Parkeston Quay (Harwich), Shandon (Gareloch) and, after the war, at Teddington (Middlesex). In the earlier days he was mainly concerned in research work on hydrophones and in underwater acoustics. Some of this work was published after the war, viz. " On light body hydrophones and the directional properties of microphones " (*Proc. Roy. Soc.* A, 1921, **100,** 252) and " On the acoustic disturbance produced by small bodies on plane waves transmitted through water, with special reference to the single-plate direction finder " (*Proc. Roy. Soc.* A, 1921, **100,** 261). This had an important bearing on the design of directional hydrophones. At a later stage of the 1914–18 war he carried out important researches on the generation of electric currents in the sea (*a*) due to the presence of steel ships, and (*b*) due to the tidal flow of a conducting medium (the sea) in the earth's field. Some of the experiments and conclusions reached in the latter were published in *Phil. Mag.*, 1920, **40,** 149, in an article entitled " Electrical disturbances due to tides and waves " by F. B. Young, H. Gerrard and W. Jevons. At this time he was also interested in the development of a new method of locating faults in submarine cables—using alternating currents and silver-chloride electrode search gear. This method has since been extensively used by cable companies and by the G.P.O. Soon after the end of the 1914–18 war he obtained the degree of D.Sc. (Bristol 1919). On the removal of the Admiralty research establishment from Shandon (Gareloch) to Teddington he worked on course plotters for ships and developed what is now known as the A.R.L. (Admiralty Research Laboratory) Course Plotter. Another line of research which he directed related to the preservation of the rubber insulation of cables in ships. It will be understood that much of his research work for the Admiralty remained unpublished on grounds of security. In July 1934 he became Superintendent of the Admiralty Research Laboratory, Teddington, a post which he filled until his retirement on reaching the age limit in October 1937. Whilst in this post he was awarded the O.B.E.

In 1939 he returned to Admiralty work in Portsmouth soon after the outbreak of the 1939–45 war, taking charge of an important section of research on the degaussing of ships as a protection against enemy magnetic mines. He finally retired from Admiralty service in 1941, taking on various unpaid wartime duties in Bristol.

He eventually settled in Portsmouth after the war where he revived his old-time interests in music and in sketching and water colour painting, He was of a retiring disposition, very reliable, thorough and conscientious in all his work, and generous in giving more than their share of credit to others who worked with him. He will be missed by those who, like myself, knew him well.

A. B. WOOD.

ARNOLD SOMMERFELD

On 26th April 1951, Arnold Sommerfeld, Honorary Fellow of the Physical Society, died from the consequences of a street accident at the age of eighty-two.

He was born in 1868 at Königsberg, East Prussia, and attended school and university in his native town. In 1893 he went to Göttingen and came under the influence of Felix Klein. Here he had a thorough mathematical training and acquired the skill in the theory of differential equations, analytical functions and complex integration which he later applied with great success to physical problems. The direct fruit of his co-operation with Klein was their famous book on the spinning top (1895–1910).

In 1895 Sommerfeld became lecturer in Göttingen, in 1897 professor at the Mining College in Clausthal and in 1900 he was appointed to a chair of mechanics at the Technical

College in Aachen. From 1906 until his death he was professor of theoretical physics in Münich. He declined several attractive positions, as for instance the chair of Planck in Berlin.

Sommerfeld's scientific work covers a vast field of which only some major points can here be mentioned. His contributions to classical physics were in hydrodynamics, by work on the stability of laminar motion, and in optics which he enriched by ingenious rigorous solutions of some diffraction problems. But soon he directed his attention to the new ideas of relativity and quantum mechanics. Combining these two subjects he developed Niels Bohr's theory of atomic spectra by taking into account the relativistic variability of mass, and obtained in 1915 his celebrated fine structure formula for hydrogen-like spectra. Sommerfeld's fine structure constant dominates not only these phenomena but the whole of quantum electrodynamics. In 1917 be began to write his great book on the structure of atoms and spectral lines which has so immensely contributed to the understanding and general acceptance of quantum theory. The advent of quantum mechanics led him first to write a short complementary volume which was later extended to a comprehensive representation containing a wealth of information. The study of wave mechanics in combination with Pauli's principle led Sommerfeld to another great success, its application to the electron theory of metals.

Sommerfeld was a brilliant teacher and attracted pupils from all over the world. When in 1938 he retired from his Chair, he began to prepare the publication of his lectures, of which all but one volume have appeared, and it is hoped that this last one will also be published. His style and power of representation is such that his books read like novels. But still greater was the charm of his personality which won him the devotion of his pupils, amongst whom were Pauli, Heisenberg, Brillouin, F. London and many other outstanding men.

Sommerfeld was a member of many academies and learned societies, amongst them the Royal Society. He received the Max Planck Medal of the German Physical Society and many other honours. He was at one time Karl Schurz Professor at the University of Wisconsin and visiting professor at the Californian Institute of Technology and at several other American universities.

MAX BORN.

STUART ARTHUR FRANK WHITE

STUART ARTHUR FRANK WHITE, who died on 12th January 1951, aged 80 years, was elected a Fellow of the Physical Society in 1895. He was for many years Professor of Mathematics at King's College, London, Dean of the Faculty of Science and latterly Vice-Principal and Fellow of the College. He retired in 1933 after occupying his Chair for thirty years.

White's education began at Portsmouth Grammar School from which he proceeded (with a scholarship or exhibition, I believe) to Wadham College, Oxford, at Michaelmas 1887. In his student days he seems to have been as much interested in physics and astronomy as in mathematics, and before going to King's College he held an appointment at Oxford under Professor Clifton. In 1894 he was appointed Demonstrator of Natural Philosophy—strangely enough, on the recommendation of the Engineering Committee—under Professor Grylls Adams, and in 1903 he succeeded W. H. Hudson in the Chair of mathematics. The appointment to this Chair of the demonstrator of natural philosophy, rather than of a mathematician *vom Fach*, appears to have been due to the desire of the Council to infuse a more vivid and practical spirit into the teaching of mathematics to the students of such subjects as engineering, physics, etc., whose interest lay less in mathematics for its own sake than in its practical applications. For such students White was ideal. He was a most able teacher, lucid and always interesting. He was moreover whole-heartedly devoted to his teaching duties and to the progress and welfare of his students, whose affection and esteem he undoubtedly won.

White was a keen golfer and skier and for a long period spent part of every Christmas vacation in Switzerland. He was intensely devoted to the college he served and his wise counsel and guidance were greatly valued, not only by the Professorial Board of the College, but also by his mathematical colleagues in the university.

WM. WILSON.

Miss JESSIE S. CHREE

Fellows of the Physical Society will be sorry to learn of the death of Miss Jessie S. Chree, sister of the late Dr. Charles Chree, F.R.S.

Dr. Chree was at one time President of the Physical Society, and the Society's *Charles Chree Medal and Prize* was instituted in memory of him through the generosity of Miss Jessie Chree.

ALLAN FERGUSON

We record with regret the death on 9th November 1951 of Dr. Allan Ferguson who was the Papers Secretary of the Physical Society from 1928 to 1938 and President from 1938 to 1941.

An appreciation will be published with next year's Obituary Notices.

CONTENTS FOR SECTION B

PAGE

Professor S. Chapman (President 1949–50) . . . . . *Frontispicee*

Mr. J. H. Andreae and Dr. John Lamb. Ultrasonic Relaxation Processes in Pure Liquids 1021

Mr. E. A. Neppiras and Dr. B. E. Noltingk. Cavitation Produced by Ultrasonics: Theoretical Conditions for the Onset of Cavitation 1032

Dr. M. Blackman. Self-Magnetic Field in High Current Discharges . . . 1039

Dr. J. R. Tillman. Space Current Changes in Thermionic Valves following Small Pulses of Current 1046

Mr. D. A. Bell. Ionospheric Interaction in Disturbed Conditions . . . 1053

Mr. K. Johnsen. Heavy Beam Loading in Linear Electron Accelerators . . 1062

Mr. E. K. Inall. Currents in a High-Voltage Ion Accelerator Tube . . . 1068

Dr. K. J. Le Couteur. The Regenerative Deflector for Synchro-cyclotrons . . 1073

Letters to the Editor:

Dr. E. O. Hall. The Lüders Deformation of Mild Steel 1085

Mr. A. N. Hunter. Ultrasonic Absorption in Supercooled Liquids . . 1086

Dr. D. G. Avery. The Optical Constants of Lead Sulphide and Lead Telluride in the Region 0·5–3 microns 1087

Dr. W. Ehrenberg and Mr. R. E. Siday: Dr. W. Glaser. The Refractive Index in Electron Optics 1088

Obituary Notices:

Leslie John Comrie 1090

Leonard George Grimmett 1092

John R. Loofbourow 1093

Edward Mallett 1094

Hantaro Nagaoka 1095

Frank Bennett Young 1096

Arnold Sommerfeld 1097

Stuart Arthur Frank White 1098

Miss Jessie S. Chree 1099

Allan Ferguson (brief note: Obituary Notice next year) 1099

Contents for Section A 1099

Abstracts for Section A 1100

Subject Index, Section B, Vol. **64** 1102

Index of Authors (with Titles), Section B, Vol. **64** 1108

Index to Reviews of Books, Section B, Vol. **64** 1114

ABSTRACTS FOR SECTION B

Ultrasonic Relaxation Processes in Pure Liquids, by J. H. Andreae and John Lamb.

SUMMARY. The assumptions made by Hall and Herzfeld in previous theories of ultrasonic absorption are interpreted on the basis of a new and more general analysis. The formulae given by them are discussed, and it is suggested that the conditions implicit in Herzfeld's formula should be modified. By this modification a new relation is derived, which provides a satisfactory explanation of the observed relaxation effects in those liquids which have been studied.

A method of 'curve fitting' is employed to compare experimental results with theoretical requirements. Finally, it is concluded that the ultrasonic behaviour of acetic acid and propionic acid is governed by the excitation of bending vibrations of carbon–hydrogen bonds. Measurements in carbon disulphide indicate that in this case also a bending vibration is responsible. Some incomplete data for toluene suggest that here a stretching vibration of the carbon–hydrogen bonds in the methyl group is involved.

Cavitation Produced by Ultrasonics: Theoretical Conditions for the Onset of Cavitation by E. A. Neppiras and B. E. Noltingk.

ABSTRACT. An attempt is made to define theoretically the conditions for the appearance of cavitation in liquids subjected to alternating pressure changes. It is found that cavitation is restricted to a definite range of variations of the following parameters: (i) alternating pressure amplitude, (ii) frequency of the pressure wave, (iii) radius of the bubble nucleus, (iv) hydrostatic pressure. Under certain conditions, the change from non-cavitating to cavitating conditions is found to be exceedingly sharp, and in these cases it is shown that the threshold for cavitation can be accurately expressed in very simple terms.

Self-Magnetic Field in High Current Discharges, by M. Blackman.

ABSTRACT. The theory of the self-magnetic field in high current discharges, originally developed by Tonks, has been investigated omitting a special assumption used in the work of Tonks. The influence of the parameters describing the discharge conditions has been considered in some detail. A comparison is also made with a simple, though more approximate, version of the theory due to Thonemann and Cowhig. The two theories are shown to be in good agreement.

Space Current Changes in Thermionic Valves following Small Pulses of Current, by J. R. Tillman.

ABSTRACT. A train of regularly spaced rectangular pulses of voltage, amplitude modulated at a frequency f_m and applied to the control grid of a commercial valve working conventionally, caused space current changes of up to 0·01 amp/cm^2 from the oxide-coated cathode. An unmodulated pulse train, interlacing the first with a delay of t_d, sampled the anode current; the samples contained a component at the frequency f_m of low level. The component decayed as t_d increased, with a time constant of about 1 msec. It was sometimes in phase with the component obtained when $t_d=0$, and sometimes in antiphase. The magnitude and phase were often dependent on the history of the valve. Thus an operation known to poison the cathode was usually followed, temporarily, by a large antiphase component.

An in-phase component denotes an enhancement of emission following a positive pulse; an antiphase component denotes fatigue. There is evidence that the impedance at the interface between cathode core and coating is not responsible for the effects. The fatigue may well be largely a surface, rather than a bulk or matrix, effect. It bears some relationship to effects reported elsewhere with pulses involving current densities of 10 amp/cm^2.

Ionospheric Interaction in Disturbed Conditions, by D. A. Bell.

ABSTRACT. Measurements of ionospheric interaction depend on special radio transmissions which are only available on a limited number of occasions, and only on some of these occasions are ionospheric conditions steady enough for direct comparison between experiment and theory. This paper describes the use of averaging methods to extract some information from observations made when conditions are not steady. The results confirm the existence of a 'low-frequency anomaly' observed by Huxley, but show no exceptional interaction for a variation of the frequency of the disturbing wave around the nominal gyromagnetic resonance frequency.

Heavy Beam Loading in Linear Electron Accelerators, by K. Johnsen.

ABSTRACT. The influence of the beam current on the length, the obtainable particle energy and the efficiency of a linear accelerator is considered. The beam loading is especially important if the accelerator waveguide has low losses. The efficiency, defined as the ratio of H.F. power transformed into kinetic energy to the total H.F. power fed to the accelerator, can have a high value, 70–80%, but the particle energy obtainable drops considerably with heavy beam loading.

Currents in a High-Voltage Ion Accelerator Tube, by E. K. Inall.

ABSTRACT. It is well known that a large electron current passes through a vacuum tube when used for the electrostatic acceleration of positive ions. This paper deals with experiments which show that many of the electrons are produced by neutral particles bombarding the lower end of the tube. The particles are formed in the region of the ion source canal and have a low energy due to the extraction potential. It has been found possible to suppress all the electrons produced below the bottom of the accelerator tube.

The Regenerative Deflector for Synchro-cyclotrons, by K. J. Le Couteur.

ABSTRACT. Tuck and Teng have proposed to extract the beam from a synchro-cyclotron by modifying the normal magnetic field in such a way as to build up the amplitude of radial oscillations until protons can escape from the magnet. In the present paper the method is studied analytically and formulae are derived which express the performance in terms of the magnetic field perturbations : these formulae have been evaluated numerically in sufficient detail to guide practical design.

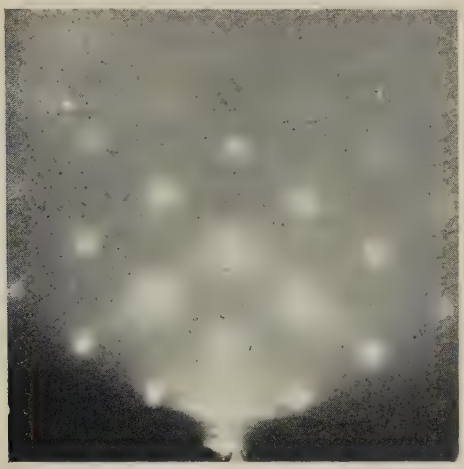

Figure 3. Electrolytically etched (100) silver surface. [011] azimuth.

Figure 6. Specimen as for Figure (3); +4° from [011] azimuth.

Figure 8. Electrolytically etched (110) silver surface. [1$\bar{1}$0] azimuth.

Figure 9. Electrolytically etched (flat) (111) silver surface. [1$\bar{1}$0] azimuth.

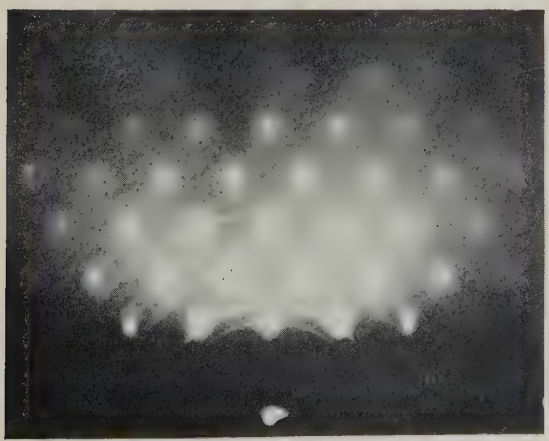

Figure 11. Electrolytically polished (110) silver surface. [1$\bar{1}$0] azimuth.

Figure 10. Electrolytically etched (rough) (111) silver surface. [2$\bar{1}\bar{1}$] azimuth.

SUBJECT INDEX

PAGE

Absorption bands, ultra-violet, probably due to InH and GaH (Letter) . . 509
Absorption edges M_{IV} and M_V of ^{68}Er (Letter) 318
Absorption of light by alkali metals 765
Absorption spectra, ultra-violet, of tin vapour in atmospheres of helium and hydrogen (Letter) 591
Abstracts—Section B . . 103, 215, 325, 438, 519, 599, 679, 762, 858, 954, 1059, 1151
Accelerators, particle, gas scattering 10
Air showers, extensive, temperature effect. 1061
Alloys, ferromagnetic, saturation magneto-resistance of 447
Alpha-particle irradiation, deterioration of anthracene under (Letter) . . . 511
Alpha-particles from the proton bombardment of phosphorus (Letter) . . . 313
Alpha-particles, and reaction $^{12}C(\gamma, 3\alpha)$ (Letter). 1056
Angular correlation in the reaction $^{6}Li(d, p)^{7}Li^{*}(\gamma)^{7}Li$ (Letter) 938
Angular distribution of long-range neutron groups of reaction $^{16}O(d, n)^{17}F$ (Letter) . 756
Angular distribution of 3 MEV. neutrons scattered by protons and by deuterons . 546
Angular distribution of neutrons from the (d, n) reaction in light elements . . 797
Angular distribution of the neutron groups from the reaction $^{12}C(d, n)^{13}N$ (Letter) . 1055
Angular distribution of protons in $F(\alpha, p)Ne$ resonance reactions (Letter) . . 88
Anthracene, crystal, $^{12}C(n, 2n)^{11}C$ reaction in (Letter) 211
Anthracene, deterioration under α-particle irradiation (Letter) 511
Antiferromagnetism by Bethe method 1108
Aromatic systems, large, diamagnetic anisotropy of: Parts I and II 261
Aromatic systems, large, diamagnetic anisotropy: III—Structures of hexagonal symmetry 921
Asymmetrical electron diffraction effects from single crystals of silver . . . 1113
Atomic energy states, experimental determination of lifetimes 458
Auger and conversion electrons of radium D 791

Balmer line widths in hydrogen arcs 574
Band spectra, emission band of the Cd_2 molecule at λ 2212 (Letter) . . . 430
Band spectrum of carbon monofluoride 481
Band system ascribed to the CH molecule (Letter) 592
Band system, ultra-violet, new, of SiF (Letter) 98
Band systems of diatomic molecules, transition probabilities in 772
Band systems, hydrocarbon flame, isotope effect in (Letter) 428
Band systems of N_2 and C_2, calculation of oscillator strengths (Letter) . . . 99
Band systems of thorium oxide and hafnium oxide (Letter) 852
Bands, C_2 (Swan), in krypton (Letter) 210
Bands, first negative of N_2^+, calculation of relative transition probabilities (Letter) . 209
Beryllium, excitation function for the production of, by the bombardment of ^{12}C by protons 902
Bethe method, applied to antiferromagnetism 1108
Beta-decay of ^{32}P, theoretical discussion (Letter) 1138
Beta-rays in cloud chamber, and sudden large changes of energy 1006
Beta-rays, identity with electrons (Letter) 846
Beta-spectrometer, wide-angle, using a spheroidal magnetic field 163
Bitter patterns on a single crystal of nickel 691
Black sphere, influence on neutron density in infinite non-capturing medium . . 881

Calculation of the oscillator strength for the $^2\Pi - ^2\Delta$ transition in the CH molecule (Letter) 666
Calibration of absolute neutron sources 638
Cascade theory, fluctuation problem, and probability distribution function . . 807
Cascade theory including ionization loss 1

PAGE

Čerenkov effect, for detection of charged particles in cosmic radiation . . . 82
Cerium ethylsulphate, paramagnetism at low temperatures (Letter) . . . 931
Cerium ethylsulphate, paramagnetism, theory (Letter) 932
Charged particles, nuclear excitation by electric interaction with 619
Chromium $^{53}_{24}$, nuclear spin (Letter) 1135
Cloud chamber, sudden large changes of energy of beta-rays in 1006
Cobalt ammonium sulphate, adiabatic demagnetization (Letter) 316
Combinatorial problem in counting cosmic rays. 1040
Conductivity, *see* Heat; Electrical conductivity; Thermal conductivity
Conversion and Auger electrons of radium D 791
Copper 63 and 65, quadrupole moments (Letter) 758
Copper sulphate, magnetic susceptibility 124
Correspondence principle and quantum theory of reciprocal fields . . . 957
Cosmic radiation, detection of fast charged particles in, by Čerenkov effect . . 82
Cosmic radiation in the air, average numbers for the development of the nucleon component 726
Cosmic radiation, penetrating bursts 733
Cosmic radiation, penetrating non-ionizing component 1042
Cosmic radiation, star-producing, measurements with a scintillation counter (Letter) 662
Cosmic-ray air showers, density of penetrating particles 915
Cosmic-ray beam, vertical, at sea level, proton component 404
Cosmic-ray mesons and stars under carbon absorbers 175
Cosmic-ray particles, ionization (Letter) 96
Cosmic-ray protons, momentum spectrum (Letter) 948
Cosmic-ray showers, penetrating, latitude effect 745
Cosmic-ray showers, penetrating, nuclear interaction length of the particles . . 4
Cosmic rays, counting, combinatorial problem in 1040
Cosmic rays, differential cross section for high energy nucleon–nucleon collisions and the mean square angle of scatter 1083
Cosmic rays, *see also* Cascade theory
Counter, scintillation, measurements of the star-producing radiation (Letter). . 662
Cross section, fall and re-increase, $^{12}C(\gamma, 3\,^4He)$ (Letter) 201
Cross section, total, of beryllium, aluminium, sulphur and lead for neutrons of energies from 2 MeV. to 6 MeV. 388
Crystal growth, epitaxial, of silver on rock-salt (110) and (111) faces . . . 283
Crystal, zinc single, structure of thin layers of zinc oxide grown on (Letter) . . 943
Crystals, deformed, X-ray asterisms from (Letter) 844
Crystals, first order Raman effect, in 1012
Crystals, lithium fluoride, quantum mechanical treatment 276
Crystals, oriented overgrowth, theory (Letter) 941
Crystals, with periodicities within the unit cell, X-ray diffraction by . . . 1003
Crystals, slip, twinning, cohesion, and boundaries of 329

Decay process, alternative, for the neutral π-meson (Letter) 667
Deformation, plastic, theory 140
Delayed coincidence method for measuring fast neutron velocities (Letter) . . 847
Demagnetization, adiabatic, of cobalt ammonium sulphate (Letter) 316
Demagnetization experiments, two-stage, the production of very low temperatures . 861
Determining uranium and thorium in rocks by the nuclear photographic plate . . 25
Deuteron bombardment of boron and proton bombardment of aluminium, gamma-rays from 906
Deuteron bombardment of neon 801
Diamagnetic anisotropy of large aromatic systems : Parts I and II 261
Diamagnetic anisotropy of large aromatic stsyems : III—Structures with hexagonal symmetry 921
Diamond, first order Raman effect in 1012
Dielectric constant, field dependence 1125

PAGE
Dielectric films, electron-bombardment conductivity 362
Dielectrics, mechanical action in (Letter) 665, 945
Differential cross section for high energy nucleon–nucleon collisions and mean square angle of scatter 1083
Diffraction, *see* X-ray diffraction
Dipole–dipole interaction in the rare-earth ethylsulphates (Letter) . . . 933
Discharge constriction by self-magnetic field and distribution of electron energies . 587
Disintegration of light nuclei by meson capture 1064
Disintegrations produced by nuclear capture of slow negative μ-mesons . . 193
Dislocation widths, factors controlling 156
Divergencies, elimination from classical electrodynamics 50
Divergencies, elimination from classical electrodynamics (Letter) . . . 427
Divergencies, elimination from quantum electrodynamics (Letter) . . . 426

Elastic scattering, secondary, in electron diffraction 609
Electrical conductivity of metals at low temperatures : equilibrium between electrons and phonons 1030
Electrical conductivity of simple p-type semiconductors (Letter) 589
Electrical properties of degenerate electronic semiconductors, cadmium oxide . 350
Electrical properties of non-metals, effect of the mean free path of electrons . . 984
Electrodynamics, classical, elimination of divergencies 50
Electrodynamics, classical, elimination of divergencies (Letter) 427
Electrodynamics, quantum, elimination of divergencies (Letter) 426
Electrodynamics, quantum, renormalization 54
Electrodynamics, quantum, supplementary condition (Letter) 850
Electrolyte, symmetrical, free energy of double layers of two plates in . . . 287
Electrolyte, symmetrical, free energy of double layers of two plates in (Letter) . 431
Electron-bombardment conductivity of dielectric films 362
Electron branching, positron (Letter) 311
Electron diffraction, determination of lattice constants by 465
Electron diffraction effects, asymmetrical, from single crystals of silver . . 1113
Electron diffraction, secondary elastic scattering 609
Electron voltaic effect (Letter) 424
Electronic transitions in B_2 and Na_2, calculation of oscillator strengths (Letter) . 425
Electrons, conversion, interference in directional correlation of (Letter) . . . 1136
Electrons, internal-conversion, successive, directional correlation 238
Electrons, mean free path, effect on electrical properties of non-metals . . . 984
Emission bands, *see* Band system
Emulsion study of ionium decay, and investigations using β-sensitive emulsions . 535
Emulsions, Ilford C2 dry, for proton range–energy relations in 1079
Energy, free, of the double layer of colloidal particle 781
Energy, free, of double layers of two plates in symmetrical electrolyte (Letter) . 431
Energy, free, of double layers of two plates in symmetrical electrolyte . . . 287
Energy levels of F-centres 648
Energy levels of the ^{5}Li nucleus, and reaction ^{6}Li(γ, n)^{5}Li (Letter) . . . 212
Epitaxial crystal growth of silver on rock-salt (110) and (111) faces . . . 283
Equations of motion in general relativity 57
Equations of motion in general relativity : II—The coordinate condition . . . 302
Erbium-167, nuclear spin (Letter) 204
Ethylene and tetra-deutero-ethylene, planar vibrations : critical analysis of potential function 32
Excitation function for production of ^{7}Be by the bombardment of ^{12}C by protons . 902
Excitation of HCO, C_2 and CH bands in flame spectra (Letter) 310
Excitation temperatures of hydrogen arcs 562

F-centres, energy levels 648
Fermi–Thomas model, applications to nucleus 937
Ferromagnetic alloys, *see* Alloys, ferromagnetic
Ferromagnetic crystals, scattering of neutrons by (Letter) 207

PAGE

Ferromagnetic crystals, slow neutron scattering 1097
Ferromagnetic resonance and internal field in ferromagnetic materials . . . 968
Ferromagnetism, free electron, theory 814
Field dependence of the dielectric constant 1125
Field theory, reciprocal (Letter) 657
First sound in liquid helium, velocity 826
Fission and neutron yields, and the average neutron energy in the photo-disintegration of uranium (Letter) 95
Flame bands, *see* Band systems
Flow of liquid helium through fine channels 554
Flow of liquid helium II through wide capillaries 833
Flow, sub-critical, in helium II film (Letter) 512
Flow, *see also* Superflow
Fluorescence, specific, of organic crystals 874
Forbidden energy zones, effect of lattice parameter on width 878
Fröhlich's theory of superconductivity 867

Gamma-ray momenta, measurement of, and thresholds of photo-disintegrations $^{12}C \rightarrow 3\,^4He$ and $^{16}O \rightarrow 4\,^4He$ (Letter) 93
Gamma-rays from deuteron bombardment of boron and proton bombardment of aluminium 906
Gamma-rays from light elements under proton bombardment 199
Gamma-rays from polonium, investigation of 493
Gamma-rays, resonant nuclear scattering : theory and preliminary experiments . 76
Gas scattering in particle accelerators 10
G.L.E.E.P. as an absolute standard of thermal neutron density (Letter) . . 1139
Gray's theory of ionization, correction factor (Letter) 509
Ground state of ^5He, and reaction $^7Li(d, \alpha)$ 452

Half-life of ^8Be, experimental determination of the (Letter) 849
Heat conduction, radially symmetrical phase growth controlled by (Letter) . . 208
Heat flow, transient, approximate solution (Letter) 1132
Helium and hydrogen and ultra-violet absorption spectra of thin vapour . . 591
Helium, liquid, flow through fine channels 554
Helium, liquid, velocity of first sound 826
Helium, solid, thermal conductivity (Letter) 89
Helium II film, sub-critical flow (Letter) 512
Helium II, liquid, flow through wide capillaries 833
Helium II, liquid, second sound 114
Helium II, liquid, theory of propagation of 'temperature waves' of finite amplitude 105
Hydrogen arcs, Balmer line widths 574
Hydrogen arcs, excitation temperatures 562

Infra-red photoconductivity in PbSe, long wave limit (Letter) 1054
Infra-red spectrum of polythene, vibrations of an infinitely long chain of CH_2-groups 521
Interference in directional correlation of conversion electrons (Letter) . . . 1136
Ionization of cosmic-ray particles (Letter). 96
Ionization, Gray's theory, correction factor (Letter) 509
Isotope effect in hydrocarbon flame bands (Letter) 428
Isotopes, radioactive, produced by nuclear photo-disintegration 395

K-capture in ^{128}I (Letter) 753

Latitude effect of penetrating showers 745
Lattice constants, determination by electron diffraction 465
Lattice constants of very small crystallites, variations in 465
Lattice parameter, effect of change on the width of the forbidden energy zone according to Kronig and Penney's one-dimensional lattice model 878
Lattice stability and oriented overgrowth 683

PAGE
Lead compounds, superconductivity in (Letter) 751
Lead sulphide, superconductivity (Letter) 667
Lifetimes of atomic energy states, experimental determination 458
Light elements, angular distribution of neutrons from the (d, n) reaction . . 797
Liquid helium, specific heat, at temperatures between 0·6° and 1·6° K. . . . 379
Low temperatures, electrical conductivity of metals : equilibrium between electrons and phonons 1030
Low temperatures, production by two-stage demagnetization 861

Magnetic analysis of α-particle groups from (d, α) reactions (Letter) . . . 754
Magnetic field, cadmium in, thermal conductivity at low temperature (Letter) . 1057
Magnetic *g*-factors of a nucleon 999
Magnetic moment and nuclear spin of rhodium, $^{103}_{45}Rh$ 1090
Magnetic susceptibility of copper sulphate 124
Magneto-resistance, saturation, of ferromagnetic alloys 447
Matter, dense, thermal conductivity. 441
Mechanical action in dielectrics (Letter) 665, 945
Meson capture and disintegration of light nuclei 1064
Meson field, β-formalism of, and nuclear reactions 659
Meson field, vector, Stueckelberg's treatment 695
Meson, neutral π-, alternative decay process (Letter) 667
Mesons, μ-, multiple scattering (Letter) 660
Mesons, μ-, at sea level, charge–ratio measurements 417
Mesons, μ-, slow negative, disintegrations produced by nuclear capture . . 193
Mesons, μ-, underground observations on interactions (Letter) 1134
Mesons, *see also* Cosmic rays
Metal transfer during sliding, using radioactivation analysis (Letter) . . . 939
Metals, alkali, absorption of light 765
Metals, electrical conductivity at low temperatures : equilibrium between electrons and phonons 1030
Metals, resistance of, θ values in 681
Modes of disintegration of ionium : an investigation using β-sensitive emulsions . 535
Molecular chain, CH_2-groups, vibrations of, and infra-red spectrum of polythene . 521
Molecular orbital treatment of the system H_4, complete 249
Molecule, CH, band spectrum ascribed to 592
Molecule, CH, calculation of the oscillator strength for the transition in $^2\Pi$–$^2\Delta$ (Letter) 666
Moments, quadrupole, of copper 63 and 65 (Letter) 758
Momentum spectrum of cosmic-ray protons (Letter) 948

Neon, deuteron bombardment 801
Neutron density, in infinite non-capturing medium, influence of black sphere or cylinder 881
Neutron energy 2–6 MeV., total cross section of beryllium, aluminium, sulphur and lead 388
Neutron scattering, slow, by ferromagnetic crystals 1097
Neutron sources, method of absolute calibration 638
Neutron velocities, fast, measurement by delayed coincidence (Letter) . . . 847
Nickel ammonium sulphate, paramagnetic resonance in (Letter) 583
Nuclear capture of slow negative μ-mesons, disintegrations produced . . . 193
Nuclear disintegrations and slow mesons in photographic plates exposed under carbon absorbers 175
Nuclear emulsions, accuracy and reproducibility of depth measurements (Letter) . 91
Nuclear emulsions, detection of $^{14}N(\gamma, d\,3\alpha)$ and $^{14}N(\gamma, pn\,3\alpha)$ reactions (Letter) . 312
Nuclear excitation by electric interaction with charged particles 619
Nuclear interaction length of the particles in penetrating cosmic-ray showers. . 4
Nuclear interactions, remarks on the use of β-formalism of the meson field for (Letter) 659

PAGE

Nuclear photographic plate, method for determining uranium and thorium in rocks 25
Nuclear reaction, long-range tritons from reaction $^{9}Be(d, t)^{8}Be$ (Letter) . . . 947
Nuclear reaction $^{6}Li(d, p)^{7}Li^{*}(\gamma)^{7}Li$, angular correlation in 938
Nuclear reaction $^{14}N(\gamma, d\,3\alpha)$ and $^{14}N(\gamma, pn\,3\alpha)$, detection in nuclear emulsions (Letter) 312
Nuclear reaction, polarized 700
Nuclear reaction, *see also* Angular distribution; Cross section; Reaction; Scattering
Nuclear scattering, resonant, of gamma-rays : theory and preliminary experiments. 76
Nuclear shell structure and nuclear density 632
Nuclear spin of erbium-167 (Letter) 204
Nuclear spin and magnetic moment of rhodium, $^{103}_{45}Rh$ 1090
Nuclear spin of $^{53}_{24}$ chromium (Letter) 1135
Nuclei, light, disintegration by meson capture 1064
Nuclei, spatial alignment (Letter) 315
Nuclear surface energy 226
Nucleon component of the cosmic radiation in air, average numbers for . . 726
Nucleon, magnetic g-factors of 999
Nucleon–nucleon collisions, differential cross section for high energy, mean square angle of scatter 1083
Nucleus, applications of Fermi–Thomas model to (Letter) 937

Obituary notices 1141
Observations on interactions of μ-mesons underground (Letter) 1134
Oscillator strength of $X\,^{2}\Pi - A\,^{2}\Delta$ transition of CH radicle (Letter) . . . 936
Oscillator strengths for certain band-systems of N_2, calculation 99
Oscillator strengths for certain electronic transitions in B_2 and Na_2, calculations (Letter) 425
Overgrowth, oriented, of crystals, theory (Letter) 941
Overgrowth, oriented, and lattice stability. 683

Paramagnetic resonance in nickel ammonium sulphate (Letter) 583
Paramagnetic resonance phenomena observed in rare earth ethyl sulphates, a preliminary survey (Letter) 205
Paramagnetic resonance in vanadous ammonium sulphate 601
Paramagnetic salts, spin-lattice relaxation in (Letter) 507
Paramagnetism of cerium ethylsulphate at low temperatures (Letter) . . . 931
Paramagnetism of cerium ethylsulphate : theory (Letter) 932
Particle accelerators, *see* Accelerators, particle
Particle, colloidal, free energy of the double layer 781
Penetrating particles, in extensive cosmic-ray air showers, density 915
Penetrating showers, *see* Cosmic-ray showers, penetrating
Phase growth, radially symmetrical, controlled by heat conduction (Letter) . . 208
Photocells, electron voltaic effect 424
Photoconductivity in the elements (Letter) 590
Photoconductivity, infra-red, long-wave limit of, in PbSe (Letter) 1054
Photodisintegration, nuclear, new radioactive isotopes produced by 395
Photo-disintegration of oxygen into two ^{8}Be nuclei (Letter) 94
Photo-disintegration of uranium, determination of fission and neutron yields and average neutron energy in (Letter) 95
Photo-disintegrations $^{12}C \rightarrow 3\,^{4}He$ and $^{16}O \rightarrow 4\,^{4}He$, thresholds and gamma-ray momenta (Letter) 93
Photoelectric effect at a metal surface, second order 135
Planar vibrations of ethylene and tetra-deutero-ethylene : critical analysis of the potential function 32
Plastic deformation, theory 140
Polarized nuclear reactions 700
Polonium, investigation of the γ-rays from 493

PAGE

Positron electron branching (Letter) 311
Pressure gradients in superflow 558
Proton bombardment of aluminium, and deuteron bombardment of boron, gamma-rays from 906
Proton bombardment of ^{12}C and production of ^{7}Be 902
Proton bombardment, gamma-rays from light elements under 199
Proton bombardment of phosphorus, alpha-particles from (Letter) 313
Proton component of vertical cosmic-ray beam at sea level 404
Protons, cosmic-ray, momentum spectrum 948
Protons, emitted in F(α, p)Ne resonance reactions, angular distribution (Letter) . 88
Protons, range of, from the reaction ^{14}N(n, p)^{14}C in Ilford C2 emulsion (Letter) . 584
Protons, range–energy relation in Ilford C2 dry emulsion 1079

Quantum electrodynamics, *see* Electrodynamics, quantum
Quantum mechanical treatment of the lithium fluoride crystal 276
Quantum theory of reciprocal fields and the correspondence principle . . . 957

Radiations, soft, from ^{239}Pu (Letter). 586
Radioactivation analysis of metal transfer during sliding (Letter) 939
Radioactive ^{159}Dy (Letter) 428
Raman effect, first order, in crystals, diamond 1012
Range–energy relation for protons in Ilford C2 dry emulsion 1079
Rare-earth ethylsulphates, dipole–dipole interaction (Letter) 933
Rare-earth ethylsulphates, paramagnetic resonance phenonema in . . . 205
Reaction ^{9}Be(d, p) (Letter) 848
Reaction $^{12}C(\gamma, 3\alpha)$ and a 16·9 MEV. level of ^{8}Be emitting alpha-particles (Letter) . 1056
Reaction ^{12}C(n, 2n)^{11}C, in anthracene crystal (Letter) 211
Reaction $^{13}C(\alpha, n)^{16}O$ (Letter) 756
Reaction (d, α), magnetic analysis of α-particle groups from 754
Reaction (d, n), angular distributions 797
Reaction $^{6}Li(\gamma n)^{5}Li$ and energy levels of the ^{5}Li nucleus (Letter) . . . 212
Reaction ^{7}Li(d, α) and the ground state of ^{5}He 452
Reaction ^{14}N(n, p)^{14}C in Ilford C2 emulsion, proton range (Letter) . . . 584
Reaction ^{23}Na(d, α)^{21}Ne (Letter) 203
Reciprocal field theory (Letter) 657
Reciprocal fields, and quantum theory of, correspondence principle . . . 957
Rectifiers, contact, breakdown voltage, and effect of temperature on the height of potential barriers (Letter). 752
Relativity, general, equations of motion 57
Relativity, general, equations of motion : II—Coordinate condition . . . 302
Relaxation, spin–lattice, in diluted paramagnetic salts (Letter) 507
Renormalization of quantum electrodynamics 54
Resistance, residual, in an extremely impure semiconductor (Letter) . . . 949
Resonance, ferromagnetic, *see* Ferromagnetic resonance
Rutherford Lecture, 5th : Lord Rutherford, 1907–19 : a Partial Portrait . . 217

Scattering, multiple, of μ-mesons (Letter) 660
Scattering of neutrons by ferromagnetic crystals (Letter) 207
Scattering of neutrons by protons and deuterons 546
Scattering phase shifts of two-nucleon systems 712
Scintillations from organic crystals : specific fluorescence and relative response to different radiations 874
Second sound in liquid helium II 114
Second sound pulses and waves of finite amplitude 105
Self-magnetic field, discharge constriction and distribution of electron energies . 587

PAGE
Semiconductors, change of activation energy with impurity concentration in (Letter) 663
Semiconductors, electronic, degenerate, variation with temperature, as exemplified by cadmium oxide 350
Semiconductors, excess, parameters of 476
Semiconductors, impure, residual resistance (Letter) 949
Semiconductors, p-type, electrical conductivity (Letter) 589
Silver, single crystals, and asymmetrical electron diffraction effects . . . 1113
Slip, twinning, cohesion, growth and boundaries of crystals. 329
Specific heat of liquid helium at temperatures between 0·6° and 1·6° K. . . 379
Spectra, flame, excitation of HCO, C_2 and CH bands (Letter) 310
Spectra, secondary electron, of ^{198}Au 13
Spectra, ultra-violet absorption bands probably due to InH and GaH : extension of line series in the arc spectrum of indium 509
Spectra, *see also* Infra-red; Absorption
Spectrometer, Geiger counter for soft x-rays (Letter) 935
Spectrum, arc, indium: extension of line series (Letter) 509
Spin–lattice relaxation in diluted paramagnetic salts (Letter) 507
Spin, nuclear, *see* Nuclear spin
Stueckelberg's treatment of the vector meson field 695
Superconducting state, theory: II—Magnetic properties at the absolute zero of temperature 129
Superconductivity, Fröhlich's theory 867
Superconductivity in lead compounds, investigation of (Letter) 751
Superconductivity of lead sulphide (Letter) 667
Superflow, pressure gradients 558
Surface energy, nuclear 226

Temperature effect of extensive air showers 1061
Temperature variation of the electrical properties of a degenerate electronic semiconductor as exemplified by cadmium oxide 350
Thermal conductivity of cadmium in a magnetic field at low temperatures (Letter). 1057
Thermal conductivity of dense matter 441
Thermal conductivity of solid helium (Letter) 89
Theta values in the resistance of metals 681
Thin layers of zinc oxide grown on a zinc single crystal, structure (Letter) . . 943
Transition probabilities in band-systems of diatomic molecules: a modified ' distortion ' process for the wave functions 772
Tritons, long-range, from reaction $^{9}Be(d, t)^{8}Be$ (Letter) 947
Two-nucleon systems, scattering phase shifts of 712

Vibrations of an infinitely long chain of CH_2-groups and the infra-red spectrum of polythene 521

X-ray asterisms from deformed crystals (Letter) 844
X-ray diffraction by a crystal possessing periodicities within the unit cell. . . 1003
X-rays, soft, Geiger counter spectrometer for (Letter) 935

INDEX OF AUTHORS (WITH TITLES)

PAGE

Allen, J. E. : The distribution of electron energies in a discharge constricted by its self-magnetic field (Letter) 587
Allen, R. A., *see* Grace, M. A.
Andrews, E. B., and Barrow, R. F. : The band-spectrum of carbon monofluoride, CF. 481
Ansbacher, F., and Ehrenberg, W. : Electron-bombardment conductivity of dielectric films 362
Ashmore, A., and Raffle, J. F. : Magnetic analysis of α-particle groups from (*d*, α) reactions (Letter). 754
Atkins, K. R. : The flow of liquid helium II through wide capillaries . . . 833
Atkins, K. R., and Chase, C. E. : The velocity of first sound in liquid helium . 826

Barker, K. H., and Butler, C. C. : The nuclear interaction length of the particles in penetrating cosmic-ray showers 4
Barrow, R. F., *see* Andrews, E. B.
Barrow, R. F., *see* Dovell, W. H.
Barton, J. C. : Observations of the penetrating non-ionizing component of the cosmic radiation 1042
Barton, J. C., George, E. P., and Jason, A. C. : Observations of slow mesons and nuclear disintegrations in photographic plates exposed under carbon absorbers . 175
Bates, D. R. : On the oscillator strength of the $x^2\Pi - A^2\Delta$ transition of the CH radicle (Letter) 936
Bates, L. F., and Wilson, G. W. : Some new bitter patterns on a single crystal of nickel 691
Benson, G. C., and Wyllie, G. : A quantum mechanical treatment of the lithium fluoride crystal 276
Benzie, R. J. : Spin-lattice relaxation in diluted paramagnetic salts (Letter) . . 507
Benzie, R. J., and Cooke, A. H. : The magnetic susceptibility of copper sulphate . 124
Billig, E. : Effect of the change in lattice parameter on the width of the forbidden energy zone according to Kronig and Penney's one-dimensional lattice model . 878
Billig, E. : Effect of temperature on the height of potential barriers and on the breakdown voltage of contact rectifiers (Letter) 752
Birks, J. B. : Scintillations from organic crystals : Specific fluorescence and relative response to different radiations 874
Birks, J. B., and Black, F. A. : Deterioration of anthracene under α-particle irradiation (Letter) 511
Black, F. A., *see* Birks, J. B.
Blackman, M. : On θ values in the resistance of metals 681
Blackman, M., *see* Frank, F. C.
Blackman, M., *see* Smollett, M.
Blackwell, J. H., and Misener, A. D. : Approximate solution of a transient heat flow problem 1132
Bleaney, B. : Note on the adiabatic demagnetization of cobalt ammonium sulphate (Letter) 316
Bleaney, B. : On the spatial alignment of nuclei (Letter) 315
Bleaney, B., and Bowers, K. D. : Nuclear spin of $^{53}_{24}$Chromium 1135
Bleaney, B., Bowers, K. D., and Ingram, D. J. E. : Quadrupole moments of copper 63 and 65 (Letter) 758
Bleaney, B., Elliott, R. J., and Scovil, H. E. D. : Dipole–dipole interaction in the rare-earth ethylsulphates (Letter) 933
Bleaney, B., Ingram, D. J. E., and Scovil, H. E. D. : Paramagnetic resonance in vanadous ammonium sulphate 601
Bleaney, B., and Scovil, H. E. D. : Nuclear spin of Erbium-167 (Letter) . . 204
Blin-Stoyle, R. J. : Polarized nuclear reactions 700
Bogle, G. S., Cooke, A. H., and Whitley, S. : Paramagnetism of cerium ethyl-sulphate at low temperatures (Letter) 931
Booker, D. V., *see* Cavanagh, P. E.

PAGE

Boswell, F. W. C. : Precise determination of lattice constants by electron diffraction and variations in the lattice constants of very small crystallites . . . 465
Bowers, K. D., *see* Bleaney, B.
Bowers, R., and White, G. K. : Pressure gradients in superflow 558
Braid, T. H., and Richardson, H. O. W. : Further studies—experimental and theoretical—of a wide-angle beta-spectrometer which uses a prolate spheroidal magnetic field 163
Bremner, J. W. : A method for determining uranium and thorium in rocks by the nuclear photographic plate 25
Brinkley, T. A., *see* Titterton, E. W.
Brodie, W. D., *see* Butt, D. K.
Brú, L., and Gharpurey, M. K. : Epitaxial crystal growth of silver on rock-salt (110) and (111) faces 283
Buckingham, M. J., *see* Makinson, R. E. B.
Butcher, P. N., : The absorption of light by alkali metals 765
Butement, F. D. S. : New radioactive isotopes produced by nuclear photodisintegration 395
Butement, F. D .S. : Radioactive ^{159}Dy (Letter) 428
Butler, C. C., *see* Barker, K. H.
Butt, D. K., and Brodie, W. D. : The conversion and Auger electrons of radium D. 791

Cade, R. : On mechanical action in dielectrics (Letter) 665
Candler, C. : The magnetic g-factors of a nucleon 999
Capelhorn, W. F., and Rundle, G. P. : The angular distribution of 3 MeV. neutrons scattered by protons and by deuterons 546
Carver, J. H., and Wilkinson, D. H. : Some gamma-rays from light elements under proton bombardment 199
Cavanagh, P. E., Turner, J. F., Booker, D. V., and Dunster, H. J. : An investigation of the secondary electron spectrum of ^{198}Au 13
Chalklin, R. C., *see* Rogers, J. L.
Champion, F. C., *see* Jolley, J. D.
Chandrasekhar, B. S., and Mendelssohn, K. : Sub-critical flow in the helium II film (Letter) 512
Chase, C. E., *see* Atkins, K. R.
Chi-Shi Lang, *see* Ehrenberg, W.
Clark, A. C., and Ruddlesden, N. : The disintegration of light nuclei by meson capture 1064
Cooke, A. H., *see* Benzie, R. J.
Cooke, A. H., *see* Bogle, G. S.
Cowley, J. M., Rees, A. L. G., and Spink, J. A. : Secondary elastic scattering in electron diffraction 609
Craggs, J. D., *see* Edels, H.
Crewe, A. V. : The multiple scattering of μ-mesons (Letter) 660

Dalitz, R. H. : On an alternative decay process for the neutral π-meson (Letter). 667
Darby, J., Hatton, J., Rollin, B. V., Seymour, E. F. W., and Silsbee, H. B. : Experiments on the production of very low temperatures by two-stage demagnetization 861
Davies, W. T., and Grace, M. A. : On the identity of β-rays with electrons (Letter) 846
Davies, W. T., and Shaw, D. F. : A search for sudden large changes of energy of beta-rays in a cloud chamber 1006
Davison, B. : Influence of a black sphere and of a black cylinder upon the neutron density in an infinite non-capturing medium 881
Dawson, J. K., *see* West, D.
Dickson, J. M., and Randle, T. C. : The excitation function for the production of ^{7}Be by the bombardment of ^{12}C by protons 902
Dovell, W. H., and Barrow, R. F. : A new ultra-violet band-system of SiF (Letter) 98
Dunster, H. J., *see* Cavanagh, P. E.

PAGE

Edels, H., and Craggs, J. D. : Balmer line widths in hydrogen arcs . . . 574
Edels, H., and Craggs, J. D. : Excitation temperatures of hydrogen arcs . . 562
Ehrenberg, W., *see* Ansbacher, F.
Ehrenberg, W., Chi-Shi Lang, and West, R. : The electron voltaic effect (Letter) . 424
El-Bedewi, F. A. : The long-range tritons from the reaction ^{9}Be(d, t)^{8}Be (Letter) . 947
El-Bedewi, F. A. : The range of protons from the reaction ^{14}N(n, p)^{14}C in Ilford C2 photographic emulsion (Letter) 584
El-Bedewi, F. A. : Range–energy relation for protons in Ilford C_2 dry emulsion. 1079
El-Bedewi, F. A., Middleton, R., and Tai, C. T. : Angular distributions of the neutron groups from the reaction ^{12}C(d, n)^{13}N (Letter) 1055
El-Bedewi, F. A., Middleton, R., and Tai, C. T. : Angular distributions of the two long-range neutron groups of the reaction ^{16}O(d, n)^{17}F (Letter) . . . 756
Elliott, R. J., *see* Bleaney, B.
Elliott, R. J., and Stevens, K. W. H.: The paramagnetism of cerium ethylsulphate: theory (Letter) 932
Elliott, R. J., and Stevens, K. W. H. : A preliminary survey of the paramagnetic resonance phenomena observed in rare earth ethyl sulphates (Letter) . . 205
Evans, J., *see* George, E. P.

Feast, M. W. : On a band system ascribed to the CH Molecule (Letter) . . 592
Foreman, A. J., Jaswon, M. A., and Wood, J. K. : Factors controlling dislocation widths 156
Frank, F. C. : Blackman, M. : The theory of oriented over-growth of crystals (Letter) 941
Freeman, J. M., and Seed, J. : Alpha-particles from the proton bombardment of phosphorus (Letter) 313
French, A. P., and Thomson, D. M. : The reaction ^{23}Na(d, α)^{21}Ne (Letter) . . 203
French, A. P., and Treacy, P. B. : The reaction ^{7}Li(d, α) and the ground state of ^{5}He 452
Fröhlich, H. : Theory of the superconducting state : II—Magnetic properties at the absolute zero of temperature 129

Gardner, J. W. : Directional correlation between successive internal-conversion electrons : II 238
Gardner, J. W. : Interference in the directional correlation of conversion-electrons (Letter) 1136
Gardner, J. W. : On the elimination of divergencies from classical electrodynamics (Letter) 427
Garton, W. R. S. : Emission band of the Cd_2 Molecule at λ2212 (Letter) . . 430
Garton, W. R. S. : Extension of line series in the arc spectrum of indium: ultra-violet absorption bands probably due to InH and GaH (Letter) . . . 509
Garton, W. R. S. : Ultra-violet absorption spectra of tin vapour in atmospheres of helium and hydrogen (Letter) 591
Gay, P., and Honeycombe, R. W. K. : X-ray asterisms from deformed crystals (Letter) 844
Gaydon, A. G., and Wolfhard, H. G. : The excitation of HCO, C_2 and CH bands in flame spectra (Letter) 310
Geist, D. : A note on the radially symmetrical phase growth controlled by heat conduction (Letter) 208
George, E. P., *see* Barton, J. C.
George, E. P., and Evans, J. : Disintegrations produced by the nuclear capture of slow negative μ-mesons 193
George, E. P., *see* Michaelis, E. G.
George, E. P., and Trent, P. T. : Observations on the interactions of μ-mesons underground 1134
George, E. P., and Trent, P. T. : Penetrating bursts of cosmic radiation . . 733
Gharpurey, M. K., *see* Brú, L.
Gibson, A. F., Lawson, W. D., and Moss, T. S. : The long-wave limit of infra-red photoconductivity in PbSe (Letter) 1054

PAGE

Goodman, P., Nicholson, K. P., and Rathgeber, H. D. : The ionization of cosmic-ray particles (Letter) 96
Goward, F. K., Jones, E. J., Watson, H. H. H., and Lees, D. J. : Determination of fission and neutron yields, and the average neutron energy in the photodisintegration of uranium (Letter) 95
Goward, F. K., and Wilkins, J. J. : Detection of $^{14}N(\gamma, d\,3\alpha)$ and $^{14}N(\gamma, pn\,3\alpha)$ reactions in nuclear emulsions (Letter) 312
Goward, F. K., and Wilkins, J. J. : Measurements of gamma-ray momenta and the thresholds of the photo-disintegrations $^{12}C \rightarrow 3^4He$ and $^{16}O \rightarrow 4^4He$ (Letter) . 93
Goward, F. K., and Wilkins, J. J. : The photodisintegration of oxygen into two ^8Be nuclei (Letter) 94
Goward, F. K., *see* Wilkins, J. J.
Grace, M. A., Allen, R. A., West, D., and Halban, H. : Investigation of the γ-rays from polonium 493
Grace, M. A., *see* Davies, W. T.
Green, H. S., and Messel, H. : The differential cross section for high energy nucleon–nucleon collisions and the mean square angle of scatter 1083
Griffiths, J. H. E., and Owen, J. : Paramagnetic resonance in nickel ammonium sulphate (Letter) 583
Gupta, S. N. : On the elimination of divergencies from classical electrodynamics . 50
Gupta, S. N. : On the elimination of divergencies from quantum electrodynamics (Letter) 426
Gupta, S. N. : On Stueckelberg's treatment of the vector meson field . . . 695
Gupta, S. N. : On the supplementary condition in quantum electrodynamics (Letter) 850

Halban, H., *see* Grace, M. A.
Halban, H., *see* Mims, W. B.
Hatton, J., Rollin, B. V., and Seymour, E. F. W. : Superconductivity of lead sulphide (Letter) 667
Hatton, J., *see* Darby, J.
Hodson, A. L. : The temperature effect of extensive air showers . . . 1061
Honeycombe, R. W. K., *see* Gay, P.
Huang, Kun : A note on Fröhlich's theory of superconductivity 867
Huby, R., and Newns, H. C. : Nuclear excitation by electric interaction with charged particles 619
Hudson, R. P. : Investigation of superconductivity in lead compounds (Letter) . 751
Hughes, J. : The angular distribution of neutrons from the (d, n) reaction in light elements 797
Hull, R. A., Wilkinson, K. R., and Wilks, J.: The specific heat of liquid helium at temperatures between 0·6° and 1·6° K 379

Ibrahim, Ali A. K. : A correction factor to Gray's theory of ionization (Letter) . 509
Ingram, D. J. E., *see* Bleaney, B.

James, D. B., and Treacy, P. B. : Measurement of fast neutron velocities by delayed coincidence (Letter) 847
Jánossy, L., and Messel, H. : Cascade theory including ionization loss. . . . 1
Jarvis, C. J. D., and Ross, M. A. S. : Modes of disintegration of ionium : an investigation using β-sensitive emulsions 535
Jason, A. C., *see* Barton, J. C.
Jaswon, M. A., *see* Foreman, A. J.
Jeffery, J. W. : X-ray diffraction by a crystal possessing periodicities within the unit cell 1003
Jelley, J. V. : Detection of μ-mesons and other fast charged particles in cosmic radiation, by the Čerenkov effect in distilled water 82
Jolley, J. D., and Champion, F. C. : The angular distribution of protons emitted in some F(α, p)Ne resonance reactions (Letter) 88
Jones, E. J., *see* Goward, F. K.
Jones, G. A., and Wilkinson, D. H. : The Reaction $^{13}C(\alpha n)^{16}O$ (Letter) . . 756

PAGE

Keam, D. W., *see* McAlister, J. M.
Kellner, L.: The vibrations of an infinitely long chain of CH_2-groups and the infrared spectrum of polythene 521
Klemens, P. G.: Electrical conductivity of metals at low temperatures: equilibrium between electrons and phonons 1030
Krishnamurty, S. G.: The band systems of thorium oxide and hafnium oxide (Letter) 852
Kuhlmann, D.: On the theory of plastic deformation 140
Kuhn, H., and Woodgate, G. K.: Nuclear spin and magnetic moment of rhodium $^{103}_{45}Rh$ 1090
Kushneriuk, S. A., and Preston, M. A.: The scattering phase shifts of two-nucleon systems 712

Landsberg, P. T., Mackay, R. W., and McRonald, A. D.: The parameters of simple excess semiconductors 476
Lawson, W. D., *see* Gibson, A. F.
Lee, P. A., *see* Stewardson, E. A.
Lees, D. J., *see* Goward, F. K.
Lempicki, A.: The electrical conductivity of simple p-type semiconductors (Letter) 589
Levine, S.: The free energy of the double layer of a colloidal particle . . . 781
Levine, S., and Suddaby, A.: Free energy of the double layers of two plates at large separations (Letter) 431
Levine, S., and Suddaby, A.: Simplified forms for free energy of the double layers of two plates in a symmetrical electrolyte 287
Lidiard, A. B.: On the theory of free electron ferromagnetism 814
Littler, D. J.: A method of calibrating neutron sources absolutely 638
Littler, D. J., Lockett, E. E., and Price, B. T.: The G.L.E.E.P. as an absolute standard of thermal neutron density 1139
Lockett, E. E., *see* Littler, D. J.
Lucas, L. N. D.: The structure of thin layers of zinc oxide grown on a zinc single crystal (Letter) 943

McAlister, J. M., and Keam, D. W.: Factors involved in the accuracy and reproducibility of depth measurements on nuclear research emulsions (Letter) . 91
McCusker, C. B. A., and Messel, H.: The momentum spectrum of cosmic-ray protons (Letter) 948
McCusker, C. B. A., and Millar, D. D.: The density of the penetrating particles in extensive cosmic-ray air showers 915
Macdonald, J. R.: Ferromagnetic resonance and the internal field in ferromagnetic materials 968
Mackay, R. W., *see* Landsberg, P. T.
McRonald, A. D., *see* Landsberg, P. T.
McWeeny, R.: The diamagnetic anisotropy of large aromatic systems: Parts I and II 261
McWeeny, R.: The diamagnetic anisotropy of large aromatic systems: III—Structures with hexagonal symmetry 921
Makinson, R. E. B., and Buckingham, M. J.: The second order photoelectric effect at a metal surface 135
Mehta, G. K., and Rajeswari, V.: C_2 (Swan) bands in krypton (Letter) . . 210
Mendelssohn, K., and Rosenberg, H. M.: The thermal conductivity of cadmium in a magnetic field at low temperatures (Letter) 1057
Mendelssohn, K., *see* Chandrasekhar, B. S.
Messel, H.: Average numbers for the development of the nucleon component of the cosmic radiation in air 726
Messel, H.: Further results on the fluctuation problem in electron–photon cascade shower theory and the probability distribution function 807
Messel, H., *see* Green, H. S.
Messel, H., *see* Jánossy, L.
Messel, H., *see* McCusker, C. B. A.

PAGE

Michaelis, E. G., and George, E. P. : Measurements of the star-producing radiation with a scintillation counter (Letter) 662
Middleton, R., *see* El-Bedewi, F. A.
Middleton, R., and Tai, C. T. : Deuteron bombardment of neon . . . 801
Millar, D. D., *see* McCusker, C. B. A.
Mims, W. B., and Halban, H. : K capture in ^{128}I (Letter) 753
Mims, W., and Halban, H. : Positron electron branching (Letter) . . 311
Misener, A. D., *see* Blackwell, J. H.
Moon, P. B.: Resonant nuclear scattering of gamma-rays : theory and preliminary experiments 76
Moorhouse, R. G. : Scattering of neutrons by ferromagnetic crystals (Letter) . 207
Moorhouse, R. G. : Slow neutron scattering by ferromagnetic crystals . . 1097
Moss, T. S. : Photoconductivity in the elements (Letter) 590
Moss, T. S., *see* Gibson, A. F.
Mylroi, M. G., and Wilson, J. G. : On the proton component of the vertical cosmic-ray beam at sea level 404

Newns, H. C., *see* Huby, R.
Newton, J. O. : Angular correlation in the reaction ^{6}Li(d, p)^{7}Li*(γ)^{7}Li (Letter) . 938
Nicholson, K. P., *see* Goodman, P.

O'Dwyer, J. J. : Field dependence of the dielectric constant 1125
Osborne, D. V. : Second sound in liquid helium II 114
Owen, B. G., and Wilson, J. G. : Further measurements of the charge ratio of μ-mesons at sea level 417
Owen, J., *see* Griffiths, J. H. E.

Paneth, H. R. : On certain applications of the Fermi-Thomas model to the nucleus (Letter) 937
Papapetrou, A. : Equations of motion in general relativity 57
Papapetrou, A.: Equations of motion in general relativity: II—The coordinate condition 302
Parker, R. : The saturation magneto-resistance of ferromagnetic alloys . . 447
Pashley, D. W. : Asymmetrical electron diffraction effects from single crystals of silver 1113
Pillow, M. E. : Transition probabilities in band-systems of diatomic molecules : a modified ' distortion ' process for the wave functions 772
Pincherle, L. : Change of activation energy with impurity concentration in semi-conductors (Letter) 663
Pincherle, L. : Energy levels of F-centres 648
Preston, M. A., *see* Kushneriuk, S. A.
Price, B. T., *see* Littler, D. J.
Pursey, D. L. : Theoretical discussion of the beta decay of ^{32}P (Letter) . . 1138

Rabinowicz, E. : A study of metal transfer during sliding, using radioactivation analysis (Letter) 939
Rae, E. R., *see* Rutherglen, J. G.
Raffle, J. F., *see* Ashmore, A.
Rajeswari, V., *see* Mehta, G. K.
Randle, T. C., *see* Dickson, J. M.
Rathgeber, H. D., *see* Goodman, P.
Rayski, J. : On the quantum theory of reciprocal fields and the correspondence principle 957
Rayski, J. : On the reciprocal field theory (Letter) 657
Rees, A. J. G., *see* Cowley, J. M.
Richardson, H. O. W., *see* Braid, T. H.
Riddiford, L. : The importance of gas scattering in particle accelerators . . 10
Rogers, J. L., and Chalklin, R. C.: A Geiger counter spectrometer for soft x-rays (Letter) 935

PAGE

Rollin, B. V., *see* Darby, J.
Rollin, B. V., *see* Hatton, J.
Rosenberg, H. M., *see* Mendelssohn, K.
Ross, M. A. S., *see* Jarvis, C. J. D.
Ruddlesden, N., *see* Clark, A. C.
Rundle, G. P., *see* Caplehorn, W. F.
Russell, A. S. : Lord Rutherford, 1907–19 : a Partial Portrait 217
Rutherglen, J. G., Rae, E. R., and Smith, R. D. : Gamma-rays from the deuteron bombardment of boron and the proton bombardment of aluminium . . 906

Salmon, A. J. : An investigation of the reaction ^{9}Be(d, p) (Letter) . . . 848
Schrödinger, E. : A combinatorial problem in counting cosmic rays 1040
Scovil, H. E. D., *see* Bleaney, B.
Seed, J., *see* Freeman, J. M.
Seymour, E. F. W., *see* Darby, J.
Seymour, E. F. W., *see* Hatton, J.
Sharpe, J., and Stafford, G. H. : The ^{12}C(n, 2n)^{11}C reaction in an anthracene crystal (Letter) 211
Shaw, D. F., *see* Davies, W. T.
Silsbee, H. B., *see* Darby, J.
Singwi, K. S., and Sundaresan, M. K. : Thermal conductivity of dense matter . 441
Smith, R. D., *see* Rutherglen, J. G.
Smith-White, W. B. : On the mechanical action in dielectrics (Letter) . . 945
Smollett, M., and Blackman, M. : Lattice stability and oriented overgrowth . . 683
Spink, J. A., *see* Cowley, J. M.
Stafford, G. H. : The total cross section of beryllium, aluminium, sulphur and lead for neutrons of energies from 2 MeV. to 6 MeV. 388
Stafford, G. H., *see* Sharpe, J.
Stephenson, G. : Calculation of the oscillator strengths for certain band-systems of N_2 and C_2 (Letter) 99
Stephenson, G. : Calculation of oscillator strengths for certain electronic transitions in B_2 and Na_2 (Letter) 425
Stephenson, G. : Calculation of the oscillator strength for the $^2\Pi - ^2\Delta$ transition in the CH molecule (Letter) 666
Stephenson, G. : Calculation of relative transition probabilities for first negative bands of N_2^+ (Letter) 209
Stephenson, G. : On the experimental determination of the lifetimes of atomic energy states 458
Stevens, K. W. H., *see* Elliott, R. J.
Stewardson, E. A., and Lee, P. A. : The M_{IV} and M_V absorption edges of ^{68}Er (Letter) 318
Sturgess, J. W. : Observations of the latitude effect of penetrating showers . . 745
Suddaby, A., *see* Levine, S.
Sundaresan, M. K., *see* Singwi, K. S.
Swiatecki, W. J. : The nuclear surface energy 226

Tai, C. T., *see* El-Bedewi, F. A.
Tai, C. T., *see* Middleton, R.
Taylor, R. : Complete molecular orbital treatment of the system H_4 . . . 249
Temperley, H. N. V. : The theory of the propagation of liquid helium II of ' temperature-waves ' of finite amplitude 105
Theimer, O. : The first order Raman effect in crystals, particularly in diamond . 1012
Thomson, D. M., *see* French, A. P.
Titterton, E. W., and Brinckley, T. A. : The reaction ^{6}Li(γ, n) ^{5}Li and energy levels of the ^{5}Li nucleus (Letter) 212
Torkington, P. : The planar vibrations of ethylene and tetra-deutero-ethylene : a critical analysis of the potential function 32
Treacy, P. B., *see* French, A. P.

PAGE

Treacy, P. B., *see* James, D. B.
Trent, P. T., *see* George, E. P.
Turner, J. F., *see* Cavanagh, P. E.

Vachaspati : Some remarks on the use of β-formalism of the meson field for nuclear interactions (Letter) 659
Vaidya, W. M. : Isotope effect in hydrocarbon flame bands (Letter) . . . 428

Ward, J. C. : On the renormalization of quantum electro-dynamics 54
Watson, H. H. H., *see* Goward, F. K.
West, D., and Dawson, J. K. : Soft radiations from ^{239}Pu (Letter) . . . 586
West, D., *see* Grace, M. A.
West, R., *see* Ehrenberg, W.
White, G. K. : Flow of liquid helium through fine channels 554
White, G. K., *see* Bowers, R.
Whitley, S., *see* Bogle, G. S.
Wilks, J., *see* Hull, R. A.
Wilks, J., *see* Wilkinson, K. R.
Wilkins, J. J., and Goward, F. K.: Fall and re-increase of the ^{12}C (γ, 3 ^{4}He) cross section (Letter) 201
Wilkins, J. J., and Goward, F. K.: Note on experimental determination of the half-life of ^{8}Be (Letter) 849
Wilkins, J. J. and Goward, F. K. : The Reaction ^{12}C(γ, 3α) and a 16·9 MEV. level of ^{8}Be emitting alpha-particles (Letter) 1056
Wilkins J. J., *see* Goward, F. K.
Wilkinson, D. H., *see* Carver, J. H.
Wilkinson, D. H., *see* Jones, G. A.
Wilkinson, K. R., *see* Hull, R. A.
Wilkinson, K. R., and Wilks, J. : The thermal conductivity of solid helium (Letter) 89
Wilman, H : The slip, twinning, cohesion, growth and boundaries of crystals . 329
Wilson, G. W., *see* Bates, L. F.
Wilson, J. G., *see* Mylroi, M. G.
Wilson, J. G., *see* Owen, B. G.
Wolfhard, H. G., *see* Gaydon, A. G.
Wood, J. K., *see* Foreman, A. J.
Woodgate, G. K., *see* Kuhn, H.
Wright, R. W. : Residual resistance in an extremely impure semiconductor (Letter) 949
Wright, R. W. : The effect of the mean free path of electrons on the electrical properties of non-metals 984
Wright, R. W. : The variation with temperature of the electrical properties of a degenerate electronic semiconductor as exemplified by cadmium oxide. . 350
Wyllie, G., *see* Benson, G. C.

Yang, L. M. : Nuclear shell structure and nuclear density 632

Ziman, J. M. : Antiferromagnetism by the Bethe method 1108

INDEX TO REVIEWS OF BOOKS

PAGE

Alfvén, H. : *Cosmical Electrodynamics* 593

Becker, R. : *Vorstufe zur theoretischen physik* 101
Berkeley, E. C. : *Giant Brains or Machines that Think* 513
Bouman, J. (Ed.) : *Selected Topics in S-Ray Crystallography* 951
Broda, E. : *Advances in Radio-chemistry* 678
Buckley, H. E. : *Crystal Growth* 952

Centre National de la Recherche Scientifique (Colloques Internationaux du C.N.R.S., VII) : *Diffusion Moléculaire de la Lumière et Effet Raman* . . 677
Centre National de la Recherche Scientifique : *Méthodes de calcul dans des problèmes de mécanique* 101
Comrie, L. J. : *Shorter Six-figure Mathematical Tables* 669
Crammer, J. L., and Peierls, R. E. : *Atomic Energy* 514
Curran, S. C., and Craggs, J. D. : *Counting Tubes* 319

Dingle, H. : *Practical Applications of Spectrum Analysis* 435

Einstein, A. : *The Meaning of Relativity* 433

Fabry, C. : *The Elements of Thermodynamics* 953
Finkelnburg, W. : *Atomic Physics* 595
Finkelnburg, W. : *Einführung in das Studium der Physik* 951
Frisch, O. R. (Ed.) : *Progress in Nuclear Physics* 674

Glasstone, S. : *Sourcebook on Atomic Energy* 854
Goldstein, H. : *Classical Mechanics* 434

Halliday, D. : *Introductory Nuclear Physics* 854
Harned, H. S., and Owen, B. B. : *Physical Chemistry of Electrolyte Solutions* . 596
Harrison, G. R., Lord, R. C., and Loofbourow, J. R. : *Practical Spectroscopy* . 597
Hartree, D. R. : *Calculating Instruments and Machines* 670
Heisenberg, W. : *Two Lectures* 594
Herzberg, G. : *Molecular Spectra and Molecular Structure* : Vol. I—*Spectra of Diatomic Molecules* 760

Institute of Physics : *The Acceleration of Particles to High Energies* . . . 675

Jellinek, K. : *Weltsystem, Weltäther und die Relativitätstheorie* 852
Jordan, P. : *Beiträge zum neuzeitlichen Weldbild der Physik* : *Das Plancksche Wirkungsquantum* 324

Kern, D. Q. : *Process Heat Transfer* 856
Knopp, K. : *Theory and Application of Indefinite Series* 953

Leverenz, H. W. : *An Introduction to Luminescence of Solids* 436
London, F. : *Superfluids*: Vol. I—*Macroscopic Theory of Superconductivity* . . 855

Margenau, H. : *The Nature of Physical Reality* : *A Philosophy of Modern Physics* . 323
Martin, T. : *Faraday's Discovery of Electromagnetic Induction* 437
Massey, H. S. W. : *Negative Ions* 760
Michaud, R. : *Contribution a l'Étude des Réactions Mutuelles des Cristaux dans la Déformation des Métaux Polycristallins* 517
Milne-Thomson, L. M. : *Theoretical Hydrodynamics* 320
Mott, N. F., and Massey, H. S. W. : *Theory of Atomic Collisions* 323

PAGE

Noakes, G. R. : *Textbook of General Physics* 671

Orear, J., Rosenfeld, A. H., and Schluter, R. A. : *Nuclear Physics* . . . 674

Parker, P. : *Electronics* 676
Pearse, R. W. B., and Gaydon, A. G. : *The Identification of Molecular Spectra* . 677

Roberts, J. K. : *Heat and Thermodynamics* 953
Rosenfeld, L. : *Theory of Electrons* 952

Schrödinger, E. : *Space–Time Structures* 673
Scott, M. : *Mechanics* 598
Sommerfeld, A. : *Vorlesungen über theoretische Physik*. 515
Soodak, H., and Campbell, E. C. : *Elementary Pile Theory* 595
Spring, K. H. : *Photons and Electrons* 436
Starling, S. G., and Woodall, A. J. : *Physics* 672
Syrkin, Y. K., and Dyatkina, M. E. : *Structure of Molecules and the Chemical Bond* 516

Weizel, W. : *Lehrbuch der theoretischen Physik*: I—*Physik der Vorgänge* . . 673
Wilkinson, D. H. : *Ionization Chambers and Counters* 517
Wright, D. A. : *Semiconductors* 678

Zweiling, K. : *Dialektrischer Materialismus und theoretische Physik* . . . 324

THE PHYSICAL SOCIETY

MEMBERSHIP

Membership of the Society is open to all who are interested in Physics:

FELLOWSHIP. A candidate for election to Fellowship must as a rule be recommended by three Fellows, to two of whom he is known personally. Fellows may attend all meetings of the Society, are entitled to receive Publications 1 (either Section A or Section B), 4 and 5 below, and may obtain the other publications at much reduced rates.

STUDENT MEMBERSHIP. A candidate for election to Student Membership must be between 18 and 26 years of age and must be recommended from personal knowledge by a Fellow. Student Members may attend all meetings of the Society, are entitled to receive Publications 1 (either Section A or Section B) and 4, and may obtain the other publications at much reduced rates.

Books and periodicals may be read in the Society's Library, and a limited number of books may be borrowed by Fellows and Student Members on application to the Honorary Librarian.

Fellows and Student Members may become members of the *Colour Group*, the *Optical Group*, the *Low Temperature Group* and the *Acoustics Group* (specialist Groups formed in the Society) without payment of additional annual subscription.

PUBLICATIONS

1. *The Proceedings of the Physical Society*, published monthly in two Sections, contains original papers, lectures by specialists, reports of discussions and of demonstrations, and book reviews. Section A contains papers mainly on atomic and sub-atomic subjects; Section B contains papers on macroscopic physics.

2. *Reports on Progress in Physics*, published annually, is a comprehensive review by qualified physicists.

3. *The Handbook of the Physical Society's Annual Exhibition of Scientific Instruments and Apparatus*. This Exhibition is recognized as the most important function of its kind, and the Handbook is a valuable book of reference.

4. *The Bulletin*, issued at frequent intervals during the session, informs members of programmes of future meetings and of the business of the Society generally.

5. *Physics Abstracts* (*Science Abstracts A*), published monthly in association with the Institution of Electrical Engineers, covers the whole field of contemporary physical research.

6. *Electrical Engineering Abstracts* (*Science Abstracts B*), published monthly in association with the Institution of Electrical Engineers, covers the whole field of contemporary research in electrical engineering.

7. *Special Publications*, critical monographs and reports on special subjects prepared by experts or committees, are issued from time to time.

MEETINGS

At approximately monthly intervals throughout each annual session, meetings are held for the reading and discussion of papers, for lectures, and for experimental demonstrations. Special lectures include: the *Guthrie Lecture*, in memory of the founder of the Society, given annually by a physicist of international reputation; the *Thomas Young Oration*, given biennially on an optical subject; the *Charles Chree Address*, given biennially on Geomagnetism, Atmospheric Electricity, or a cognate subject; and the biennial *Rutherford Memorial Lecture*. Meetings are generally held each year at provincial centres, and from time to time meetings are arranged jointly with other Societies for the discussion of subjects of common interest.

Each of the four specialist Groups holds about five meetings in each session.

SUBSCRIPTIONS

Fellows pay an Entrance Fee of £1 1*s*. and an Annual Subscription of £3 3*s*. Student Members pay only an Annual Subscription of 15*s*. Second Section of *Proceedings* 30*s*. No entrance fee is payable by a Student Member on transfer to Fellowship.

Further information may be obtained from the Secretary-Editor at the Offices of the Society:

1 LOWTHER GARDENS, PRINCE CONSORT ROAD, LONDON S.W. 7
Telephone: KENsington 0048, 0049

The

PHILOSOPHICAL MAGAZINE

(First Published 1798)

A Journal of Theoretical, Experimental and Applied Physics

EDITOR:
PROFESSOR N. F. MOTT,
M.A., D.Sc., F.R.S.

EDITORIAL BOARD:
SIR LAWRENCE BRAGG,
O.B.E., M.C., M.A., D.Sc., F.R.S.
ALLAN FERGUSON,
M.A., D.Sc.
SIR GEORGE THOMSON,
M.A., D.Sc., F.R.S.
PROFESSOR A. M. TYNDALL,
C.B.E., D.Sc., F.R.S.

Established 150 Years

ANNUAL SUBSCRIPTION
£6 0s. 0d.

OR

12s. 6d.
EACH MONTH
POST-FREE

Contents for December 1951

L. J. GRIFFIN (H. H. Wills Physical Laboratory, University of Bristol). "Microscopic Studies on Beryl Crystals.—II. Dislocations and the Growth of {10$\bar{1}$0} Prism Faces."

J. C. GUNN & J. IRVING (Department of Natural Philosophy, University of Glasgow). "The Photo-electric Disintegration of Three- and Four-Particle Nuclei."

J. SAWKILL & N. THORLEY (Physics Department, King's College, Newcastle-upon-Tyne). "The Recrystallization Texture of Drawn Aluminium Wire."

O. PENROSE (Royal Society Mond Laboratory, Cambridge). "On the Quantum Mechanics of Helium II."

R. H. DALITZ & D. G. RAVENHALL (Department of Mathematical Physics, University of Birmingham). "On the Tomonaga Method for Intermediate Coupling in Meson Field Theory."

V. VAND (Chemistry Department, The University, Glasgow). "Application of Dislocation Theory to the Polytypism of Silicon Carbide."

J. G. HAYES & T. VICKERS (National Physical Laboratory, Middlesex). "The Fitting of Polynomials to Unequally-Spaced Data."

J. D. ESHELBY & A. N. STROH (H. H. Wills Physical Laboratory, University of Bristol). "Dislocations in Thin Plates."

F. H. J. CORNISH & D. K. C. MacDONALD (Clarendon Laboratory, Oxford). "The Influence of Deviations from the Debye Spectrum on the Electrical Conductivity of Metals."

O. KOFOED-HANSEN (Institute for Theoretical Physics, University of Copenhagen). "Effects of the Recoil on Allowed β-Transitions."

W. B. THOMPSON (University of Toronto). "Thermal Convection in a Magnetic Field."

L. HOWARTH (Department of Mathematics, University of Bristol). "The Boundary Layer in Three Dimensional Flow.—Part II. The Flow near a Stagnation Point."

CORRESPONDENCE:

M. BLACKMAN (Physics Department, Imperial College, London). "On the Calculation of Characteristic Temperatures from the Elastic Constants."

R. HUBY & H. C. NEWNS (Department of Theoretical Physics, The University of Liverpool). "Inelastic Scattering of Deuterons."

R. BOWERS, D. F. BREWER & K. MENDELSSOHN (Clarendon Laboratory, Oxford). "Experiments on the Unsaturated Helium II Film."

O. KOFOED-HANSEN (Institute for Theoretical Physics, University of Copenhagen). "The Upper Limit for the Neutrino Rest Mass."

BOOK REVIEWS

TAYLOR & FRANCIS LTD., Red Lion Court, Fleet St., LONDON, E.C.4

Printed by TAYLOR & FRANCIS, LTD., Red Lion Court, Fleet Street, London E.C.4